UiT The Arctic University of Norway

Faculty of Health Sciences

Microbial evolution in biofilms

Øyvind Myrvoll Lorentzen

A dissertation for the degree of Philosophiae Doctor - September 2024

Front page image: Montage of stereomicroscope images of *V. cholerae* colonies.

A dissertation for the degree of Philosophiae Doctor

Microbial evolution in biofilms

Øyvind Myrvoll Lorentzen

Tromsø – September 2024

Department of Pharmacy

Faculty of Health Sciences

UiT The Arctic University of Norway

Acknowledgements

This work was carried out at the Department of Pharmacy at UiT – The Arctic University of Tromsø between 2016 and 2024. I am thankful to the Faculty of Healthy Sciences, UiT – The Arctic University of Tromsø and the medical student research program for funding and supporting my research over several years. Thanks to funding from the medical student research program and the PhD schools IBA, Digital Life and NDPIA, I have had the privilege to present my research at several conferences, which I am very grateful for.

First, I would like to extend my gratitude to my supervisors **Pål Jarle Johnsen** and **Sören Abel**. **Pål**, thank you for welcoming me into MicroPop and the world of evolutionary biology. I am grateful for your support and how you have always encouraged my curiosity-driven approach to research and given me the freedom to follow my own research interests. **Sören**, you introduced me to research in general as a medical research student. Your guidance and encouragement in those years have undoubtedly impacted my approach to research and research interests. This PhD would not have been possible without support and guidance from both of you.

To my office buddy **Chris**. Collaborating with you has been a joy and has greatly influenced this thesis. More importantly, I am grateful for our friendship over the last years. Thank you for all the good times, office beers, and fun wine evenings with you and **Alex**.

I am very grateful for the hospitality of colleagues and friends in **MicroPop** and the Department of Pharmacy. Thank you, **Elizabeth**, **Vidar**, **Julia**, **João**, **Klaus**, **Xana**, **Nina**, **Mikkel**, **Ørjan**, **Francois**, **Miriam,** and **Silje**. A special thank you to **João, Elizabeth**, **Vidar**, **Julia**, and **Klaus** for always being open to discuss ideas, helping me with technical questions and for introducing me to the world of evolutionary biology, mobile genetic elements and AMR. I also want to thank former lab mates and members of **InfBio**, especially **Christina, Bhupender,** and **Merete**.

This work would have not been possible without the contribution of all my co-authors and collaborators. I am thankful to all my co-authors, which I have had the pleasure to work alongside with during this PhD. I am grateful to the Advanced Microscopy Core

Facility, Genomics Support Centre Tromsø (GSCT) and The Norwegian Sequencing Centre (NGC) for assisting my research with technical support and equipment.

Throughout this PhD, I have had invaluable support from friends and family. To my closest friends in PW, thank you for years of friendship. Happenings with you have always been a welcoming distraction from work. Life would be much grayer without you. To my closest family - **Mom**, **Dad**, **Elias**, **Ingrid** and **Isabell** - your encouragement over all these years have meant everything to me. Your presence in my life is always a source of joy. To my dear brother **Elias,** we have walked this path together. Thank you for the “millions” of lunches and coffees, countless discussions, and for sharing so many passions with me.

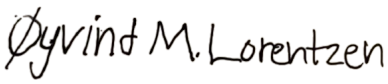

Tromsø, September 2024

«Og vi sier

ingenting, vi, før noen

hogger oss ut»

Tor Ulven

Table of Contents

Abbreviations

AMR	Antimicrobial resistance
AIs	Autoinducers
AmpC	Ampicillinase C (class C β-lactamase)
AphA	Activator of *tcpP* and *tcpH* expression
A-site	Active site
ATR	Acid tolerance response
Bap1	Biofilm associated protein 1
CACHE	Calcium channels and chemotaxis receptors
c-di-GMP	Cyclic diguanylate
CTX	Cholera toxin
CTX-M	Cefotaximase (CTX) from Munich (M) (class A β-lactamases)
CTXφ	CTXφ bacteriophage
DGC	Diguanylate cyclase
DNA	Deoxyribonucleic acid
ESBL	Extended-spectrum β-lactamase
FP	Fluorescent protein
HapR	Hemagglutinin/protease regulatory protein
HDOD	HD-related output domain
HGT	Horizontal gene transfer
GAF	cGMP-specific phosphodiesterases, adenylyl cyclases and FhlA
ICE	Integrative and conjugative element
IncC	Incompatibility group C
I-site	Inhibitory site
KPC	*Klebsiella pneumonia* carbapenemase
LB	Lysogeny broth
LTEE	Long-term evolution experiment
LuxO	Luminescence regulatory protein
MbaA	Maintenance of biofilm architecture
MBLs	Metallo-b-lactamase
MDR	Multidrug resistance
MGE	Mobile genetic element

MIC	Minimal inhibitory concentration
NDM	New Delhi metallo-b-lactamase (class B)
OD_{595}	Optical density at 595 nm
OD_{600}	Optical density at 600 nm
OXA	Oxacillinase
PAS	Per-Arnt-Sim domain
PBPs	Penicillin binding proteins
PCR	Polymerase chain reaction
PDE	Phosphodiesterases
QS	Quorum sensing
RbmA	Rugosity and biofilm structure modulator A
RbmC	Rugosity and biofilm structure modulator C
REC	Phosphoacceptor receiver domain
RNA	Ribonucleic acid
RpoS	RNA polymerase, sigma S
SBLs	Serine β-lactamases
SNP	Single nucleotide polymorphism
SXT	Sulfamethoxazole
T6SS	Type VI secretion system
TCP	Toxin co-regulated pilus
TEM	Named after the patient (Temoneira) (class A β-lactamases
VIM	Verona integron-encoded metallo-β-lactamase (class B)
VPI-1	*Vibrio* pathogenicity island-1
VPI-2	*Vibrio* pathogenicity island-2
VPS	*Vibrio* polysaccharide
VSP-1	*Vibrio* seventh pandemic island 1
VSP-2	*Vibrio* seventh pandemic island 2
WASA	West African-South American
WHO	World health organization

List of papers

This thesis is based on the following scientific works:

1. Øyvind M. Lorentzen, Christina Bleis and Sören Abel. A comparative genomic and phenotypic study of *Vibrio cholerae* model strains using hybrid sequencing. (**Manuscript, accepted in Microbiology**).

2. Øyvind M. Lorentzen, Sören Abel, Pål J. Johnsen and Christopher Frøhlich. Biofilm evolution selects for constitutive synthesis of c-di-GMP by the bifunctional enzyme MbaA. (**Manuscript, not published)**

3. Øyvind M Lorentzen, Anne Sofie B Haukefer, Pål J Johnsen, Christopher Frøhlich. The biofilm lifestyle shapes the evolution of β-lactamases. Genome Biology and Evolution, Volume 16, Issue 3, March 2024, evae030, https://doi.org/10.1093/gbe/evae030

Abstract

Formation of biofilms is an important adaptive strategy that bacteria employ to endure challenging conditions. This thesis delves into the evolution of the pathogen *Vibrio cholerae* in biofilms with a focus on biofilm adaptation, c-di-GMP signaling and β-lactamase evolution.

Paper 1 improved upon the genome of *V. cholerae* C6706 and linked every open reading frame to the current reference strain *V. cholerae* N16961. A genetic analysis identified multiple differences between *V. cholerae* C6706 and N16961. Experimental evidence suggested that these genetic differences affected biofilm formation and motility through alterations in quorum sensing and c-di-GMP turnover.

Paper 2 examined biofilm adaptation during biofilm evolution. Strong selection for biofilm formation markedly improved the biofilm forming capacity of *V. cholerae* through mutations in the polyamine-regulated, bi-functional c-di-GMP-metabolizing enzyme MbaA. Mutagenesis studies and enzyme kinetics indicated that mutations in MbaA activated the diguanylate cyclase activity of the GGDEF-domain, reduced phosphodiesterase activity of the EAL-domain and decoupled MbaA from polyamine-mediated regulation via NspS. This suggests that the increase in biofilm formation comes from shifting the enzymatic output of MbaA from degradation to synthesis of c-di-GMP.

Paper 3 investigated how β-lactamases affect biofilm formation in *V. cholerae* and how the biofilm lifestyle can affect the evolution of β-lactamases. A wide range of β-lactamases impaired biofilm formation in *V. cholerae*. Directed evolution coupled with selection for biofilm formation selected for mutations that reversed biofilm inhibition. This suggests that the biofilm environment can influence the evolutionary trajectories of β-lactamases.

Overall, this thesis expands our understanding of the biology and evolution of *V. cholerae* and underscores the importance of understanding pathogen evolution in biofilms. Additionally, it suggests that the c-di-GMP signaling system is a potent evolutionary target for bacterial adaptation.

1 Vibrio cholerae

1.1 Cholera

Vibrio cholerae is a pathogenic Gram-negative bacterium and the causative agent of cholera [1]. This is an acute and severe diarrheal disease. If left untreated, the disease can cause fluid loss of up to 1000 milliliters per hour and rapidly lead to severe dehydration, hypovolemic shock and death [1]. The pathogen is believed to have afflicted humans with disease for centuries and ancient accounts from the Bay of Bengal (from 500 BCE) have described a severe diarrheal disease similar to cholera [2]. Since the 1800s, cholera has spread globally and caused seven pandemics [1–3]. During this time, the pathogen has become endemic in multiple regions globally and cholera still represents a major global health threat. Annually, *V. cholerae* infects approximately 3 000 000 people worldwide and is associated with 95 000 deaths [4].

Cholera outbreaks usually occur in areas with poor water, sanitation, and hygiene infrastructure [1]. Either because of inadequate infrastructure to begin with, or due to destruction of infrastructure by war or natural disasters. During outbreaks, the number of cases can increase explosively and rapidly overwhelm public health services. In the last decades, devastating cholera outbreaks in Haiti and Yemen have underlined this [5–8]. As a result, WHO launched the global initiative “Ending cholera” with the goal of reducing cholera deaths globally by 90% by 2030 [9, 10]. Despite the ongoing coordinated global initiative, cholera has seen a resurgence recently [11].

V. cholerae strains are divided into serogroups based on their polysaccharide O antigens. To date, around 200 different serogroups have been identified [1, 12]. Despite the large number of serogroups, pandemic strains only belong to two serogroups, O1 and O139, with O1 being most frequently associated with disease. The remaining serogroup diversity is in nonpathogenic environmental strains of *V. cholerae*. These non-O1/O139 *V. cholerae* strains can cause sporadic diseases with mild cholera-like diarrhea, but do not cause pandemics [1]. Historically, the O1 serogroup has been the most common among circulating pathogenic *V. cholerae* strains. However, around 1992 a strain belonging to the O139 serogroup caused an outbreak on the Indian sub-continent [1, 13, 14]. Initially, this strain successfully outcompeted the O1 serogroup strains, and cause several outbreaks around the Bay

of Bengal. Puzzlingly, the O139 serogroup strains vanished rapidly and after the 2000s this serogroup has rarely been isolated [13]. Consequently, the O1 serogroup still remains the dominant serogroup among pathogenic *V. cholerae* strains.

V. cholerae O1 strains are further classified in the two biotypes classical and El Tor, respectively. The classical biotype is the original biotype of pathogenic *V. cholerae* O1 and believed to be the cause of the first six pandemics [1, 15, 16]. The El Tor biotype emerged around 1900 and is named after the quarantine station it was first isolated at (El Tor quarantine station in Egypt) [2, 15]. After its emergence, the El Tor strains have completely outcompeted the classical biotype [1, 17, 18]. It is the current circulating biotype and culprit of the ongoing 7th cholera pandemic. On the one hand, El Tor strains commonly induce less severe disease and fewer fatalities and are more frequently associated with asymptomatic infections [19–21]. On the other hand, El Tor strains exhibit increased environmental persistence and transits between the aquatic environment and the human host more efficiently than classical biotype strains [21–23]. This is believed to be one of the reasons behind the displacement of classical strains by El Tor strains. The two biotypes can be distinguished by the presence of specific phenotypic traits [22]. Additionally, the two biotypes can be differentiated by multiple genetic differences. Among them are the genetic islands *Vibrio* seventh pandemic island-1/2 (VSP-1/2), which are genetic hallmarks of 7th pandemic O1 El Tor biotype strains [1, 22, 24].

1.2 The 7th cholera pandemic

Since 1817, there has been seven global cholera pandemics. The 7th and currently ongoing pandemic began in Indonesia in 1961. Since then, it has spread globally in three distinct transmission waves (Fig. 1) [3, 15, 18, 21].

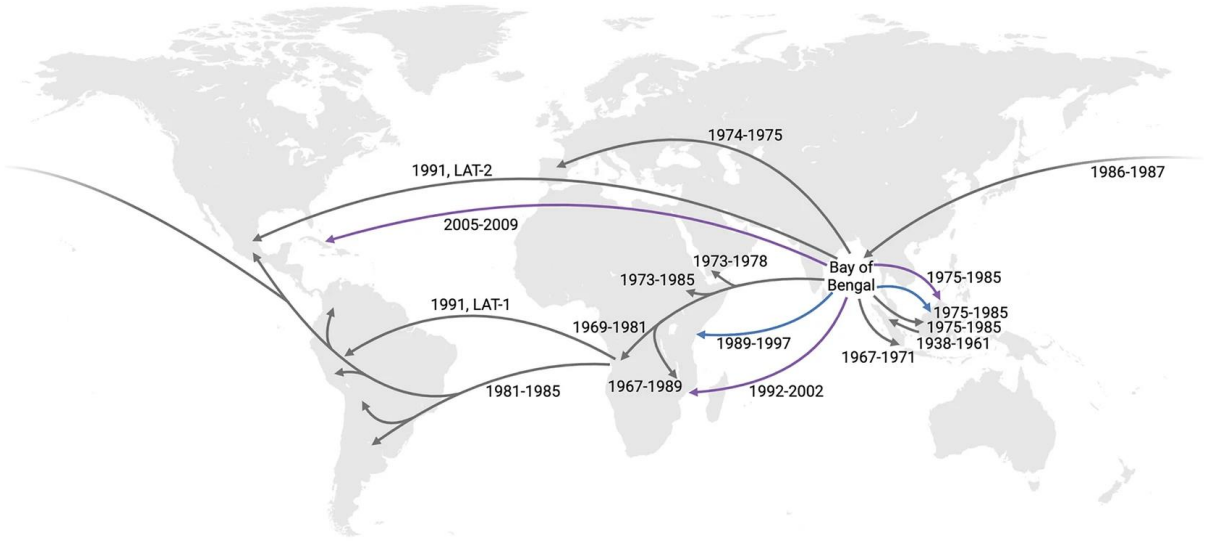

Figure 1 Global spread of 7th cholera pandemic
The global spread of *V. cholerae* during the 7th pandemic. The pandemic originated in Indonesia in 1961 and spread globally in three waves: wave 1 (gray), wave 2 (blue) and wave 3 (purple) [18]. Adopted with permission from [3].

Wave 1 represents the first global transmission and spread cholera to Africa, Europe, the Americas and across Asia. Many of the commonly used model strains of *V. cholerae* stem from wave 1 of the 7th pandemic including *V. cholerae* N16961, which functions as the current reference genome, C6706, A1552 and E7946 [25–29]. The acquisition of the SXT-element, which is an integrative, conjugative element, marks the transition from wave 1 to wave 2 [18]. This has been predicted to occur between 1978-84, several years before the first SXT-element was isolated in Southeast Asia (first isolated in 1993) [18, 30]. In addition, wave 2 strains harbor changes in the CTX prophage in the form of a tandem repeat of CTX on chromosome 2. Wave 3 strains have been deemed hybrid El Tor strains since they have acquired the *ctxB* allele of the classical biotype and some of these strains have been deemed hypervirulent [31]. In addition, wave 3 strains also harbor the SXT-element [3, 18, 22]. Wave 3 strains have caused several devastating outbreaks globally in the last decade (e.g. Haiti,

Yemen, and Zimbabwe) [7, 8, 32, 33]. The study of the 7th cholera pandemic clearly demonstrates how *V. cholerae* continuously evolve and acquires novel traits as it spreads throughout the world.

1.3 Evolution of *V. cholerae* by mobile genetic elements

Mobile genetic elements (MGEs) are DNA-segments that can move within or between bacterial genomes. These two types of movements are named intracellular and intercellular mobility, respectively (Fig. 2a) [34]. MGEs are widespread throughout the bacterial kingdom and can encode proteins that ensure their own mobility and spread, but many parasitize the mobility apparatus of other MGEs [35–38]. MGEs often encode genes providing novel adaptive traits to the host, including antibiotic and heavy metal resistance, phage and plasmid defense systems and virulence/pathogenicity factors [35–37]. Because of this, MGEs are crucial drivers of adaptive evolution in bacteria. A classic example of this is how horizontal transfer of MGEs have facilitated the spread of AMR in the last decades [34, 35, 37].

Over the years multiple types of MGEs have been discovered, which can be categorized based on their ability to move between or within genomes [34]. Plasmids, integrative, conjugative elements (ICEs), bacteriophages, phage satellites and genomic islands primarily move between genomes, while transposon and integrons move within genomes (Fig. 2a) [34]. Although, integrons are non-mobile themselves, they encode site-specific recombination systems that allows them to recognize and capture genes [39, 40]. Importantly, transposon and integrons are often associated with other MGEs, thereby enabling their movement between genomes as well (e.g. the SXT-element encodes both a transposon and an integron) [41].

Horizontal gene transfer (HGT) refers to any transfer of genetic material into a bacterial cell and mediates intercellular spread of MGEs [42]. The three major types of HGT are transduction, natural transformation, and conjugation (Fig. 2b). Transduction relies on bacteriophages and represents the accidental transfer of genetic material between bacterial cells due to bacteriophages infecting in bacterial cells. This happens when DNA is packaged together with the phage genome into the phage particles (Fig. 2b) [42]. Phages can also integrate into the host chromosome to become prophages [43, 44]. Natural transformation refers to uptake of extracellular DNA from the environment which can only be done by bacterial species that are naturally competent [45]. After uptake from the environment, the DNA can be integrated into the genome, often through homologous recombination, via RecA (Fig. 2b). Lastly, conjugation refers to

the direct transfer of MGEs between two bacterial cells in close proximity of each other, which relies on conjugative pili (Fig. 2b) [42]. This is the primary transfer mechanism of plasmids and ICEs and the main mechanism for horizontal spread of AMR determinants [34, 37, 42]. In addition, there are so called non-canonical HGT-mechanisms, which among other can involve outer membrane vesicles, tiny pilus-like structures, or gene transfer agents (Fig. 2b) [42].

It is clear that MGEs play a key role in microbial evolution, yet MGEs often impose a fitness burden that reduces the reproductive ability of the MGE-harboring bacteria in the absence of selection for MGE-encoded traits [42, 46–48]. This has been defined as MGE-imposed fitness cost. If this cost is too large, bacterial cells harboring MGEs will be outcompeted by bacteria without MGEs. Although MGE-imposed fitness costs can be reduced over time through the acquisition of compensatory mutations, the initial MGE-imposed cost is a crucial constraint on the vertical and horizontal spread of MGEs [46–49]. Therefore, the MGE-imposed fitness cost represents a major barrier to long-term spread and persistence of MGEs [48].

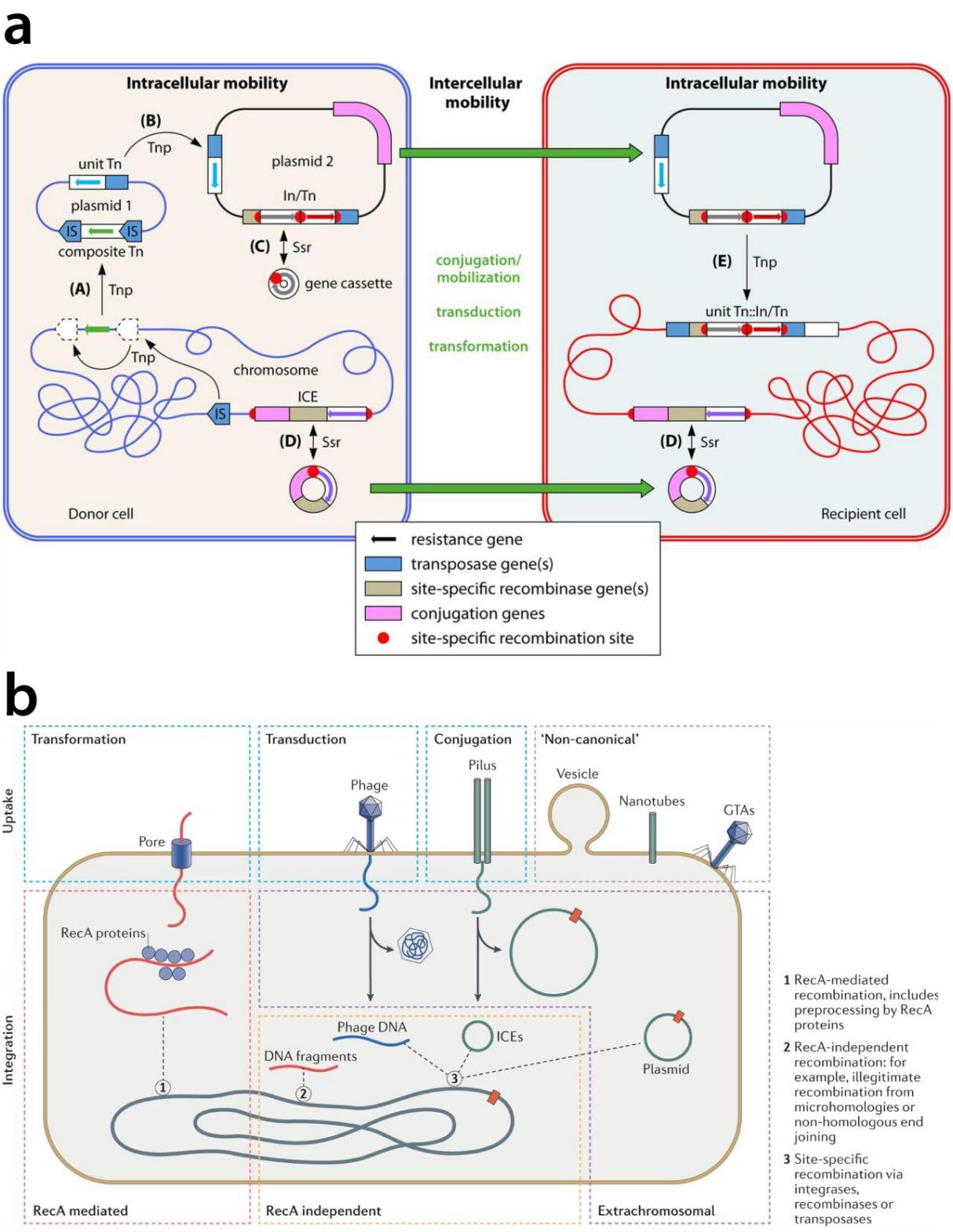

Figure 2 Overview of different types of horizontal gene transfer within and between genomes

a. Overview of mobile genetic elements (MGEs) and examples of intracellular and intercellular mobility. Two different bacterial cells are depicted, with one acting as donor (blue) and one acting as recipient (red). Multiple MGEs are present in each cell. Functions of the individual genes encodes by the MGEs are color coded and depicted in the box underneath the cells.

Intracellular mobility is depicted as a thin black arrow. Intracellular mobility mediated by transposases are labeled Tnp, while those mediated by site-specific recombinases are labeled Ssr. Intercellular mobility is depicted as a thick green arrow. A plasmid can mediate its own intercellular transfer by conjugation if it encodes the conjugation machinery. It may also be mobilized by another conjugative plasmid if it lacks the conjugation machinery. Different types of intracellular mobility are depicted as **(A)-(E)**. (**A**)Transposons (Tn) can move from the chromosome to an MGE (plasmid 1). (**B**) Transposons can also move between different MGEs e.g., move from plasmid 1 to plasmid 2. (**C**) Gene cassette can move between different transposon/integrons via circular intermediates. Certain MGEs can also move via circular intermediates. (**D**) For example, ICEs can excise and circularize before conjugating into a recipient bacterial cell. Once there, it can reintegrate into the chromosome of the recipient cell. Plasmids can move between bacteria by horizontal gene transfer as depicted by the movement of plasmid 1 into the recipient cell. (**E**) Once in the recipient cell, if the plasmid carries transposons, these may jump into the chromosome of the recipient host. Figure is adopted with permission from [34]. ***b.*** Overview of different modes of HGT and the downstream processing of the DNA in the recipient cell. Transformation depends on the uptake of DNA from the environment. After uptake, the DNA can be integrated into the chromosome either through RecA-mediated or RecA-independent recombination. Transduction relies on phage-mediated transfer of DNA by packaging of DNA into phage particles. After entry in to the cell, the phage can replicate and form new phage particles. Alternatively, the phage can also integrate into the host chromosome to become a prophage. Conjugative plasmids or elements are transferred into bacterial cells via the conjugative pilus in a contact-dependent manner. After conjugating into the recipient cells, plasmids are maintained as extrachromosomal elements. In contrast, some conjugative elements (e.g. ICEs) integrate into the host chromosome. In addition to the three above-mentioned mechanisms, several non-canonical mechanisms have also been described, including HGT mediated by membrane vesicles, tiny pilus-like structures and gene transfer agents (GTAs). Figure is adopted with permission from [42].

The origin and evolution of *V. cholerae* have been shaped by MGEs (Fig. 3a-b) [3, 15, 17]. Thus, it serves as an excellent example of how MGEs affect microbial evolution. Notably, the generation of a toxigenic *V. cholerae* strain with pandemic potential depends on the acquisition of multiple MGE-encoded virulence factors, such as the cholera toxin and toxin co-regulated pilus (TCP) (Fig. 3a). The *vibrio* pathogenicity island-1 (VP-1) encodes the TCP, crucial for intestinal colonization of *V. cholerae*, and the key virulence regulator ToxT [23, 50]. Furthermore, TCP is indispensable for acquisition of the cholera toxin genes since it acts as the receptor for the CTXφ bacteriophage (CTXφ), which encodes cholera toxin. Thus, it enables the acquisition of CTXφ and the conversion of a non-toxigenic *V. cholerae* strain into a toxigenic strain. After infection of the bacterial cell, CTXφ is irreversibly integrated into the chromosome of *V. cholerae* [1, 3]. Thus, becoming a prophage, and granting *V. cholerae* the ability to the produce cholera toxin (CTX) and induce the cholera disease.

The emergence of the *V. cholerae* O1 El Tor biotype responsible for the ongoing 7th pandemic was also mediated by the acquisition of novel MGEs (Fig. 3a-b) [3, 15, 17, 24]. One of the drivers behind the success of the El Tor biotype is believed to be related to the acquisition of the two novel genomic islands VSP-1 and VSP-2 [3, 15, 24, 51]. These two islands have been linked to both pathogenicity, phage defense, plasmid defense systems, and novel metabolic traits [3, 15, 24, 51]. In support of this, the classical biotype is outcompeted to a lesser degree against an El Tor biotype strain with ΔVSP1-2 [51]. Furthermore, before the acquisition of VSP-1/2, *V. cholerae* El Tor biotype strains only caused minor sporadic outbreaks [15].

In addition to the MGEs that facilitate the transformation of *V. cholerae* into a toxigenic pathogen, it can possess other MGEs that grant additional traits (Fig. 3a) [51–55]. This includes the beforementioned SXT-element as well as novel MDR plasmids that emerged in recent large cholera outbreaks [7, 8, 33, 56]. These plasmids encode multiple antibiotic resistance genes and induce multidrug resistance (MDR) towards many commonly used antibiotics [1, 7, 8, 33, 56]. Taken together, MGE acquisition has been linked to key evolutionary transitions and *V. cholerae* represents a suitable model system to study how MGEs or MGE-harbored genes evolve.

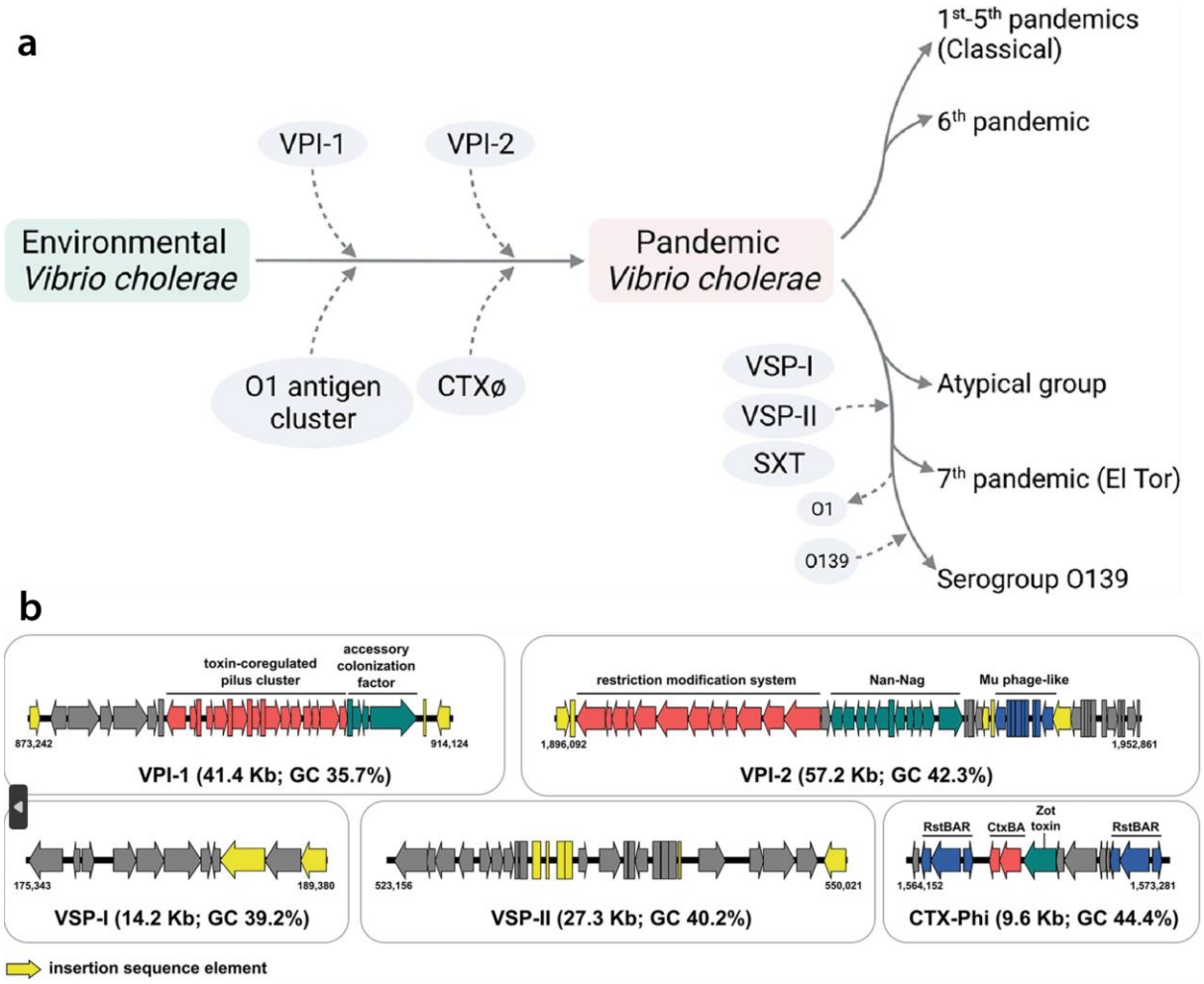

Figure 3 Evolution and emergence of pathogenic *Vibrio cholerae*
a. Overview of the transformation of an environmental non-pathogenic *V. cholerae* strain into a pathogenic strain with pandemic potential. VPI-1 = *Vibrio* pathogenicity island-1, VPI-2 = *Vibrio* pathogenicity island-2, CTXΦ, CTX bacteriophage, VSP-1 = *Vibrio* seventh pandemic island-1, VSP-2 = *Vibrio* seventh pandemic island-2, SXT = SXT-element, an integrative and conjugative element. **b.** Genomic maps of the MGEs (VP-1, VP-2, VSP-1, VSP-2, CTXΦ) encoding the major virulence factors in 7th pandemic *V. cholerae* strains. Adopted with permission from [3].

1.4 Antimicrobial resistance in *V. cholerae*

The introduction of antimicrobials in the 1940s represents a major paradigm shift in modern medicine, enabling the treatment of bacterial infections. To this day, it remains one of the most important advances in the history of modern medicine. Currently, multiple classes of antimicrobials exist and are regularly used [57]. In general, antimicrobials target one of four indispensable cellular processes:

I. Nucleic acid synthesis
II. Folate synthesis or other metabolic processes
III. Cell wall synthesis
IV. Protein synthesis

Unfortunately, due to bacteria's remarkable adaptive ability, AMR has become an increasing problem over the last few decades [57]. From a clinical standpoint, AMR represents a troublesome bacterial trait, which is associated with millions of deaths annually [58]. So far, no classes of antimicrobials have managed to escape resistance development. In general, antimicrobial resistance is achieved through four mechanisms [57]:

I. Prevention of access to the target through increased efflux or reduced permeability.
II. Alteration, modification, or protection of the target that prevent efficient antimicrobial binding.
III. Enzymatic modifications or degradation of antimicrobial drugs.
IV. Antimicrobial target bypass which makes the antimicrobial target redundant.

Administration of antimicrobials are currently recommended for patients with cholera with moderate/severe dehydration [59]. The most frequently used classes of antimicrobials to treat cholera are tetracyclines, fluroquinolones and macrolides. Due to the widespread use of antimicrobials, AMR has emerged in *V. cholerae* over the last decades. Consequently, multidrug resistant (MDR) isolates of *V. cholerae* have become common and currently circulate globally. The most important mediator of AMR in *V. cholerae* is the previously mentioned SXT-element, which commonly encodes resistance towards streptomycin, sulfamethoxazole, florfenicol and trimethoprim [41].

Worryingly, in some of the last major outbreak (e.g. Zimbabwe and Yemen) MDR plasmids encoding multiple additional AMR genes have emerged [7, 8, 33]. These plasmids encode resistance genes against several antimicrobials, including macrolides, sulfonamides and β-lactams.

Although β-lactams are infrequently used to treat cholera, they are one of the most important classes of antimicrobials. All β-lactams share a common structural feature in the form of the β-lactam ring [60, 61]. The class is further divided into four subclasses: penicillins, cephalosporins, monobactams and carbapenems [60, 61]. The antibacterial effect of β-lactams comes from disruption of bacterial cell wall synthesis through inhibition of penicillin-binding proteins (PBPs). PBPs are crucial for the synthesis of peptidoglycans, the major component of bacterial cell walls. β-lactams binds to PBPs and inactivates them, which disrupts bacterial cell wall homeostasis and triggers bacterial cell lysis [57, 60, 62].

The widespread use of β-lactams over several decades have strongly selected for β-lactam resistance. In Gram-negative bacteria, the most troublesome resistance mechanism against β-lactams is the expression of β-lactamases [57, 58, 63]. These are enzymes that can hydrolyze and thereby inactivate β-lactams. Furthermore, β-lactamase-encoding genes are often associated with MGEs, which facilitated their spread globally [64]. Because of this, β-lactamases represents an important cause of AMR and a major public health threat. β-lactamases display significant sequence- and functional-variability and can be classified either by sequence diversity (Ambler class A to D) or active site (A-site) properties (serine-type or metallo-β-lactamases) [61, 65].

Serine- and metallo-β-lactamases differ in their A-site characteristics and employ different mechanisms to hydrolyze β-lactams. In general, serine-β-lactamases (SBLs) employ an acylation-deacylation mechanism. This approach relies on a nucleophilic serine to form a covalent acyl-enzyme intermediate with the β-lactam. Next, an activated water molecule hydrolyzes the acyl-enzyme intermediate and frees the degraded β-lactam. Different classes of SBLs utilized different residues to activate the water molecule that mediate deacylation. Class A enzymes (e.g. KPC-2), utilize E166, class C enzymes (e.g., AmpC) utilize K67 via Y150 and class D enzymes (e.g. OXA-

48) utilize carboxylated K73. In contrast, metallo-β-lactamases (MBLs) utilize zinc metals to activate a water molecule that subsequently hydrolyzes the β-lactam.

1.5 The *Vibrio cholerae* life cycle

V. cholerae has a complex life cycle and survives year-round in estuarine and coastal environments in endemic areas [1, 23, 66, 67]. Because of this, it is considered an environmental pathogen that can infect humans through contaminated water and food [1, 3, 23, 66]. In both the aquatic environment and the human host, sensing and adapting to changing conditions is essential for *V. cholerae*`s ability to survive and cause disease [1, 3, 23, 66].

1.5.1 Environmental persistence and survival of *V. cholerae*

The aquatic environment that *V. cholerae* reside in is harsh and continuously fluctuates. To survive, *V. cholerae* needs to sense and adapt to challenges such as predation, osmotic stress, temperature shifts, nutrient limitations, phage infections, antimicrobial compounds and inter-microbial competition [23, 66, 68, 69]. One of the most important adaptive strategies *V. cholerae* employs to ensure environmental survival is biofilm formation [66, 70]. Biofilms, expanded upon in section 3, can be defined as bacterial communities enclosed in a self-produced protective matrix [71]. In the environment, *V. cholerae* often colonizes crustaceans (e.g. phytoplankton and zooplankton) by adhering to their chitinous exoskeleton and use them as surfaces to form biofilms on [23, 72, 73]. Biofilm formation enhance environmental persistence and protects against external stressors like predation, bacteriophages, and salinity and temperature shifts. In support of this, a hyper-biofilm variant (rugose variation) of *V. cholerae* exhibit increased tolerance to multiple external stressors [74–77].

Chitin is a key nutrient and an important source of carbon and nitrogen for *V. cholerae* [23]. Furthermore, chitin is an important lifestyle que and association with it triggers natural competence, which allows *V. cholerae* to take up new genetic material from its environment [23, 78]. Because of this, biofilm formation on chitin surfaces increases both persistence, nutrient acquisition and HGT. Furthermore, biofilm-derived *V. cholerae* has been shown to be hyper-infectious and readily induce cholera disease in humans [23, 66, 69, 79–81]. Therefore, biofilm formation seems to increase the environmental survival of *V. cholerae*, while simultaneously priming the pathogen for human infection. Altogether, biofilm formation seems to be a key survival strategy and lifestyle for *V. cholerae*. In agreement with this, a simple filtration system that removes

particles >20 µm has been shown to reduce the incidence of cholera in endemic regions in Bangladesh [82].

1.5.2 Pathogen entry into the human host

Upon oral uptake by the human host, *V. cholerae* experiences a radical shift in conditions. This continues through the host and the pathogen must sense and adapt to changes throughout the infection cycle [23]. The first and perhaps greatest challenge for *V. cholerae* is the human gastric fluid. *V. cholerae* is sensitive to pH and the low pH of 1 - 3 in the human stomach represents a major challenge [23, 83]. Because of this, only a small fraction of the initial bacterial inoculum will manage to pass into the small intestine [84]. Therefore, unless gastric fluid is buffered, large oral doses, often greater than 10^8 are needed to consistently induce clinical cholera disease [1, 85, 86].

Once again, formation of biofilms is a key strategy that facilitates the passage of *V. cholerae* through the harsh conditions of the stomach. The biofilm matrix is believed to shield the biofilm-embedded bacteria from the acidic environment of the stomach. As a result, the *V. cholerae* biofilms are more tolerant to the acidic environment and are able to better transit into the small intestine [23, 66, 87, 88]. In addition, a study also demonstrated that acidic pH induces surface-attachment through increased expression of mannose sensitive hemagglutinin (MSHA) pili [89]. Therefore, biofilm formation seems to be an important adaptive strategy to survive entry into the stomach. In support of this, as already stated, biofilm-derived *V. cholerae* are hyper-infectious and seems to be primed for host infection [23, 66, 69, 79–81, 87].

V. cholerae also possess molecular systems that can induce an acid tolerance response (ATR) upon exposure to acidic environments. The main actor in ATR is a lysine decarboxylase (CadA), which consumes H^+ ions to produce the polyamine cadaverine and carbon dioxide [90–92]. It is believed that CadA pumps H^+ ions out of the cell, thereby increasing the internal pH of the cell and its acid tolerance. In support of this, previous work has demonstrated that *V. cholerae* cells lacking *cadA* are not able to withstand acid shock [90]. Furthermore, acid adapted *V. cholerae* outcompete non-adapted *V. cholerae* in infection models [93]. Interestingly, the fitness benefit of acid-adapted *V. cholerae* does not manifest until >3h post-infection, suggesting that

the observed fitness benefit is not due to greater passage through the gastric phase, but occurs later in the infection cycle [93].

1.5.3 Colonization of the small intestine and pathogenesis

After passage through the stomach, the pathogen enters the small intestine. Once there, *V. cholerae* penetrates the mucus barrier to colonize the small intestine, multiply and induce diarrhea by secretion of cholera toxin (CTX) [1]. If the pathogen still resides in a biofilm upon entry in the small intestine, it must disperse from the biofilm, orient itself in the lumen and translocate to the walls of the intestine [23]. It has been demonstrated that *V. cholerae* senses multiple cues during infection, including bile, bicarbonate and pH [23, 66, 68]. These are believed to function as spatial cues that *V. cholerae* use to orient itself within the intestine [94]. Most bile salts lead to increased biofilm formation, while bicarbonate and alkaline pH increase biofilm dispersal and swim speed [89, 95]. This supports a model were *V. cholerae* transits through the stomach and into the small intestine in a biofilm form. Upon approaching the mucosal lining with increasing amounts of bicarbonate and higher pH, it disperses from the biofilm and penetrates the mucus barrier to reach the mucosal lining of the small intestine [23, 66, 94, 96–98].

After penetrating the mucus barrier, *V. cholerae* makes contact with the intestinal lining. There it attaches to the epithelial cells and divides to form microcolonies [23, 66, 99–102]. The formation of microcolonies is mediated by the toxin co-regulated pilus (TCP), one of two key virulence factors expressed by *V. cholerae* [100, 101]. To establish microcolonies, *V. cholerae* must displace the already present gut microbiota within the small intestine. Evidence suggests that *V. cholerae* employ the type 6 secretion system (T6SS), a contact-dependent toxin-delivery system, to displace the host microbiota and open up the intestinal niche [103]. This is supported by experimental data demonstrating that T6SS is active in the intestine and contributes to virulence and colonization [103–107].

After forming microcolonies in the small intestine, *V. cholerae* initiates secretion of CTX, which penetrates into the host cells and activates adenylate cyclase. This causes an increase cyclic AMP (cAMP) levels, which leads to excessive secretion of chloride ions and water into the intestinal lumen, thereby causing severe watery diarrhea, the

hallmark of cholera disease [1]. Expression of CTX mediates a fitness advantage to *V. cholerae* through modulation of the host-microbe metabolism [108, 109]. This supports the intestinal growth of *V. cholerae* to incredibly high numbers (>10^{11} CFUs in diarrheal fluid) from low levels, after eradication of a large fraction of the initial inoculum in the stomach [85]. The high *V. cholerae* load in diarrheal fluid towards the end of the infection facilitates further dissemination of the pathogen during outbreaks.

1.5.4 Mucosal escape and exit of the host

The final phase of the infection cycle of *V. cholerae* is characterized by the expulsion of the pathogen from the human host. Host exit is a key step in the life cycle of *V. cholerae* and a major contributor to the explosive nature of cholera outbreaks [23]. Human-shed *V. cholerae* are hyper-infectious and can efficiently re-infect other individuals, thereby, driving further spread of the pathogen [110–112]. To successfully exit the host, the pathogen must detach from the epithelial cells and migrate into the intestinal lumen, so that it can be shed in the stool [23, 66].

In the late stages of infection, *V. cholerae* initiates the mucosal escape response to exit the host [23, 113]. The mucosal escape response is controlled by the stationary phase alternative sigma factor (RpoS) [113]. As the infection progresses, and the intestinal *V. cholerae* population expands, nutrients become scarcer. This leads to growth deceleration and entry into stationary growth phase, triggering the activation of a genetic stress program by RpoS [26, 113]. This initiates the mucosal escape response by downregulating virulence related genes and increasing motility and detachment [23, 113]. As the pathogen exits its intestinal niche it prepares to re-enter the aquatic environment by inducing a specialized physiological state, which primes it for environmental survival and dissemination. This state is hallmarked by modulation of its metabolism, activation of phosphate and nitrogen acquisition systems, activation of chitin degrading enzymes, and activation of specific c-di-GMP genes [23, 114, 115]. *In vivo* studies of *V. cholerae* host exit, have demonstrate that biofilm-like aggregates can be isolated from the stool of cholera patients [79]. This indicates that once in the intestinal lumen, biofilm formation is yet again beneficial, and prepares the pathogen to reenter the aquatic environment [23, 66, 116].

2 C-di-GMP signaling

The cyclic diguanylate (c-di-GMP) signaling system is central to bacterial homeostasis and allows bacteria to sense and respond to a wide range of signaling cues [117–121]. It is a conserved nucleotide-based second messenger that is ubiquitous across the bacterial kingdom [117]. Second messengers are intracellular signaling molecules involved in the translation of extracellular or intracellular signals into physiological responses [117–121].

The research group of Moshe Benziman discovered c-di-GMP in 1987 [122]. In their seminal paper, they demonstrated that c-di-GMP regulates a bacterial cellulose synthase in the model organism *Acetobacter xylinum*. One of the most central roles of c-di-GMP is regulating the switch between a motile planktonic lifestyle and sessile biofilm-associated lifestyle [117–119]. In addition to this, c-di-GMP is involved in the regulation of numerous additional bacterial processes, including virulence, cell size, stress tolerance, cell shape, cell cycle regulation, secretion of extracellular enzymes, and antibiotic production [117–119, 123–131]. Therefore, understanding c-di-GMP signaling is crucial to understand biofilm regulation, but also bacterial decision-making and how bacteria maintain homeostasis under changing conditions.

2.1 General principles of c-di-GMP signaling

2.2 C-di-GMP control module

The c-di-GMP control module is made up of four key actors: two antagonistic enzymes that degrade or synthesis c-di-GMP based on signaling inputs, a c-di-GMP effector that binds c-di-GMP and a cellular target, which the effector modulates upon binding of c-di-GMP, to produce a physiological response (Fig. 4) [117–119]. This system allows bacteria to sense and adapt to a wide range of conditions through a single signaling system, thereby, facilitating adaptation and survival in rapidly changing environments [117–119].

Diguanylate cyclases (DGCs) synthesize c-di-GMP, while c-di-GMP-specific phosphodiesterases (PDEs) hydrolyze c-di-GMP. The function of DGCs and PDEs are linked to specific conserved protein domains, DGCs with GGDEF-domains and PDEs with EAL- or HD-GYP-domains [117–119]. All three domains are named after sequence motifs that make up parts of their A-site. The functional domains of DGCs and PDEs are often linked to various sensory domains that regulate their activity based on specific signaling inputs [132, 133]. The sensory domains most frequently associated with c-di-GMP-metabolizing enzymes are PAS-, GAF-, CACHE-, and REC-domains [132, 133]. Examples of signaling inputs are oxygen, bile acids, bicarbonate, and light [94, 134–137]. C-di-GMP modulates cell behavior through various c-di-GMP-responsive effectors [118, 138]. These effectors regulate downstream cellular targets in response to c-di-GMP-binding. So far, several classes that regulate a variety of cellular targets have been described (e.g., mRNA riboswitches, rRNA methylases, transcriptional regulators, PilZ-domain containing proteins and degenerate GGDEF/EAL-domains) [138–141].

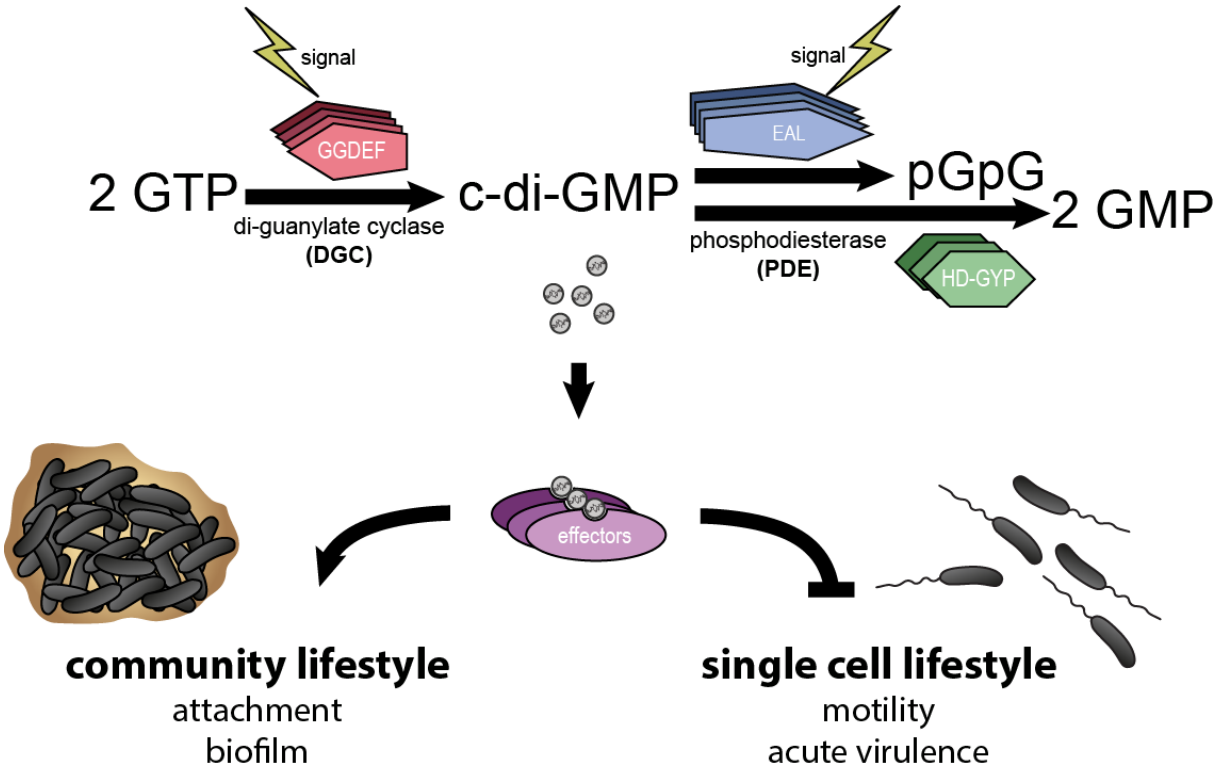

Figure 4 The C-di-GMP control module
External or internal signaling inputs (yellow flash) modulate the intracellular concentration of c-di-GMP by regulating the enzymatic activity of c-di-GMP-metabolizing proteins. Proteins containing GGDEF-domains (red pentagon) synthesize c-di-GMP, while EAL- and HD-GYP-domain containing proteins (blue pentagon or green hexagon, respectively) degrade it. C-di-GMP (grey circles) translates the signal inputs into functional outputs by binding to and regulating the activity of c-di-GMP effectors (violet ovals). Upon binding of c-di-GMP, these effectors regulate downstream cellular targets that produce cellular responses. In general, high levels of c-di-GMP promotes biofilm formation and inhibit motility and acute virulence.

2.3 Producers and degraders of c-di-GMP

2.3.1 Diguanylate cyclases synthesize c-di-GMP

DGCs, hallmarked by the GGDEF-domain, synthesize c-di-GMP [117–119]. The GGDEF-domain consists of a five-stranded central β-sheet surrounded by α-helices. It is closely related to the catalytic domain of adenylate cyclases and share the same βααββαβ-fold as adenylate cyclases [142, 143]. The domain is named after the amino acid motif Gly-Gly-Asp-Glu-Phe (GGDEF) that makes up an essential part of the enzyme's A-site (Table 1). This motif is crucial for the enzymatic activity of GGDEF-domains and most amino acid changes in this motif will severely impair enzymatic activity. So far, only four functional variants of this motif are known to exist (GGDEF, GGEEF, SGDEF, AGDEF) [142, 144–148]. The A-site is located at the dimer-interface of GGDEF-domains and is involved in GTP-binding, metal coordination and catalysis. In addition to the A-site, GGDEF-domains contain three additional residues important for both metal-binding, catalysis and guanyl binding (Table 1) [142]. The domain also contains additional conserved amino acid residues, but their function remains elusive [142].

DGCs synthesize c-di-GMP through the fusion of two GTP molecules. GGDEF-domains only contain one GTP binding site, therefore, c-di-GMP synthesis depends on the dimerization of two GGDEF-domains [142]. Since dimerization is essential for the enzymatic activity of DGCs, it is also an important point of regulation. Regulatory signals can modulate the activity of DGCs by either facilitating or impeding dimerization [136, 142, 143, 149–152]. GGDEF-domains are often part of multi-domain proteins that contain N-terminal sensory domain (e.g. PAS-, GAF-, CACHE-, and REC-domains). These sensory domains regulate the activity of the GGDEF-domain based on specific signaling inputs that either stimulate or inhibit c-di-GMP synthesis [117–119, 132]. In addition, many DGCs are regulated through product inhibition. C-di-GMP can bind specific inhibitory sites (I-sites) in the GGDEF-domain, which locks the protein in a conformation that is unable to form an enzymatically competent dimer (Table 1) [142, 143, 149, 151–153].

Table 1 Residues in GGDEF-domains important for enzymatic activity

Conserved residues	PleD	MbaA	Residue role (interaction)	References
#1	D327	D376	Mg++ binding and catalysis	[142, 143, 149]
#2	N335	N384	Guanyl binding	[142, 143, 149]
#3	D344	D393	Guanyl binding	[142, 143, 149]
#4	R359	K408	Primary I-site	[142, 143, 149]
#5	D362	S413	Primary I-site	[142, 143, 149]
#6-10	G368GEEF	S424GDEF	Active half-site hairpin	[142, 143, 149]
#11	R390	R448	Primary I-site	[142, 143, 149]

2.3.2 C-di-GMP-specific phosphodiesterase degrade c-di-GMP

2.3.2.1 EAL-domain proteins

EAL- and HD-GYP-domain are hallmark domains of the c-di-GMP-specific PDEs and a prerequisite for c-di-GMP hydrolysis. The EAL-domain is the most common of the two domain types and hydrolyzes c-di-GMP by catalyzing the asymmetric opening of c-di-GMP to 5′-pGpG [117–119]. In contrast to GGDEF-domains, some EAL-domains seem to retain some of their enzymatic activity in their monomeric state [154]. Nonetheless, most characterized EAL-domains form dimers or high-order oligomers and dimerization usually increases enzymatic activity [119, 134, 155, 156]. Therefore, dimerization is also a point of regulation for EAL-domain proteins and PDE-stimulating signaling inputs can facilitate dimerization of EAL-domain proteins [119, 155].

Like the GGDEF-domain, the EAL-domain is named after three highly conserved residues essential for the domain's enzymatic activity (Glu-Ala-Leu) (Table 2). EAL-domain proteins form multi-domain proteins less frequently than the GGDEF-domain. Furthermore, they are more often associated with C-terminal domains with additional enzymatic functions than N-terminal sensory domains [133]. The HDOD-domain, which can degrade 5′-pGpG to GMP, is the enzymatic domain second-most frequently associated with EAL-domains. Interestingly, the most frequently associated domain is the GGDEF-domain, which is more common than single EAL-domain proteins [133]. Even though EAL-domains are less frequently associated with N-terminal sensory domains, it still occurs. In this case, their enzymatic output is often modulated by the sensory domain [132, 133]. A classic example of this is the blue-light sensitive PDE BlrP1 from *K. pneumoniae* [134].

Crystal structures of EAL-domain proteins have demonstrated that the domain forms a modified TIM-barrel fold [155, 157, 158]. This is a conserved protein structure consisting of alternating α-helices and β-strands that form a central β-barrel with flanking α-helices. In TIM-barrel folds, the active sites are comprised of amino acid residues from the C-terminal ends of the β-strands [155, 158]. As a consequence, the A-site of the EAL-domain is more spread out in the amino acid sequence compared to the GGDEF-domain. Based on experimental data with multiple purified EAL-domains, 18 conserved residues important for enzymatic function have been identified (Table 2)

[155, 157, 159–161]. These residues are involved in both coordination of metal ions, coordination of the catalytic water molecule, substrate binding, dimerization, and stabilization of the protein quaternary structure [155, 157, 159–161].

Table 2. Conserved residues in EAL-domains important for enzymatic activity

Conserved residues	TBD1265	MbaA	Residue role (interaction)	References
#1	Q509	Q539	Unknown	[157, 161]
#2	P510	P540	Unknown	[161]
#3	E523	E553	Metal coordination	[157, 159–162]
#4	L525	L555	Unknown	[161]
#5	R527	R557	Substrate binding	[157, 159–161]
#6	P543	P573	Unknown	[161]
#7	E546	E576	Substrate binding	[157, 160, 161]
#8	N584	N612	Metal coordination, Substrate binding	[157, 159–161]
#9	E616	E644	Metal coordination	[157, 159–161]
#10	T618	T646	Unknown	[157]
#11	E619	E647	Metal ion coordination, Dimerization, substrate binding	[157, 161]
#12	D646	D672	Metal coordination, dimerization	[157, 159–161]
#13	D647	D673	Metal coordination, dimerization	[157, 159–161]
#14	K667	K693	Coordinate catalytic water molecule	[157, 159–161]
#15	D669	D695	Unknown	[157]
#16	E703	E728	Metal coordination	[157, 159–161]
#17	Q723	Q748	Metal coordination	[157, 159–161]
#18	G724	G749	Unknown	[160]

2.3.2.2 HD-GYP-domain proteins

HD-GYP-domain proteins degrade c-di-GMP into 5′-pGpG, but also catalyze the next chemical reaction that degrades 5′-pGpG into GMP [117–119]. This domain is rarer than EAL-domain proteins and not as well characterized [133, 163]. It belongs to a subset of the larger HD superfamily. Like GGDEF- and EAL-domains, the HD-GYP-domain is named after a conserved sequence motif (His-Asp-Gly-Tyr-Pro). Historically, the sequence model for the HD-GYP domain was not as refined as the GGDEF- and EAL-domains. As a consequence, it was poorly represented in domain databases, and it was more difficult to do systematic bioinformatic searches for HD-GYP-domain proteins. This was amended in a study by Galperin et al. [163], which refined the sequence model for HD-GYP-domains and create a new database over HD-GYP-domains. Furthermore, they also identified additional conserved residues in the HD-GYP-domain (Table 3).

Although less frequent than GGDEF- and EAL-domain proteins, HD-GYP domains are still widespread throughout the bacterial kingdom and many bacteria encode multiple HD-GYP-domain proteins [133, 163]. *V. cholerae* for example encodes 11 putative HD-GYP-domains [164]. Similar, to the GGDEF-domain, the HD-GYP-domains are often associated with and modulated by N-terminal sensory domains [133, 163]. Similar to EAL-domains, the HD-GYP-domain can also be associated with GGDEF-domains to form tandem GGDEF-HD-GYP proteins, but these are far less frequent than GGDEF-EAL proteins and only 7% of HD-GYP-domains form tandem proteins with GGDEF-domains [133].

Table 3. Conserved residues in HD-GYP-domains important for enzymatic activity

Conserved residues	PmGH	Residue role (interaction)	References
#1	Q185	Binds Me2 and Me3	[163]
#2	H189	Binds Me3	[163]
#3	H221	Binds Me3	[163]
#4	D222	Binds Me1 and Me2	[163]
#5	K225	Binds Me2	[163]
#6	K235	Main chain carbonyl oxygen binds N2 of c-di-GMP	[163]
#7	G237	Main chain carbonyl oxygen binds N1 of c-di-GMP	[163]
#8	H250	Binds Me1	[163]
#9	H276	Binds Me1	[163]
#10	H277	Binds Me1	[163]
#11	D278	Stabilizes the 18-aa loop between α4 and α5	[163]
#12	G284	Stabilizes the 18-aa loop between α4 and α5	[163]
#13	Y285	Binds nonbridging O of c-di-GMP ribose-phosphate ring	[163]
#14	P286	Stabilizes the 18-aa loop between α4 and α5	[163]
#15	D305	Binds Me3	[163]
#16	A309	Hydrophobic interaction with c-di-GMP guanine base Gua1	[163]
#17	L310	Hydrophobic interaction with c-di-GMP guanine base Gua1	[163]
#18	R314	Binds N7 and O6 of c-di-GMP guanine base Gua1	[163]
#19	K317	Binds O6 of c-di-GMP guanine base Gua1	[163]

2.3.3 GGDEF-EAL-domain proteins

DGCs and c-di-GMP-specific PDEs can exist together in GGDEF-EAL- or GGDEF-HD-GYP-domain proteins [133]. GGDEF-EAL are the most frequent and make up approximately 1/3 of GGDEF-domain proteins and 2/3 of EAL-domain proteins [133]. As a result, it is the second most frequent type of c-di-GMP-metabolizing protein, only exceeded by single GGDEF-domain proteins [133].

GGDEF-EAL proteins can be divided into three classes based on their enzymatic function. They can be bi-functional with the ability to both synthesize and hydrolyze c-di-GMP, mono-functional with the ability to either synthesize or hydrolyze c-di-GMP or have lost enzymatic activity in both domains. Initial biochemical studies indicated that GGDEF-EAL proteins were monofunctional and retained only one enzymatically competent domain [133, 143, 161, 165–167]. However, systematic bioinformatic studies have demonstrated that the majority of GGDEF-EAL proteins have conserved domains that are predicted to be enzymatically active [133].

As more GGDEF-EAL proteins have been characterized, several bi-functional c-di-GMP-metabolizing enzymes have been identified [136, 146, 147, 168–172]. However, most bi-functional GGDEF-EAL proteins seems to have a preference towards either synthesis or hydrolysis of c-di-GMP. The activity of the enzymes is often under strict post-translational regulation and specific signaling inputs are required to alter the enzymatic output. This ensures that the activity of the enzyme is fine-tuned to intra/extracellular signaling cues. Furthermore, it also prevents both domains from being active at the same, which could be detrimental to the bacteria due to excessive energy consumption.

MbaA from *V. cholerae* is a classic example of a bi-functional c-di-GMP-metabolizing enzyme [146, 147, 173]. This particular enzyme is regulated by polyamines *via* the polyamine sensor NspS. In its native state, MbaA functions as a PDE and inhibits biofilm formation. When high levels of the polyamine norspermidine is present, NspS binds norspermidine and interacts with MbaA, thereby, shifting the enzymatic activity of MbaA from hydrolysis to synthesis of c-di-GMP [146, 147, 173]. This preference towards either DGC- or PDE-activity under rigorous post-translational regulation is

most likely why bi-functional c-di-GMP-metabolizing enzymes were initially hard to identify.

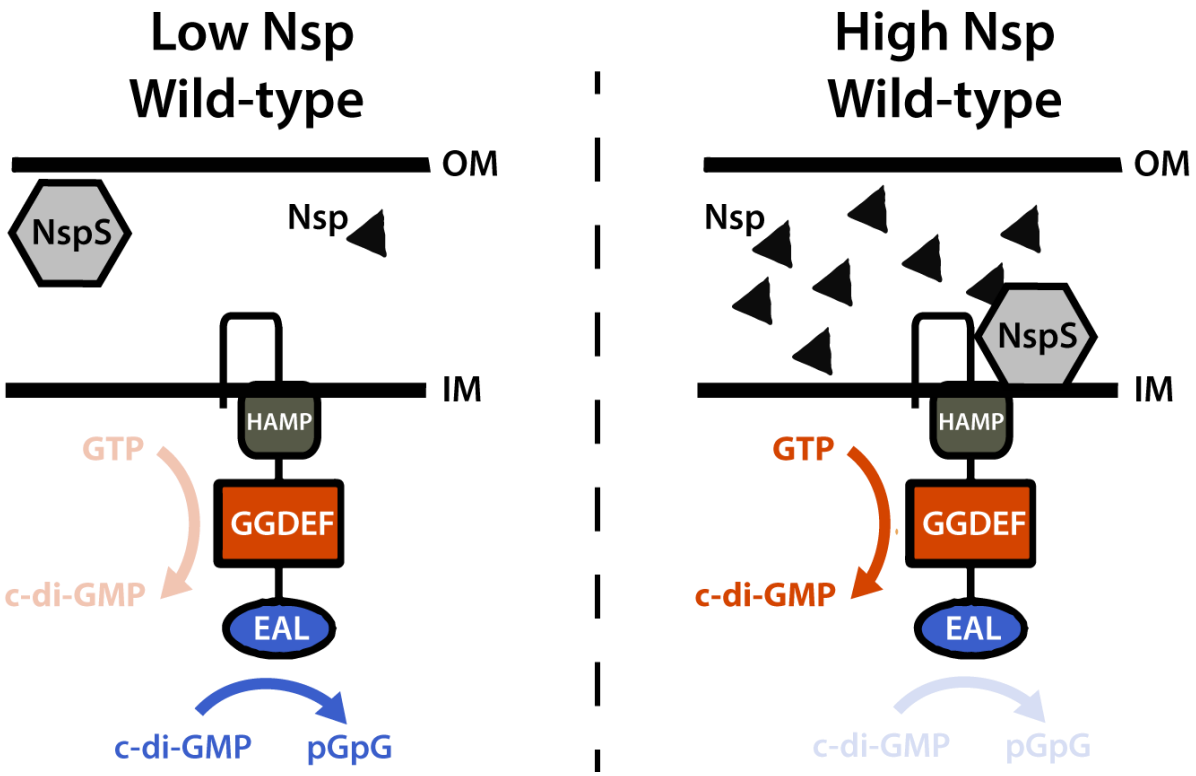

Figure 5 Regulatory model of MbaA
Model of wild-type MbaA and its response to low and high levels of norspermidine as proposed by Bridges et al [146]. During low levels of norspermidine, MbaA functions as a PDE and degrades c-di-GMP. When high levels of norspermidine is present, NspS binds norspermidine and interacts with MbaA and alters the enzymatic output from hydrolysis to synthesis of c-di-GMP. Adapted from Bridges et al. [146] with permission.

Mono-functional GGDEF-EAL proteins contain one conserved, enzymatically active domain and one inactive, degenerate domain. The non-active, degenerate domain has often evolved to become a sensory domain that modulates the activity of the remaining enzymatically competent domain [143, 161, 165–167, 174, 175]. In mono-functional GGDEF-EAL proteins, the GGDEF-domain is most frequently degenerated and partnered to an active EAL-domain [133]. In this case, the degenerate GGDEF-domain often retains the ability to bind GTP and modulate the activity of the EAL-domain upon GTP-binding [133, 143, 161, 165–167].

GGDEF-EAL proteins with two degenerate domains is the final and least frequent type [133]. These proteins possess two domains with abolished enzymatic activity. However, they typically retain the ability to bind c-di-GMP, either through the EAL-domain or an intact I-site in the GGDEF-domain. This allows them to move downstream in the c-di-GMP control module and evolve into c-di-GMP-effectors [117–119, 176, 177]. The perhaps most prominent example of this is LapD from *Pseudomonas fluorescens*, which has evolved into a c-di-GMP effector that regulates biofilm formation [177].

2.4 C-di-GMP effectors

C-di-GMP effectors convert the cellular levels of c-di-GMP into molecular outputs. Binding of c-di-GMP by effectors, alter the modulation of downstream cellular targets, which produce new molecular outputs. These effectors show much greater diversity in sequence, structure, and function than c-di-GMP-metabolizing enzymes [117–119, 139, 143, 178]. C-di-GMP effectors are made up of multiple protein classes and RNAs, making it more challenging to identify novel c-di-GMP effectors. The c-di-GMP effectors described so far include PilZ-domain containing receptors, degenerate GGDEF domain proteins, degenerate EAL/HD-GYP domain proteins, PDE-trigger enzymes, transcription factors and c-di-GMP binding riboswitches (Fig. 6)[117–119, 123, 138–141, 143, 178, 179]. These effector classes can modulate vastly different cellular targets allowing the same second messenger to control multiple diverging cellular outputs.

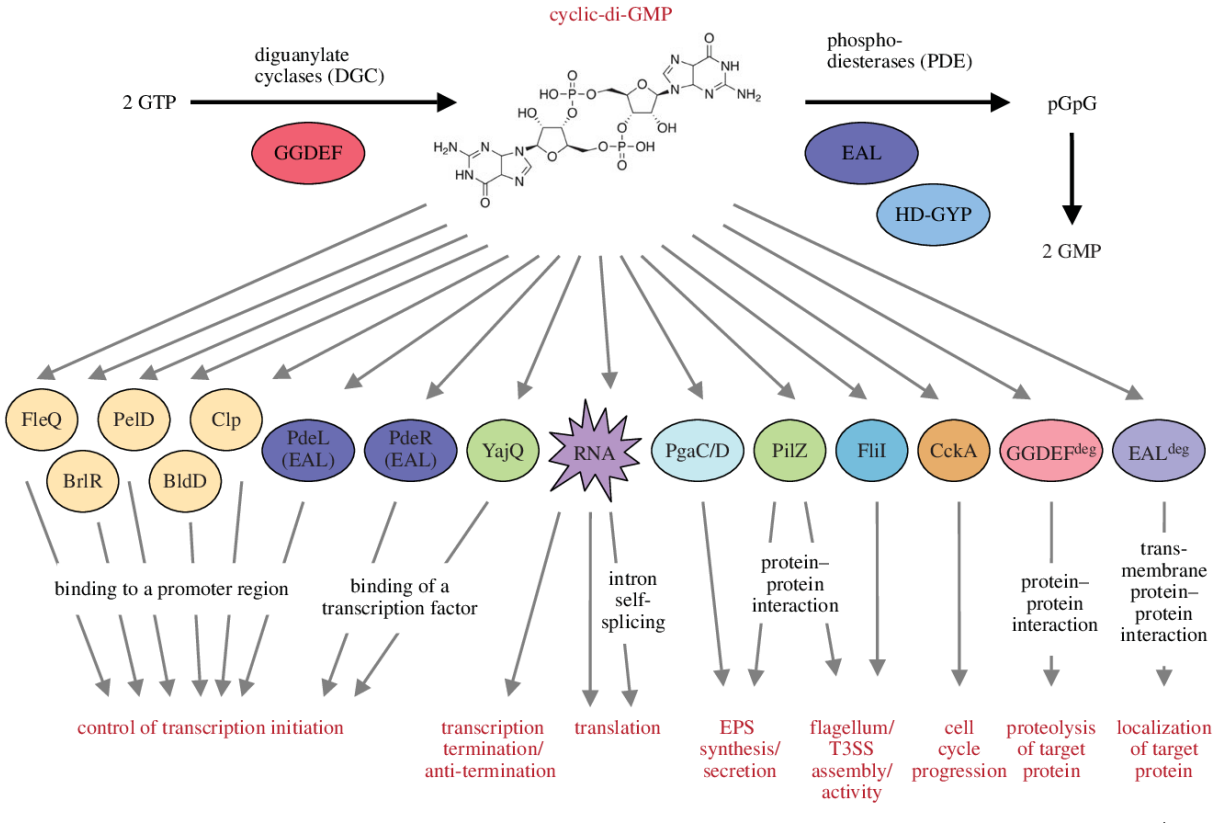

Figure 6 Overview of different c-di-GMP effectors
Diversity of discovered c-di-GMP-binding effector classes, function and target(s) that they regulate. Proteins are depicted as circles or ovals and colored according to class. RNAs are depicted as an irregularly shaped star. Adopted with permission from [178].

2.5 Regulation of motility and biofilm formation by c-di-GMP

C-di-GMP is recognized as a key regulator of the motile-to-sessile transition in bacteria. The current paradigm is that high levels of c-di-GMP leads to a sessile, biofilm-associated bacterial lifestyle, while low levels of c-di-GMP leads to a motile, planktonic lifestyle [118, 119, 123]. These two lifestyles are radically different and bacteria transitioning between them to undergo major phenotypic changes. The transition is a tightly regulated multistage process and c-di-GMP plays a key role throughout the process [119, 177, 180–184].

2.5.1 Motility

C-di-GMP is involved in regulating the assembly and function of the bacterial flagellum on multiple regulatory levels, including expression of flagellar genes, motor assembly and motor function [118, 119, 123, 185]. The bacterial flagellum is often assembled stepwise in a multistage process [186, 187]. First, the export machinery in the cytoplasmic membrane is assembled. Secondly, components that make up the basal body and hook is exported. Finally, large amounts of flagellin protein are secreted to form the filament. To ensure that the flagellum is assembled correctly, flagellar gene transcription occurs in a hierarchical order. As a result, flagellar components are transcribed depending on which phase of flagellar assembly they are involved in [187–192]. This transcriptional hierarchy is under the control of a transcriptional master regulator (FleQ/FlrA). Without this master regulator, no flagellar genes are expressed, resulting in a non-motile bacterium without flagellum [187–189, 192]. C-di-GMP has been shown to bind transcriptional regulators, including the master regulator of motility (FleQ/FlrA), to inhibit the expression of flagellar genes [193, 194]. In addition, c-di-GMP has been shown to bind and modulate the activity of flagella export AAA+ ATPases [195]. C-di-GMP can also affect the function of the flagellar motor. Binding of c-di-GMP by the effector protein YcgR triggers an interaction between YcgR and the flagellum, which functions as a molecular brake that reduces flagellar motor output [119, 196–200]. As a result, high levels of c-di-GMP reduce bacterial swim speed. Finally, the production of extracellular matrix can also impede motility by hindering flagellar rotation [193, 198]. Altogether, it is evident that c-di-GMP regulate motility through several distinct regulatory mechanisms.

2.5.2 Biofilm formation and dispersal

The biofilm life cycle is a multistep tightly regulated cycle, that can be divided into distinct phases: Aggregation and attachment, growth, accumulation and maturation, and disaggregation and detachment [184]. First, bacteria must attach to a surface or form aggregates. Currently, surface-associated biofilms are the best characterized model of biofilm formation. In this case, the bacterial cell must reach a surface, sense it and make temporary contact [180, 181, 183, 201–203]. Next, it must initiate permanent contact by decreasing motility and producing adhesins that anchors the bacterial cell to the newly discovered surface [177, 180]. Finally, the newly formed microcolony can start to produce extracellular matrix and develop into a mature biofilm [69, 184, 203]. Surface sensing triggers a rapid increase in c-di-GMP, which triggers bacterial surface adaptation. In this case, c-di-GMP mediate surface colonization through regulation of pili and flagella, promotion of adhesins/pili and production of extracellular matrix [69, 180–182, 201–206].

Once, adhered to a surface or aggregated together bacteria can form mature biofilms. This depends on the production and secretion of extracellular matrix components, which anchor the biofilm-embedded cells to each other and/or surfaces [69, 71, 184, 203]. One of the key components of bacterial biofilms are secreted exopolysaccharides. These are essential for the packing of cells in the biofilm and development of a 3D biofilm structure [69, 71, 203]. Different bacteria typically secrete different exopolysaccharides. For instance, cellulose, Pel polysaccharide and *Vibrio* polysaccharide (VPS) are examples of different exopolysaccharides commonly produced by *Escherichia coli*, *Pseudomonas aeruginosa* and *V. cholerae*, respectively [69, 207, 208]. Bacteria also secret matrix proteins that are important for the architecture and structural integrity of the biofilm [69, 71, 184, 203]. In addition to polysaccharides and matrix proteins, biofilms commonly consist of other components, such as nucleic acids, lipids, other small molecules and even outer membrane vesicles (OMVs) [71, 209]. Production and secretion of exopolysaccharides and biofilm matrix proteins are often under the regulation of c-di-GMP. In *V. cholerae* for instance, production and secretion of *Vibrio* polysaccharides and key matrix proteins are under the control of two central transcriptional regulators (VpsR and VpsT), which are both c-di-GMP responsive [69, 137, 210–216].

The end-stage of the biofilm life cycle is dispersal of biofilm-embedded cells, which can either be a passive process or an active cellular process [184, 217]. The passive process involves disruption of biofilms by external forces (e.g., fluid flow and predator grazing) and has been coined detachment [69, 203, 217]. In contrast, dispersion refers to an active process initiated by the biofilm-embedded bacteria themselves [69, 217, 218]. Biofilm dispersion can be triggered by various environmental or internal cues including polyamines, oxygen depletion, nutrition depletion, cell density and nitric oxide [69, 146, 217, 219–229]. Active biofilm dispersal often relies on the coordination of multiple parallel processes. These often include retraction/cleavage of pili/adhesins, downregulation of biofilm matrix production, production of matrix-degrading enzymes and increased motility [69, 217, 218]. Because both production of biofilm matrix and regulation of motility depends on c-di-GMP, this second messenger is crucial for proper regulation of biofilm dispersal. Therefore, many of the abovementioned triggers of biofilm dispersion do so by reducing c-di-GMP levels [69, 118, 137, 207, 217, 218, 230, 231]. Furthermore, induction of specific PDEs can also induce biofilm dispersal *in vitro* and *in vivo* [223, 232–234].

2.6 C-di-GMP signaling in *V. cholerae*

V. cholerae harbors a very complex c-di-GMP signaling system and encode >60 putative c-di-GMP-metabolizing enzymes (Fig. 7). Furthermore, the pathogen also possesses a variety of c-di-GMP effectors [137]. C-di-GMP plays a key role in the ability of *V. cholerae* to sense and adapt to changing environments throughout its life cycle. In addition to regulating biofilm formation and motility, the signaling molecule is also involved in the regulation of virulence, cell shape, DNA repair and tolerance to reactive oxygen species (ROS) and environmental persistence [69, 125–127, 137, 235–237].

In line with the current c-di-GMP paradigm, c-di-GMP represses motility and acute virulence, and stimulates biofilm formation in *V. cholerae* [137]. C-di-GMP represses motility by both inhibiting the synthesis and function of the flagellum, similar to what has been observed in other Gram-negative bacteria (e.g. *P. aeruginosa* and *E. coli*) [187, 192, 193, 236, 238]. Inhibition of virulence by c-di-GMP is mediated through a transcriptional mechanism, which inhibits the expression of virulence genes [127]. In support of this, specific PDEs are induced during infection and high levels of c-di-GMP hinders intestinal colonization by *V. cholerae in vivo* [23, 127, 137, 238–241]. Furthermore, in certain strains of *V. cholerae*, low levels of c-di-GMP activates the T6SS, which is believed to facilitate colonization through displacement of the intestinal microbiota [237, 242]. It must be mentioned that these observations are strain-specific and the link between c-di-GMP and virulence in El Tor strains are not as clear as for Classical biotype strains [137, 241, 243–245]. To muddy the waters even more, *V. cholerae* biofilms are hyper-infectious due to upregulation of virulence factors [80].

The second messenger stimulates biofilm formation through multiple mechanisms in *V. cholerae*, including attachment and production of matrix proteins and VPS. Initial attachment is initiated by the MshA pilus. C-di-GMP leads to increased production of MshA and also alters its function to facilitate surface attachment [201, 202]. Consequently, high levels of c-di-GMP increases surface attachment. In *V. cholerae*, biofilm matrix production is under transcriptional control of the two key transcriptional regulators VpsR and VpsT. Although, VpsR is the most important of the two, both regulators activate the expression of VPS biosynthesis genes and genes encoding

matrix proteins. Both VpsR and VpsT are c-di-GMP responsive and can bind c-di-GMP, which is believed to increase expression of biofilm-related genes [23, 69, 137, 210–216]. Interestingly, the c-di-GMP-VpsR/VpsT regulatory axis is not limited to solely biofilm formation and motility, but also regulate multiple other cellular processes, including DNA repair, cell shape and ROS tolerance [125, 126, 235].

Altogether, it is evident that the c-di-GMP signaling system is an important regulator of bacterial behavior in *V. cholerae* and is implicated in multiple stages of its life cycle. Although we lack a granular overview of the c-di-GMP equilibrium throughout the life cycle of *V. cholerae*, it seems to fluctuate throughout the pathogen's life cycle based on environmental cues [23, 137]. Based on the current body of knowledge, high levels of c-di-GMP and biofilm formation seems to be favorable in the aquatic environment [23, 66]. This seemingly also aids in the passage through the stomach after pathogen uptake as *V. cholerae* biofilms better tolerate the acidic environment of the stomach [87]. Moreover, *V. cholerae* biofilms are hyper-infectious compared to planktonic *V. cholerae* [80, 81]. During the intestinal phase, low levels of c-di-GMP are favored as this ensure increased motility and virulence, allowing *V. cholerae* to penetrate the mucus layer, colonize the intestine and produce cholera toxin [1, 23, 96, 127, 137, 187, 212, 236, 238, 240, 241]. Finally, during host exit, *V. cholerae* seemingly increase levels of c-di-GMP again to prepare for re-entry into the aquatic environment [23, 66, 114, 116].

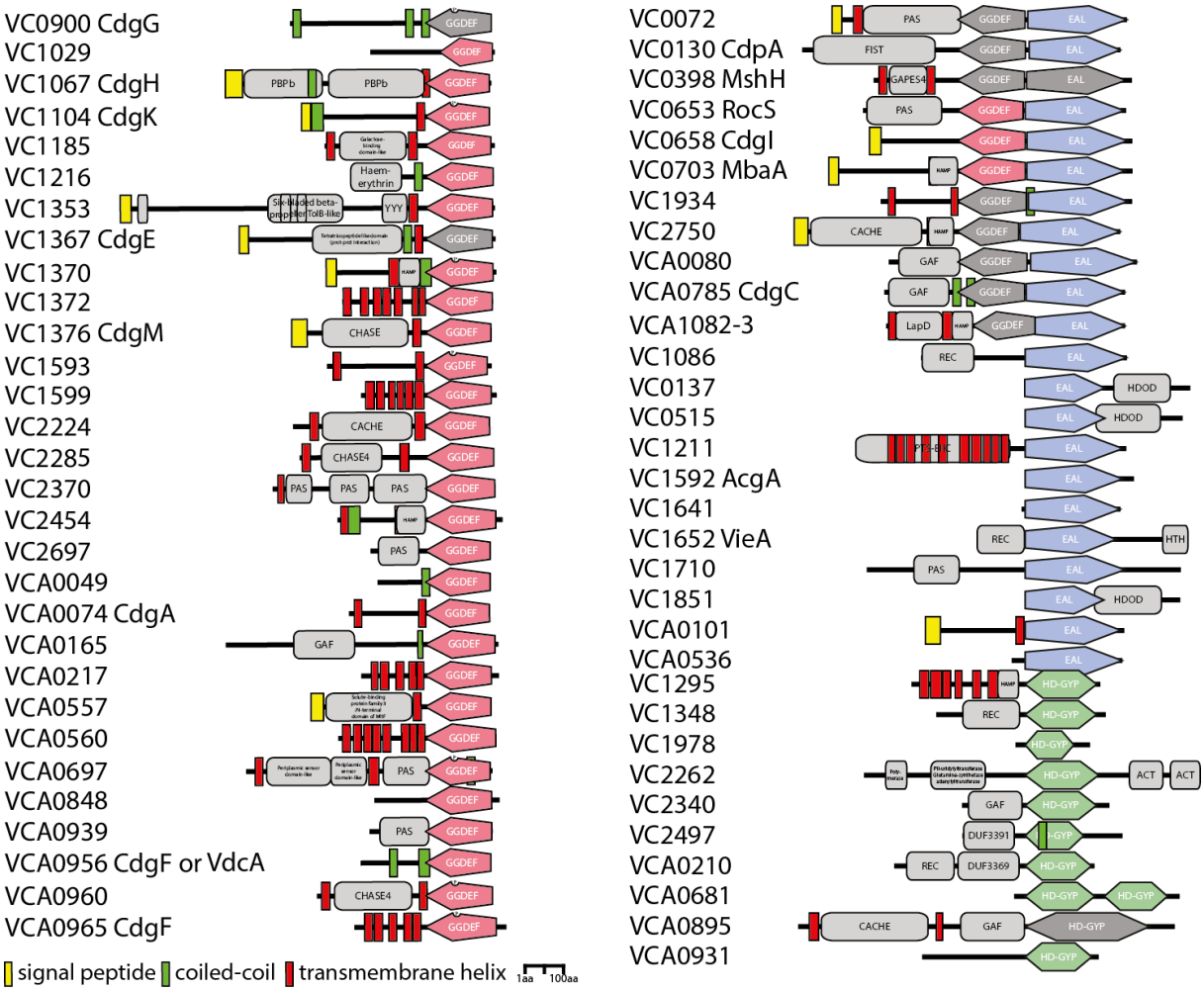

Figure 7 The genome of *V. cholerae* encodes 62 putative c-di-GMP-metabolizing proteins.

Schematic representation of the predicted domain structure of putative c-di-GMP metabolizing enzymes from *V. cholerae*. Names of genes encoding for the putative c-di-GMP metabolizing enzymes are indicated on the left of the protein schematics. Systematics names from the *V. cholerae* strain N16961 are always given; four letter protein names are given if proteins have been characterized previously. GGDEF domains are depicted as red pentagons, EAL domains are depicted as blue pentagons and HD-GYP domains are depicted as green hexagons. GGDEF, EAL or HD-GYP domains depicted in dark grey are predicted to be devoid of enzymatic activity based on the absence of catalytically essential residues. Other predicted domains, mainly putative signal input domains, are depicted by light grey rounded squares and named in the figure. Predicted signal peptides (yellow bars), coiled-coil protein-protein interaction domains (green bars), and transmembrane domains (red bars) are indicated.

2.6.1 Integration of quorum sensing and c-di-GMP signaling in *V. cholerae*

Quorum sensing (QS) is a cell-to-cell communication system that coordinate and regulate collective behavior in bacteria [246]. It relies on the production and detection of extracellular signaling molecules named autoinducers (AIs). QS allows bacterial populations to alter their behavior based on the density and composition of the population. Because of this, QS regulates several bacterial processes that rely on multicellular behavior, including biofilm formation, bioluminescence and virulence [226, 231, 246].

V. cholerae possess a complex QS signaling system and produce and detect multiple autoinducers [231, 246]. QS regulates many traits in *V. cholerae*, including biofilm formation, and it is one of the key regulators of biofilm formation along with c-di-GMP. Interestingly, QS regulates biofilm formation through multiple avenues. For instance, it directly regulates the expression of VPS and biofilm matrix proteins [69, 203, 226, 231, 247–250]. At low cell-density (LCD), levels of AIs are low and *V. cholerae* exhibit an individual behavior. Low levels of AIs induce phosphorylation of the response regulator LuxO, which in turn simultaneously represses HapR and activates AphA. Since HapR inhibits expression of VPS and biofilm matrix proteins, repression of HapR induces biofilm formation. In contrast, high cell-density (HCD) leads to dephosphorylation of LuxO, which results in repression of AphA and production of HapR, which inhibits biofilm formation [69, 203, 226, 231, 247–250]. Additionally, QS regulates the expression and activity of multiple c-di-GMP-metabolizing enzymes, thereby regulating the intracellular level of c-di-GMP [69, 203, 226, 231, 247–250]. Simplified, QS in general inhibits biofilm formation, although formation of certain biofilm aggregates depends on QS [226, 231, 251–253]. Therefore, QS-deficient *V. cholerae* strains locked into low-cell–density (LCD) forms more biofilm than strains locked into high-cell–density (HCD) [87, 247].

3 The biofilm lifestyle affects the evolution of bacteria

3.1 Biofilm formation increases the resilience of bacteria

Biofilm formation is a widespread survival strategy that facilitate the survival and persistence of bacteria under challenging conditions [71, 254]. Because of this, biofilms are common in aquatic and terrestrial environments (e.g. *V. cholerae* form biofilms on chitinous surface) and also occur in the human body [71, 254, 255]. Biofilms can be defined as bacterial aggregates covered in a self-produced extracellular matrix, which either adhere to each other and/or to surfaces [71, 184]. The biofilm matrix functions as a protective layer for the bacteria and fill in the space between the individual biofilm-embedded bacterial cells. It consists of multiple components, including extracellular polymeric substances (EPS), matrix proteins, and extracellular DNA (eDNA). EPS is often the most abundant and most important component of biofilms since they are crucial for the formation and maturation of the biofilm architecture [71, 203].

One of the hallmarks of biofilms is increased resilience against external stressor [23, 71, 254]. This includes threats often encountered in aquatic and terrestrial environments (e.g. predation, osmotic stress, and salinity and temperature shifts) as mentioned in section 1 [23, 71]. Worryingly, biofilm formation also increases resilience towards antimicrobials though multiple different mechanisms [71, 254]. Firstly, the biofilm matrix itself can function as a fortress that impairs the diffusion of certain antimicrobial drugs, thereby reducing the amount of antimicrobial drug that the biofilm-embedded cells are exposed to [71, 254]. Secondly, the biofilm lifestyle can affect the metabolic activity of the biofilm-embedded cells and increase the number of dormant cells or cells with low metabolic activity [71, 256]. This in turn can promote tolerance, a phenomenon where bacteria temporarily survive lethal concentrations of antimicrobials [254, 256–258]. Finally, biofilm formation can also promote AMR, which is permanent, in contrast to tolerance [256]. Increased AMR in biofilm is the result of a complex interplay between several phenomena that can occur in biofilms, including tolerance as a steppingstone to resistance, increased mutation rate, specific selective niches within the biofilm (further discussed in section 3.2) and increased frequency of HGT [35, 254, 258]. Because of the protective effects of the biofilm matrix and inherent properties of biofilm-embedded bacteria cells, biofilm-associated infections are often

more difficult to treat and often require higher doses of antimicrobials and prolonged treatment [259]. Therefore, biofilms can be troublesome in the setting of clinical infections as they can both promote tolerance and resistance development and increase the risk of treatment failure [254, 255, 259].

Biofilm formation is central to the life cycle of *V. cholerae*. The pathogen is an adept biofilm producer and form biofilms both in its aquatic environment and the human host. Because of this, *V. cholerae* is a commonly used model organism for biofilm research [23, 66, 69]. The main component of *V. cholerae* biofilms is VPS, which make up roughly 50% percent of the biofilm matrix [203, 260, 261]. The genes involved in the synthesis of VPS are located in two operons (*vps*-1 and *vps*-2) and deletions of these genes impair biofilm formation significantly [203, 261]. In addition to VPS, *V. cholerae* produce the matrix proteins RbmA, RbmC and Bap1, which are essential for the structural integrity and maturation of *V. cholerae* biofilms [203, 262, 263]. Current available evidence suggests that RbmA is involved in cell-cell adhesion, Bap1 facilitate surface adhesion and pellicle strength, while RbmC accumulate around cell clusters together with Bap1 in mature biofilms [203, 262, 263]. Other matrix components include the MSHA pili [264, 265], which is abundant throughout *V. cholerae* biofilms as well as eDNA and outer membrane vesicles (OMVs) [69, 203]. To summarize, a mature *V. cholerae* biofilm consists of organized cluster of *V. cholerae* cells, encapsulated in VPS, matrix proteins (RbmA, Bap1 and RbmC), eDNA and OMVs [69, 203].

While *V. cholerae* commonly form smooth colonies when growing on culture plates, certain *V. cholerae* strains can assume a rugose phenotype due to phase variation [74, 76, 77]. This variant exhibits a hyper-biofilm phenotype and form hyper-wrinkly colonies and biofilm pellicles. Furthermore, it exhibits increased biofilm formation compared to smooth variants [75, 76]. The rugose variation depends on the expression of VPS and biofilm matrix proteins [75–77, 266]. In line with the current biofilm paradigm, rugosity is believed to be an environmental adaptive strategy employed by *V. cholerae* to facilitate environmental persistence and survival. Indeed, rugose *V. cholerae* showcase multiple traits consistent with increased tolerance to environmental stress, including increased resilience against oxidative and osmotic stress, predation and bacteriophages [75–77, 266]. Many of these traits have been directly linked to the

increased biofilm forming capacity of the rugose variant, underlining how biofilm formation facilitates adaptation and survival in challenging environments.

3.2 Microbial evolution in biofilms

The matrix-imposed spatial structure of biofilms, can create a heterogenous environment and induce establishment of gradients throughout the biofilm (e.g. nutrients, oxygen, pH, antimicrobials, *etc*.) [71]. This leads to the development of distinct microenvironments within the biofilm [71]. Furthermore, the spatial structure of the biofilm results in different levels of interactions between the biofilm-embedded cells, where neighboring cells will interact closely, and cells further apart to a lesser degree. Consequently, it can foster various social interactions, including both cooperation, cheating and competition that can vary throughout the biofilm [71]. Combined, this produces several distinct ecological niches within the biofilm that bacteria can exploit and adapt towards [71, 267]. This is in stark contrast to homogenous planktonic cultures where the entire bacterial population compete against each other. Because of this, living in biofilms can open up new evolutionary trajectories not commonly available to planktonic bacteria [267].

Experimental evolution is a commonly used laboratory-based method to study the evolution of various living organisms [268, 269]. It can be defined as the study of evolutionary processes occurring in experimental populations in response to specific selective conditions [268, 269]. This makes it possible to explore evolutionary dynamics and observe natural selection in real time. The short generation time of microbes makes them ideal for experimental evolution as you can quickly evolve populations for hundreds of generations. Researchers have successfully employed experimental evolution to study a multitude of different topics (e.g. antimicrobial resistance development, adaptation to new environments, multicellularity, biofilm adaptation and metabolic adaptation) [267–269]. The most prominent example is perhaps the long-term evolution experiment (LTEE) initiated by Richard Lenski, which have evolved populations of *E. coli* for >80 000 generations [270–273]. Coupled with next-generation sequencing, experimental evolution can also be employed as a powerful screening method to identify adaptive mutations in genes linked to functions of interest (e.g. antibiotic resistance, biofilm formation and motility) [274]. Although not suited to systematic screen entire genomes, this method can also be leveraged to link genotypes to phenotype without the same bias towards gene disruption that some commonly used screening methods have [275].

Traditionally, experimental evolution of bacteria was based on propagation of liquid culture (an unstructured environment) [268, 269]. In the 1990s, a few seminal papers demonstrated how spatial structures and heterogenous environments strongly affected the evolution of bacteria and led to development of novel phenotypes and greater phenotypic diversity compared to unstructured environments [276, 277]. In the last two decades, this work has been expanded greatly as researchers started to serially propagate different types of biofilms [256, 267, 278]. This has facilitated the study of how bacteria evolve within biofilms and led to the development of multiple biofilm evolution models with varying levels of complexity (Table 4) [256, 267, 278]. These models follow the same principles: Inoculate cultures with planktonic bacteria, allow biofilms to form, transfer or harvest biofilms and use biofilm-derived bacterial cells to seed a new biofilm [256, 267]. The perhaps most important distinctions between different biofilm evolution models are the type of biofilms grown (e.g., surface-attached, floccule, and pellicle), presence/absence of flow, dynamic *versus* static systems and type of growth medium. The simplest models are based on static cultured with rich medium, while more complex models are dynamic, incorporate flow and use growth medium that mimics *in vivo* conditions. Finally, real *in vivo*- or patient-derived biofilms can also be employed to study the evolutionary processes in biofilms [256, 267].

Table 4. *In vitro* biofilm models

Model	Description	References
Static microcosm	Static cultures where a biofilm pellicle is allowed to form at the air-liquid interface. The biofilm pellicle can be harvested and subsequently used to seed a new biofilm pellicle.	[276]
Bead-based model	Biofilms are formed on glass or plastic beads in test tubes under shaking. The shaking generates flow stress that can affect the biofilm growing on the beads. Upon transfer, beads with biofilms are transferred to a new culture with a new bead. The bacteria must then disperse from the old bead and colonize the new bead to be propagated.	[279]
Colonies on solid agar plates	Bacterial cultures are spotted onto solid agar plates or on filters placed upon solid agar plates	[277]
Non-shaking microtiter plate	Biofilms are grown in static culture in microtiter plates and allowed to form biofilms at the bottom of the plate	[280, 281]
Peg-based models	Biofilm are grown in special 96-well microtiter plates with a special lid with pegs. The pegs are submerged into the growth medium so that biofilms can form at the pegs. The pegs can then be transferred to fresh medium. Alternatively, peg-based biofilms can also be harvested and used to inoculate a new culture with a new peg.	[282]
Flow models	Biofilms grown under flow conditions, which ensures that nutrients can be continuously provided, and waste products removed.	[283]

When experimentally evolved in *in vitro* biofilms, many bacterial species (e.g. *P. aeruginosa*, *K. pneumoniae*, *Burkholderia cenocepacia*) undergo adaptive changes and acquire novel traits not commonly acquired during planktonic growth [256, 267, 279, 284–288]. A commonly acquired trait in these studies is a hyper-biofilm phenotype with altered c-di-GMP signaling. Interestingly, the same tendency has been observed during *in vivo* evolution and within-patient evolution [129–131, 289, 290]. Prior studies have also used biofilm models to understand how biofilm-embedded cells evolve towards specific phenotypes (e.g., antimicrobial resistance) relative to planktonic bacteria. This has revealed that planktonic and biofilm-embedded bacteria can follow distinct evolutionary trajectories, although this not always the case [256, 291–295]. Consequently, living in biofilms can have broader evolutionary implications and affect other important traits in addition to biofilm adaptation.

Mutations in the c-di-GMP signaling system that drive biofilm adaptation can occur in the entire c-di-GMP control module. This includes sensory domains regulating c-di-GMP-metabolizing enzymes, enzymatic domains of c-di-GMP-metabolizing enzymes and c-di-GMP effectors [279, 284–288]. In several of these studies, c-di-GMP measurements have demonstrated elevated levels of c-di-GMP in evolved clones [129–131, 289, 290]. Therefore, in line with the current c-di-GMP paradigm, acquired mutations in the c-di-GMP signaling system seems to increase biofilm formation *via* mutations that increase c-di-GMP levels. So far, these mutations are poorly studied on a molecular level and the underlying molecular mechanisms that alter the activity of specific c-di-GMP-metabolizing enzymes remains elusive. Future studies focusing on how these mutations alter the activity of c-di-GMP-metabolizing enzymes are needed. In general, the c-di-GMP signaling system seems to be a potent evolutionary target to facilitate biofilm adaptation in bacteria.

Even though *V. cholerae* is a model organism to study biofilm formation, no one has experimentally evolved *V. cholerae* biofilms yet. *V. cholerae* can rapidly attain a hyper-biofilm phenotype (rugose phase variation) during specific conditions [76, 77, 296]. Furthermore, *V. cholerae* has a complex c-di-GMP signaling system and specific mutations in it can induce increase biofilm formation [77]. Therefore, *V. cholerae* should be a suitable model organism to study biofilm adaptation during experimental

evolution. This could shed new light on the regulatory mechanisms governing biofilm formation and how the biofilm lifestyle affects the evolution of *V. cholerae*.

3.3 Antimicrobial resistance determinants can inhibit biofilm formation

Many MGEs and enzymes (e.g., β-lactamases) can induce pleiotropic effects in the bacteria harboring them, such as reduced growth rate, altered biofilm forming capacity or collateral responses to antimicrobials [297–299]. Strikingly, some studies have already demonstrated that certain plasmid-borne β-lactamases inhibit biofilm formation [300, 301]. In addition, certain plasmids have also been demonstrated to influence biofilm formation, although many plasmids have a neutral effect on biofilm formation as well [300–306]. Since evolution in biofilm can alter the evolutionary path of bacteria, it seems plausible that biofilm growth could affect the evolution of specific MGEs and enzymes, especially if they influence biofilm forming capacity to begin with. In support of this, pioneering studies have already demonstrated that plasmids can evolve differently in biofilms compared to planktonic cultures [307, 308]. However, it remains to be seen how generalizable this effect is and if this is limited to certain classes of MGEs (e.g., solely plasmids).

A limited number of studies have investigated how the biofilm growth mode affects the evolution of AMR determinants [256]. Many pathogens associated with AMR and opportunistic nosocomial infections (e.g., *K. pneumoniae*, *Serratia marcescens complex* and *P. aeruginosa*) colonize either humans or hospital environments [309–312]. Since biofilm formation is known to facilitate colonization and survival in inhospitable environments, this seems like a more relevant lifestyle than unstructured planktonic cultures, to study the evolution of AMR determinants. Indeed, a previous biofilm evolution study in *K. pneumoniae* demonstrated mutational overlap between clinical outbreak isolates and isolates evolved in an *in vitro* biofilm model [288]. Therefore, evolving AMR determinants within biofilms could help us better understand how these enzymes evolve and spread. Even though *V. cholerae* is not a nosocomial pathogen, it is an environmental pathogen of global significance [1]. Furthermore, *V. cholerae* harbor multiple MGEs that are suitable for studying how clinically relevant MGEs evolve in biofilms (e.g. SXT-element and MDR IncC plasmids from cholera outbreaks in Yemen and Zimbabwe) [7, 8, 33].

4 Aims

This PhD thesis aimed to fill multiple knowledge gaps in the biology of *V. cholerae*. First, we aimed to assemble an improved version of the current reference genome for *V. cholerae* C6706. Next, we wanted to leverage this strain and the accompanying reference genome to study how living in biofilms affect the evolution of *V. cholerae*.

The following research aims were pursued:

- Project 1: Genetic and phenotypic comparison of *V. cholerae* C6706 and N16961.
    1. Establish a reference genome for the *V. cholerae* model strain (*V. cholerae* C6706) and compare its genome with the current reference genome from *V. cholerae* strain N16961.
    2. Conduct a phenotypic comparison between *V. cholerae* C6706 and N16961.

- Project 2: Experimental evolution of *V. cholerae* C6706 biofilms.
    1. Experimentally evolve *V. cholerae* C6706 biofilms.
    2. Characterize genetic and phenotypic changes that arise in *V. cholerae* C6706 during evolution in biofilms.

- Project 3: Evolution of β-lactamases in biofilms.
    1. Characterize how the expression of β-lactamases affects biofilm formation in *V. cholerae*.
    2. Investigate how selection for biofilm formation affects the evolution of β-lactamases.

5 Summary of papers

5.1 Paper I (Manuscript, accepted in Microbiology)

“A comparative genomic and phenotypic study of *vibrio cholerae* model strains using hybrid sequencing”

Øyvind M. Lorentzen, Christina Bleis and Sören Abel.

In this work, we employ hybrid sequencing technology to assemble and annotate a closed genome of *V. cholerae* C6706. To improve upon the previous version of the genome we employed hybrid sequencing, manually curated the genome annotation, and linked every open reading frame (ORF) to the corresponding ORF in the reference strain *V. cholerae* N16961 [28, 313]. This genome was then employed to conduct a genetic comparison of *V. cholerae* C6706 with N16961. This revealed a total of 76 mutations in *V. cholerae* C6706. In addition, *V. cholerae* C6706 also contained the WASA-1 prophage, which is specific to the West African–South American (WASA) clade of *V. cholerae* isolates, a different variant of VSP-2 and an inversion in chromosome 1 [18, 314, 315]. Interestingly, several of the identified mutations in *V. cholerae* C6706 were located in genes previously linked to important biological functions such as biofilm formation, motility, quorum sensing, genome stability and repair and acid tolerance.

To understand if these mutations led to phenotypic differences in *V. cholerae* C6706, we conducted a selection of assays to quantify phenotypes relevant to the life cycle of *V. cholerae*. This included mutation rate, acid tolerance, biofilm formation and motility. Quantification of mutation rate demonstrated that *V. cholerae* C6706 have an increased mutation rate, possibly related to a point mutation in RecA. No differences in acid tolerance were observed. The most strikingly differences between the two strains were the differences in biofilm formation and motility. To account for a point mutation in LuxO in our stock of *V. cholerae* C6706, which locked it in LCD, we also included a strain of *V. cholerae* C6706 with wild-type LuxO. Depending on the quorum sensing state, *V. cholerae* C6706 had either decreased or increased biofilm formation compared to N16961. Specifically, QS-deficient C6706 had a 53% increase in biofilm formation, while QS-proficient C6706 had a 17% decrease in biofilm formation compared to N16961. *V. cholerae* N16961 demonstrated increased motility compared

to C6706 regardless of QS-state and had a 13% and 30% increase in motility compared to QS-deficient and QS-proficient C6706, respectively. Thus, demonstrating that QS inhibits both biofilm formation and motility.

The difference in biofilm formation and motility between QS-deficient *V. cholerae* C6706 and N16961, which is also QS-deficient, indicated that QS was not the sole cause of the observed phenotypic differences. Indeed, *V. cholerae* C6706 contains multiple mutations in its c-di-GMP signaling system, including a frameshift mutation in an active c-di-GMP-degrading enzyme (VC1295). Further investigations demonstrated that VC1295 was expressed in *V. cholerae* and restoration of VC1295 in *V. cholerae* C6706 reversed the previously observed differences in biofilm formation and motility. Thus, indicating that the combined effects of altered QS and c-di-GMP signaling lead to differences in biofilm formation and motility between *V. cholerae* C6706 and N16961.

5.2 Paper II (Manuscript, not published)

“Biofilm adaptation selects for mutations in the bifunctional enzyme MbaA leading to constitutive synthesis of c-di-GMP

Øyvind M. Lorentzen, Sören Abel, Pål J. Johnsen and Christopher Frøhlich.

To better understand how biofilm evolution affects the regulatory systems governing biofilm formation in *V. cholerae*, we serially passaged populations of *V. cholerae* C6706 as either planktonic cultures (*n* = 2) or biofilm pellicles (*n* = 6). This demonstrated that serial passage of biofilm pellicles readily selected for a hyper-biofilm phenotype. Strikingly, all of the biofilm-evolved populations accumulated mutations in the polyamine-regulated c-di-GMP-metabolizing enzyme MbaA. We uncovered a total of 10 mutations in MbaA with a frequency ranging from 1.1% – 82.8%, including mutations in both the HAMP- (R316W), GGDEF- (E483K) and EAL-domain (E576K, L618V, S620P, T648A).

Assessment of biofilm formation in selected single mutants (E483K, E576K, L618V) recapitulated the observed hyper-biofilm phenotype. *In vivo* mutagenesis studies demonstrated that removal of MbaA or the EAL-domain failed to reproduce the hyper-biofilm phenotype. In addition, mutating the active site of the GGDEF-domain in a hyper-biofilm variant (G425A/E576K) also led to loss of the phenotype. Therefore, the hyper-biofilm phenotype seemed to depend on the function of the GGDEF-domain.

In vitro enzyme kinetics demonstrated that specific mutations in both the GGDEF- (E483K and EAL-domain (E576K, L618V) of MbaA increased the DGC-activity of the GGDEF-domain, while simultaneously reducing the PDE-activity of the EAL-domain. Finally, the selected mutations (E483K, E576K, L618V) also decoupled MbaA from polyamine-mediated post-translational regulation by NspS. Summarized, *in vivo* mutagenesis and *in vitro* enzyme kinetics suggests that the selected mutations (E483K, E576K, L618V) convert the enzymatic activity of MbaA from degradation to constitutive synthesis of c-di-GMP.

5.3 Paper III

“The biofilm lifestyle shapes the evolution of β-lactamases”

Øyvind M Lorentzen, Anne Sofie B Haukefer, Pål J Johnsen, Christopher Frøhlich. *Genome Biology and Evolution*, Volume 16, Issue 3, March 2024, evae030, https://doi.org/10.1093/gbe/evae030

In this paper, we investigated how β-lactamases affect biofilm formation and how selection for biofilm formation affects the evolution of β-lactamases in *V. cholerae.* Firstly, we examined how the expression of a broad panel of β-lactamases spanning all Ambler classes affected biofilm formation in *V. cholerae*. This demonstrated that the majority of β-lactamases mediated a strong inhibitory effect on biofilm formation ranging from 43% to 61%.

Next, we used directed evolution to create a mutational library of KPC-2, one of the β-lactamases with the biggest inhibitory effect, and transformed it into *V. cholerae*. Expression of the gene library in *V. cholerae* significantly improved biofilm formation compared to wild-type KPC-2, indicating that the library contained mutants with compensated biofilm inhibition. To identify variants with compensated biofilm inhibition, we harvested biofilm pellicles formed by *V. cholerae* expressing the KPC-2 mutant library (n = 2) and isolated 12 random clones. Sanger sequencing revealed that 33% of the selected clones contained mutations within KPC-2 at position 136 (N136K or Δ1-48/N136D/M152I/L167P).

Quantification of biofilm formation demonstrated that N136K and Δ1-48/N136D/M152I/L167P exhibited a 68% and 107% increase in biofilm formation compared to ancestral KPC-2. Thus, demonstrating that evolution in biofilms can shape the evolution of β-lactamases. Reconstruction of single mutants (N136D, L167P and Δ1-48) demonstrated that Δ1-48 was not able to compensate biofilm formation alone. In contrast, N136D and L167P increased biofilm formation significantly, suggesting that biofilm compensation relates to functional effects in KPC-2. In general, there was as trend between increased biofilm formation and lower ampicillin resistance. However, the L167P mutant maintained ampicillin susceptibility similar to

wild-type KPC-2, while compensating for biofilm formation. Thus, demonstrating that biofilm compensation can occur without compromising antimicrobial resistance.

Finally, to better understand whether the enzymatic activity of wild-type KPC-2 and evolved variants was linked to biofilm formation, we introduced S70A in wild-type KPC-2, N136K and Δ1-48/N136D/M152I/L167P variants. This creates variants that are unable to covalently bind and hydrolyze β-lactams. Introduction of S70A in wild-type KPC-2 and the Δ1-48/N136D/M152I/L167P variant caused a 45% and 73% reduction in biofilm formation, respectively. In contrast, S70A/N136K displayed only a slight reduction in biofilm formation compared to the evolved N136K variant. The exact molecular mechanisms of biofilm antagonization and compensation remain elusive. Based on our data, we hypothesize that the evolved variants compensate for biofilm inhibition either independently of enzymatic activity (N136K) or by employing its enzymatic activity (Δ1-48/N136D/M152I/L167P).

6 Methodological consideration

6.1 *Vibrio cholerae C6706* as a model strain

Since this thesis focus on the evolution of *V. cholerae* in biofilms, we naturally employed *V. cholerae* as a model strain. The chosen strain was *V. cholerae* C6706, a clinical isolate from the 1st wave of the 7th cholera pandemic, which was isolated in Peru in 1991. This particular strain is one of the clinical strains of *V. cholerae* most frequently used in research [29]. In **paper 1**, we whole-genome sequenced our laboratory stock of *V. cholerae* C6706 and compared it genetically and phenotypically to the current genetic reference strain *V. cholerae* N16961 [28]. This revealed that our frozen stock of *V. cholerae* C6706 contained a previously described point mutation in *LuxO*, which impairs quorum sensing (QS-deficient) and locks it in a low-density cell state [316]. Since, biofilm formation and motility are affected by quorum sensing state, we also included a QS-proficient version of *V. cholerae* C6706 in **paper** 1.

In **paper 2**, we wanted to serially propagate *V. cholerae* biofilm pellicles. To ensure that we could grow robust biofilms with dense bacterial populations (to ensure adequate mutational supply during biofilm evolution), which could easily be propagated, we wanted to work with a *V. cholerae* strain with a high baseline level of biofilm formation. At the start of working on **paper 2**, there was no publicly available genomes of *V. cholerae* C6706. Therefore, we used our strain of *V. cholerae* C6706, which we had recently sequenced for internal use, which also formed robust biofilms.

6.2 Biofilm evolution method

In this thesis, we employed a biofilm pellicle-based propagation regime to evolve *V. cholerae* biofilms. There are multiple established methods to evolve biofilms, but none have been used with *V. cholerae* before [267]. Our chosen strain of *V. cholerae* (C6706) forms smooth biofilm pellicles at the air-liquid interface of static cultures. Evolution of biofilm pellicles was conducted by growing *V. choler*ae C6706 in static cultures at 30 ℃ for 24 hours until biofilm pellicles formed. These biofilm pellicles were then harvested, dissolved in PBS, vortexed to disintegrate the biofilms, filtered to remove biofilm aggregates and used to inoculate a new static culture.

This method was chosen due to the ease of biofilm propagation compared to other biofilm evolution models (e.g., bead- or peg-based models) and the possibility to visually inspect the biofilm pellicle phenotype during evolution. The downside of this evolution method is the difficulty to accurately calculate generation time. Although this is not so easily determined in other biofilm evolution models either, as the initial founding population of the biofilms are unknown. Because of this, we used the number of biofilm transfers to describe the duration of the experiment.

During transfer of the biofilm populations, the PBS-suspension with harvested biofilm populations was filtered through a 5 µm filter to remove larger biofilm clumps. This was done to ensure that the transferred bacterial populations had to reproduce as much of the biofilm matrix as possible after each transfer. However, how the filtration step affects the selective conditions of the experiment remains unknown. It is possible that the filtration step creates an upper limit to biofilm-forming capacity due to the removal of bacterial cells with a highly aggregative phenotype. This could potentially also reduce the overall diversity of the biofilm-evolved populations.

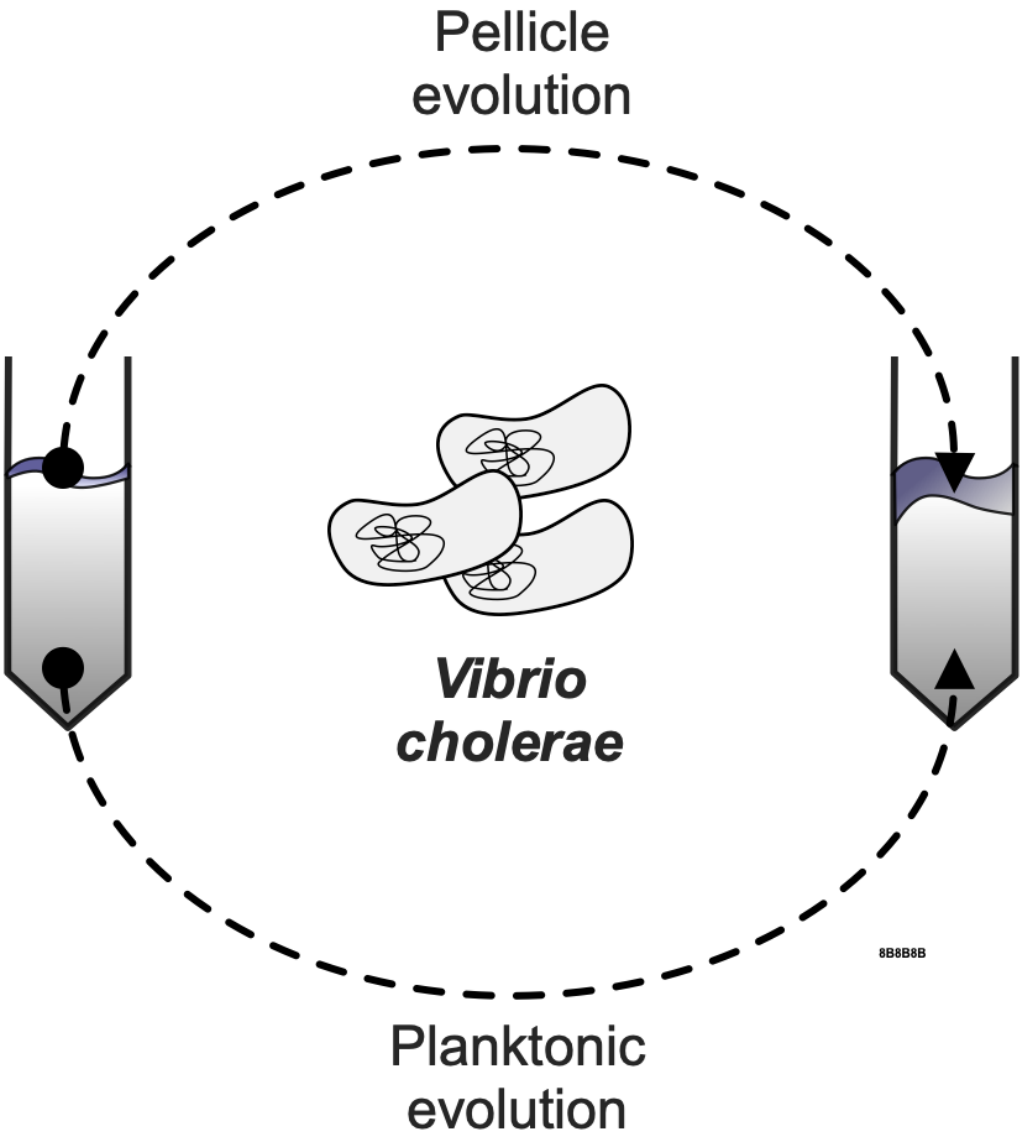

Figure 8 Evolution of biofilm pellicles

Summary of experimental workflow for evolution of *V. cholerae* biofilm pellicles. *V. cholerae* C6706 was grown in 2 ml (24-well plate) static cultures for 24 hours. After 24 hours, the bacterial cultures contained biofilm pellicles at the air-liquid interface. These biofilm pellicles were harvested and transferred with a sterile loop into 1 ml of sterile PBS. The biofilm pellicle was then broken up by vortexing to dislodge biofilm-embedded cells. After vortexing, the bacterial PBS-suspension was filter through a Whatman® Puradisc 5 µm sterile filter to remove any unbroken biofilm particles and used to inoculate a new static culture to grow a new biofilm pellicle. Six biofilm populations were evolved in parallel. In addition, two planktonic-evolved populations were passaged in parallel with a standard 1:100 dilution. All populations were propagated for a total of eight days.

6.3 Directed evolution

In **paper 3**, directed evolution by error-prone PCR coupled with biofilm evolution was employed to evolve the β-lactamase KPC-2. Random mutagenesis with a single round of error-prone PCR with an estimated mutagenesis rate of 1-2 amino acid changes was conducted to create a mutational library of KPC-2 [317]. To sample the whole sequence of KPC-2, the mutant library was constructed with >5000 mutants. Directed evolution of KPC-2 coupled with selection for biofilm formation was employed to reduce the number of confounding mutations that compensate biofilm inhibition independently of KPC-2. In this setup, random mutagenesis with error-prone PCR generates the genetic diversity within KPC-2, while selection for biofilm pellicles enriches for KPC-2 mutants with increased biofilm formation. To limit the amount of confounding chromosomal mutations. biofilm evolution was conducted for one single round. Additionally, to exclude unwanted mutations outside of KPC-2, isolated KPC-2 variants were subcloned into an isogenic vector backbone and transformed back into wild-type *V. cholerae* C6706.

6.4 Quantification of biofilm formation and motility

There are multiple ways of quantifying biofilm formation and motility in bacteria [318–322]. In **paper 1-3**, biofilm formation was quantified using a crystal violet assay. Crystal violet (CV) rapidly stains biotic biomass purple. It can be exploited to stain attached biofilms, which are subsequently dissolved in solvents, such as acetic acid or ethanol. The amount of biomass can then be quantified by measuring the absorbance of the dissolved biomass at 595 nm in a microplate spectrophotometer [323]. While it does not give detailed qualitative information like more complex imaging-based methods (e.g. Comstat or BiofilmQ) it allows for rapid quantification of biofilm formation [318, 322]. One must bear in mind that quantification of biofilm formation with CV relies on multiple phenotypes, including growth rate, production of extracellular matrix and attachment. Therefore, changes in any of these phenotypes will also affect the output of the assay.

Due to the staining and subsequent dissolving of biofilms, the CV assay only generate a single measurement. This represents a limitation, as biofilms are dynamic structured communities. Because of this, single measurements do not capture the dynamics of

biofilm formation and dispersal over time, which can potentially vary between different strains and mutants. This issue can be mitigated by advanced imaging techniques that can monitor and quantify biofilm development over time, but this requires a costly specialized microscopy system [146, 147, 318, 324] . Alternatively, one can conducting time-resolved or dilution-resolved CV assays, but this comes at the cost of less scalability [325]. Since we were working with a very distinct and easily recognizable hyper-biofilm phenotype in **paper 2**, we opted for measurements of a single endpoints. In **paper 1 and 3**, due to the high interexperiment variation of the CV assay we opted for measurements of single timepoints to ensure scalability. Measurement of biofilm formation at multiple time points or with dilution-resolved CV assays, could yield more detailed insights into biofilm dynamics and potentially highlight phenotypic differences not captured by single endpoint measurements.

In addition, we also conducted qualitative assessment of biofilm pellicle morphology in **paper 2 and 3**. This was done by imaging biofilm pellicles with a stereomicroscope. Assessment of pellicle morphology was done by eye and not with specialized software, which some research groups have employed in recent years [251, 252]. Therefore, we did no obtain quantitative measurements of differences in pellicle morphology. Nevertheless, this method can still capture large phenotypic differences reliably (e.g. smooth *versus* hyper-wrinkly biofilm pellicle).

In **paper 1** we also quantified motility, as motility is often inversely regulated with biofilm formation. To quantify motility, we employed semi-solid agar plates with 0.3% agar. This is a plate-based method to measure swimming motility, which is a unicellular flagellum-dependent type of movement [326–328]. Swimming motility is measured by inoculating a semi-solid agar plate (0.3% agar) and incubating the plates for a set amount of time. After incubation, motility is measured by measuring the size of the bacterial swarm. Thus, swarm size is employed as a proxy for motility. The method represents an easy and scalable way of measuring swimming motility. Similar to the CV assay, this method depends on multiple phenotypes, including growth rate, chemotaxis and swimming motility. Therefore, growth defects or defects in chemotaxis can affect the interpretation of the assay. Other measures of quantifying bacterial swimming include measuring the actual swim speed with direct microscopy. This assay represents a more direct measurement of motility but require specialized equipment

and is technically much more difficult. Because of this, we opted for measuring swimming motility with semi-solid agar plates.

6.5 DNA sequencing approaches

In all the projects we employed various methods of DNA sequencing to characterize the genotypes of ancestral and evolved strains and/or genes. In **paper 1**, we employed next-generation sequencing (NGS) to establish a closed, circular genome for our laboratory stock of *V. cholerae* C6706. In order to create a closed genome of high quality, we utilized a hybrid sequencing approach combining long- and short-read sequencing technology [329, 330]. Although short-read sequencing represents a cost-effective and accurate technique for whole genome sequencing of microbial genomes, it has certain caveats [330, 331]. The short read length makes it difficult to assess certain aspects of the sequenced genome, especially structure, rearrangements, repetitive regions and MGEs. Therefore, de novo assembling closed circular microbial genome based solely on short-read sequencing propose a challenge [331]. The increased read length of long-read sequencing makes it easier to fully resolve genome structure and create closed, circular genomes, although at the cost of increased sequencing error rates [331, 332]. By employing hybrid sequencing, the long reads can function as scaffolds and provide information regarding the genome structure, while the short reads are employed to call individual bases at a local scale [329, 331, 333, 334]. Consequently, hybrid assemblies with both short and long sequencing technology are well-suited to generate fully resolved, closed microbial genomes. For this reason, we employed both short- and long-read sequencing technologies to whole genome sequence our isolate of *V. cholerae* C6706.

The genome established in **paper 1** was later employed in **paper 2** as reference for the ancestral strain of *V. cholerae* C6706. To genetically characterize the evolved populations as comprehensively as possible, we opted for deep sequencing of the evolved populations. Deep sequencing refers to massive parallel sequencing with high coverage, which allows for detection of mutations at low frequencies in heterogenous populations [335–337]. Thus, employing this method makes it possible to capture the genetic diversity within the evolved populations. The main drawback of deep sequencing is the high cost due to the need of high sequencing coverage. In addition, since all populations are pooled, single colonies needs to be isolated afterwards and then re-sequenced to confirm their genotype. Depending on the genetic diversity of the populations, identifying mutations driving adaptation and linking genotypes to

phenotypes, can vary in difficulty. If working with a population with high diversity and multiple mutations at low frequencies, linking genotypes to phenotypes can be cumbersome and demand isolation, resequencing and phenotypic characterization of multiple isolates.

In **paper 3** since we were working with a single gene, we sanger sequenced a random selection of evolved KPC-2 variants [338]. Obviously, this limits our ability to assess the genetic diversity within the KPC-2 mutant library after selection and measure the frequency of individual mutations. However, it provided a fast and cheap way to characterize the genotype of individual KPC-2 variants, which we subsequently characterized phenotypically.

6.6 Measurement of DGC- and PDE-activity

In **paper 2**, we expressed and purified wild-type MbaA and various MbaA mutants to measure diguanylate cyclase (DGC) and phosphodiesterase (PDE) activity. To successfully purify MbaA, which is a membrane-bound protein, we purified a non-membrane-bound version of MbaA (GGDEF-EAL-domain, L328 – R791) linked to a maltose-binding protein (MBP). To measure the enzymatic activity of MbaA under conditions that mimic *in vivo* conditions as closely as possible, purification of the entire protein followed by cleaving of the MBP-tag would be ideal. Alas, this was deemed too difficult technically as this would require establishing a lipophilic environment for the enzyme kinetics. Furthermore, MbaA has very poor solubility and it is challenging to keep the protein soluble without the MBP-tag [339]. Therefore, the enzyme kinetics was determined with the non-membrane-bound MBP-tagged versions of MbaA. The presence of the MBP-tag could potentially affect the activity of the GGDEF- and EAL-domains of MbaA. Importantly, in previous studies with MbaA, the non-membrane-bound MBP-tagged versions of MbaA remained enzymatically active [339].

Measurement of DGC-activity was based on the measurement of pyrophosphate (Pi), which is released upon formation of c-di-GMP from GTP [152, 340–342]. DGC-activity was measured with a EnzCheck pyrophosphate kit (Invitrogen). This kit detects the production of Pi through a chemical reaction between Pi and 2-Amino-6-mercapto-7-methylpurine riboside (MESG), which is catalyzed by the purine nucleoside phosphorylase (PNP) enzyme. The conversion of MESG induces a change in absorbance maximum from 330 to 360 nm, which can be measured by a spectrophotometer. We first determined the extinction coefficient for the reaction of Pi with MESG and then used this to conduct Michaelis Menten kinetics on the DGC-activity of wild-type MbaA and the corresponding mutants.

Measurement of PDE-activity was conducted with the fluorescent c-di-GMP derivate 2'-O-(N'-methylanthraniloyl)-cyclic diguanylate (MANT-c-di-GMP) [342]. We employed fluorescence spectroscopy to measure emitted fluorescence before and after incubation of MANT-c-di-GMP with wild-type MbaA and MbaA variants. Conversion of MANT-c-di-GMP into MANT-pGpG leads to a reduction in fluorescence that can be monitored as a function of time [342]. The change in fluorescence was used to

calculate the extinction coefficient, which was subsequently used to calculate Michaelis Menten kinetics for the PDE-activity of wild-type MbaA and the corresponding mutants.

Although indirect, these methods are well established for the measurement of DGC- and PDE-activity and enable determination of enzyme kinetics. The *in vitro* enzymatic activity of wild-type MbaA has already been determined, demonstrating that wild-type MbaA only possess PDE-activity *in vitro* [339]. When measuring PDE-activity, we employed wild-type MbaA as a positive control, while MbaA with an inactivating mutation in its active site (E553A) served as a negative control [157, 159–162]. Since wild-type MbaA lack DGC-activity *in vitro*, we employed wild-type MbaA as a negative control for measurement of DGC-activity. Similar to previous studies, we did not detect any *in vitro* DGC-activity in wild-type MbaA.

7 Results and discussion

7.1 Genetic and phenotypic differences between 7th pandemic *V. cholerae* strains

V. cholerae possess a complex life cycle and cycle between its aquatic niche and the human host. Due to the continuous spread of *V. cholerae* over several hundred years, the pathogen has also been under adaptive evolution for an extended time. The prime example of this is the emergence of the El Tor biotype, which outcompeted the classical biotype due to increased fitness [1–3, 21].

The introduction of next generation sequencing technologies enabled researchers to develop powerful new tools to link genotypes to phenotypes [28, 84, 343–346]. Thus, enabling the discovery of genes and cellular processes that were essential to the life cycle of *V. cholerae* [107, 112, 114, 115, 345, 347–351]. Many of these methods rely on the availability of a reference genome to function. In **paper 1**, we *de novo* assembled the genome of *V. cholerae* C6706 using short- and long-read next-generation sequencing technologies. To improve upon the previous version of the genome we employed hybrid sequencing, manually curated the genome annotation, and linked every open reading frame (ORF) to the corresponding ORF in the current reference strain *V. cholerae* N16961 [28, 313].

Our work in **paper 1** showcases the potential dangers of employing a single strain as reference for all 7th pandemic *V. cholerae* strains. Although the strains were genetically similar overall, *V. cholerae* C6706 contained 76 genetic changes from *V. cholerae* N16961. In addition, C6706 harbored an additional prophage, a different variant of VSP-2 and a large inversion in chromosome 1 [18, 314, 315]. Many of these genetic changes were in genes linked to important biological functions such as biofilm formation, motility, chemotaxis, quorum sensing and genome stability. This also included a previously described laboratory-acquired mutation in the quorum sensing regulator LuxO, which locks *V. cholerae* C6706 in a low-cell density QS-state. QS is a key regulator of bacterial behavior and affect multiple phenotypes including biofilm formation, motility, T6SS, and natural competence [231, 352]. **Paper 1** highlights how the genotype of 7th pandemic *V. cholerae* strains can differ, which can be a potential

source of error in genetic studies of *V. cholerae*, if researchers do not use the appropriate genome as reference.

Phenotypic assays demonstrated that our stock of QS- *V. cholerae* C6706 had altered biofilm formation, motility, and mutation rate compared to *V. cholerae* N16961. This is despite the fact that *V. cholerae* N16961 is also locked in a low-cell density QS-state due to a frameshift mutation in *hapR*. Comparison of QS- *V. cholerae* C6706 and *V. cholerae* N16961 with QS+ *V. cholerae* C6706 (wild-type LuxO) demonstrated that all three strains differed from each other in both biofilm formation and motility. This once again underlines the potential dangers of a single reference strain for the 7th pandemic as seemingly small genetic changes can have large effects on important bacterial phenotypes.

Even though these strains belong to the same transmission wave (wave 1) of the 7th pandemic, they exhibit important phenotypic differences. It seems plausible that other strains from wave 1 also differ phenotypically and that clinical strains from other transmission waves could differ even more [31]. This could have important implications as findings in one given strain might not be applicable to other 7th pandemic *V. cholerae* strains. Indeed, this has to some degree already been demonstrated between classical and El Tor biotype strains [137, 241, 243–245]. Furthermore, it stresses the importance of knowing the genotype of the strain one is working with as unknown laboratory-acquired mutations can have significant phenotypic effects that potentially confound experimental results. In support of this, Stutzmann et al. [316] have already described the point mutation in LuxO in certain *V. cholerae* C6706 strains and demonstrated how the mutation induces a defect in natural competence and T6SS.

The difference in biofilm formation and motility between QS-deficient *V. cholerae* C6706 and N16961, which is also QS-deficient, indicated that QS was not the sole cause of the observed differences. Indeed *V. cholerae* C6706 contained mutations in several c-di-GMP-metabolizing enzymes, including a frameshift mutation in a known c-di-GMP-degrading enzyme (VC1295) [164]. Fluorescent microscopy demonstrated that VC1295 is expressed in *V. cholerae* and overexpression of it reversed the previously observed differences in biofilm formation and motility. Altogether, this suggests that the combined effects of altered QS and c-di-GMP turnover are

responsible for the observed differences in biofilm formation and motility between *V. cholerae* C6706 and N16961. This stresses the adaptive potential of both c-di-GMP and QS as genetic changes within these systems can significantly alter the physiology of *V. cholerae*.

As described in section 1, environmental *V. cholerae* strains convert into toxigenic strains through the acquisition of MGEs [3]. The acquisition of MGEs is also believed to be the driving force of adaptation in *V. cholerae* [3, 18, 51]. Although this seems true, our work in **paper 1** exemplifies how 7th pandemic *V. cholerae* strains also accumulate chromosomal mutations that affect central biological functions. In support of this, previous studies have demonstrated how a single SNP dramatically alters the activity of T6SS in *V. cholerae* [353–355]. Therefore, these mutations seemingly also drive adaptation in 7th pandemic *V. cholerae* strains. Broader phenotypic comparisons of *V. cholerae* 2010EL-1786 (2010, Haiti) with several commonly used strains of 7th pandemic *V. cholerae* (e.g. E7946, A1552 and N16961) displayed multiple important phenotypic differences between the strains [31]. This included differences in c-di-GMP levels, motility, biofilm formation, transformation, and virulence. *V. cholerae* 2010EL-1786 contains additional MGEs as well as genetic changes within previously acquired MGEs (SXT-element and CTXφ). Despite this, several of the described phenotypic differences (e.g., motility, biofilm formation and virulence) were also linked to chromosomal mutations, including altered c-di-GMP signaling [31]. Additionally, in regional outbreaks, adaptive evolution *via* acquisition of novel MGEs, mutations in already acquired MGEs and chromosomal mutations have been observed [6–8, 31, 356, 357]. Thus, chromosomal mutations seem to be an underappreciated, but important driver of adaptation in 7th pandemic *V. cholerae*.

7.2 Evolution of *V. cholerae* biofilms

7.2.1 Biofilm evolution induces a hyper-biofilm phenotype in *V. cholerae*

Although biofilm formation is viewed as an essential part of the life cycle of *V. cholerae*, the evolutionary effects of living in biofilms remain understudied [66, 69]. There are very few experimental studies on the evolution of *V. cholerae* and **paper 2** is to our knowledge the only existing study on the evolution of *V. cholerae* biofilms [358–362]. Similar to previous studies in other bacterial species, our study demonstrated that evolution in biofilms strongly selected for biofilm formation and induced a hyper-biofilm phenotype [267]. After propagation of biofilm pellicles over eight days, the populations exhibited a distinct hyper-biofilm phenotype with a >8-fold increase in biofilm formation and formation of hyper-wrinkly biofilm pellicles. The rapid increase in biofilm formation suggests that few mutations are needed to attain this. In support of this, previous studies have demonstrated that single mutations within the c-di-GMP signaling system can induce hyper-biofilm phenotypes in *V. cholerae* [77].

The most striking difference compared with previous biofilm evolution studies is the lack of phenotypic and genetic diversification [267]. In previous studies, evolution in biofilms quickly generate phenotypic and genetic heterogeneity. This can often be witnessed as the emergence of different morphotypes in the evolving bacterial populations [267, 276, 278, 279, 284–286, 363, 364]. In contrast, the biofilm-evolved populations in **paper 2** exhibited clear signs of convergent evolution with very high frequency of mutations in the bi-functional c-di-GMP-metabolizing enzyme MbaA. Although the phenotypic diversity of the biofilm-evolved populations was not exhaustively characterized, we observed limited phenotypic diversity within the populations. The reason for this remains elusive, but multiple factors could potentially contribute to this. Firstly, the chosen method for biofilm evolution and could contribute to convergent evolution. Many of the previous studies evolved attached biofilms in more dynamic models (e.g. bead-based biofilm model), which could generate more diversity than evolution of static biofilm pellicles. For instance, the bead-based model popularized by Poltak et al. [279] employs a cycle of colonization and dispersal. In this model, the evolving populations needs to colonize one bead which is then transferred into a new tube where the bead population must disperse and colonize a new bead.

The increased complexity of this model with selective conditions favoring colonization followed by dispersion could potentially select for increased genetic diversity. Nevertheless, previous studies with biofilm pellicles have demonstrated that diversification can occur in biofilm pellicles [278]. This includes the landmark study by Rainey *et al*. which demonstrated that evolution of static microcosms generated and sustained a high degree of diversity [276]. Unlike us, this study sampled the entire static culture. Therefore, the difference in diversity compared to this study most likely comes from differences in sampling. Secondly, we filtered the harvested biofilm populations through a 5 µm sterile filter to remove larger biofilm aggregates. This filtration step could represent a selective condition that limits diversity and function as an upper threshold for biofilm-forming capacity. The length of our biofilm evolution study was also limited and shorter than most previous studies [267, 276, 278, 279, 284–286, 363, 364]. It is possible that the diversity within the biofilm-evolved populations could increase if we increased the duration of the experiment. Alternatively, strong convergent evolution and limited diversification could be a hallmark of *V. cholerae* biofilm evolution. As our study represents the only conducted biofilm evolution study with *V. cholerae* this remains to be investigated in future studies.

7.2.2 The c-di-GMP-signaling system represent an adaptive target in bacteria

In **paper 2,** biofilm-evolved populations demonstrated strong signs of convergent evolution in the bi-functional c-di-GMP-metabolizing enzyme MbaA. Thus, indicating that MbaA and the c-di-GMP-signaling system are under strong selection during biofilm evolution. In support of this, multiple *in vitro* biofilm evolution studies have demonstrated that evolution in biofilms can select for adaptive mutations in the c-di-GMP signaling system [267, 279, 284–288]. **Paper 1** also linked mutations in c-di-GMP-metabolizing enzymes to differences in biofilm formation between clinical *V. cholerae* strains. As a key regulator of biofilm formation, c-di-GMP-associated genes seems to represent potent evolutionary targets to facilitate biofilm adaptation.

Biofilm formation is an important bacterial lifestyle that increase resilience and facilitate colonization of inhospitable niches. In support of this, c-di-GMP-associated proteins have been implicated in the infection cycle of multiple pathogens, including *V. cholerae* [23, 117, 118, 137, 365, 366]. Therefore, accumulation of mutations in the c-di-GMP

signaling system occur not only upon selection for increased biofilm formation, but can also occur in patients and during *in vivo* evolution [129–131, 289]. Taken together, it seems evident that the c-di-GMP signaling system is an evolutionary target that facilitate bacterial adaptation.

7.2.3 Domain crosstalk could regulate the enzymatic activity of bi-functional c-di-GMP-metabolizing enzymes

Paper 2 demonstrated that single mutations in the GGDEF- (E483K) or EAL-domain (E576K and L618V) of the bi-functional c-di-GMP-metabolizing enzyme MbaA increased the DGC-activity, decreased the PDE-activity and decoupled MbaA from polyamine-mediated regulation by NspS. The observation that single mutations in the GGDEF- or EAL-domain affect the enzymatic activity of the opposing domain suggests that interactions between these domains modulate the enzymatic output of MbaA. In support of this, Bridges et al. (15) demonstrated that polyamine-mediated regulation of MbaA depends on the presence of both enzyme domains. Furthermore, a study on the bi-functional c-di-GMP-metabolizing enzyme DcpA from *Mycobacterium smegmatis*, demonstrated that mutations in the EAL-domain could negatively affect both DGC- and PDE-activity [170, 171]. Homology modelling of MbaA demonstrated that the selected mutations were located at the interface between the GGDEF- and EAL-domain, thereby supporting the notion of interdomain interactions.

The molecular mechanism regulating the shift in the enzymatic activity of MbaA remains elusive. Regulation of GGDEF-EAL proteins have primarily been studied in monofunctional GGDEF-EAL proteins were one of the enzyme domains (often the GGDEF-domain) have evolved into a sensor domain that regulate the activity of the opposing enzyme domain. Regulatory crosstalk between the GGDEF- and EAL-domain have already been observed in multiple mono-functional GGDEF-EAL proteins [118, 143, 161, 165, 167]. For instance, several studies have described monofunctional GGDEF-EAL proteins, were the degenerated GGDEF-domain can induce conformational changes that increases the enzymatic output of the EAL-domain [143, 161, 165, 166, 174, 175]. A limited amount of bi-functional c-di-GMP-metabolizing enzymes have been characterized so far. However, the characterized ones can yield insights into how domain crosstalk potentially affects the enzymatic activity of MbaA.

Two of the best characterized bi-functional c-di-GMP-metabolizing enzymes are MorA and RbdA from *P. aeruginosa* [172, 367]. While they primarily function as PDEs *in vivo*, *in vitro* they exhibit a conformation that can support both synthesis and degradation of c-di-GMP. This conformation is supported by salt bridges that span between the GGDEF- and EAL-domain. Interestingly, this interaction involves regions of the GGDEF- and EAL-domains that acquired mutations in our study. MorA contains a salt bridge between K1076 and E1213, that corresponds to D440 and Q577 in MbaA, while RbdA harbors a salt bridge between D518 and R609 that corresponds to D490 and Q577 in MbaA [172, 367]. Furthermore, in the model protein LapD, a degenerate GGDEF-EAL protein that functions as a c-di-GMP receptor, the same regions participate in recruiting the DGC GcbC [177, 368, 369]. This is done *via* an interaction between the α2-helix (GRFLPWLER462-470, which corresponds to EEFIPIAEQ469-577 in MbaA) of the EAL-domain of LapD and the α5-helix (EQLLFAADK477-485, which corresponds to EKLLLNADT483-491 in MbaA) of the GGDEF-domain of GcbC [177, 368, 369]. Consequently, the regions of MbaA that accumulate mutations during biofilm evolution participate in interdomain interactions in GGDEF-EAL protein homologs (Phippen et al. 2014; Dahlstrom et al. 2015; Chong et al. 2018; David et al. 2018).

Interestingly, a study on bidirectional evolution in *P. fluorescens,* showcased how mutations (E1081A and E1082K which corresponds to E576 and Q577 in MbaA) in the EAL-domain of a MorA homolog induced a phenotype associated with increased levels of c-di-GMP [287]. This phenotype was later lost due to frameshift mutations in MorA, suggesting that the initial mutations stimulate the DGC-activity of MorA [287]. Summarized, these studies and our findings on MbaA suggest that there could be interdomain interactions that regulate the enzymatic activity of MbaA. The enzymatic activity of c-di-GMP-metabolizing enzymes are tightly linked to protein conformation. An example of this is the bi-functional c-di-GMP-metabolizing enzyme DcpG, where changes in the protein conformation affects its enzymatic activity [136]. Taken together, we hypothesize that the identified mutations in MbaA could potentially perturb interdomain interactions, thereby leading to conformational changes that alter the enzymatic output of MbaA. The presence of both intra- and interprotein interactions in multiple c-di-GMP-metabolizing enzymes could suggest that the underlying molecular

mechanism is evolutionary conserved [172, 287, 367, 368, 370]. However, further structural studies are required to confirm these findings.

7.2.4 β-lactamases evolve along different evolutionary trajectories in biofilms

It seems evident that the biofilm lifestyle can alter the evolutionary trajectories of bacteria. This holds true not only for bacteria, but also MGEs [35, 307, 308]. In Gram-negative bacteria, β-lactamases are among the most frequently carried AMR determinants and represent a major cause of AMR [35, 58, 64]. AMR determinants and plasmids frequently have pleiotropic effects, meaning that they can affect multiple phenotypic traits, such as biofilm formation and growth rate. Indeed, certain classes of β-lactamases antagonize biofilm formation in *E. coli* and *P. aeruginosa* [300, 301]. **Paper 3** demonstrated that a broad range of β-lactamases antagonize biofilm formation in *V. cholerae*. Furthermore, this inhibition could be compensated by specific mutations (N136K and Δ1-48/N136D/M152I/L167P in KPC-2) selected for during growth in biofilm pellicles, thereby indicating that the biofilm lifestyle can affect the evolution of β-lactamases.

Testing of constructed single mutants (Δ1-48, N136D and L167P demonstrated that loss of the signal peptide alone (Δ1-48) did not improve biofilm formation. In contrast, both N136D and L167P increased biofilm formation. The Δ1-48 KPC-2 mutant lacks the signal peptide, which should hinder translocation into the periplasm. Thus, suggesting that KPC-2's effect on biofilm formation is mediated by processes in the cytosol and related to functional effects in KPC-2. Class A β-lactamases have been shown to fold into functional enzymes prior to translocation and this could potentially be the case for KPC-2 [371]. Introduction of S70A, which hinders covalent binding and hydrolysis of β-lactams by KPC-2, had divergent effects on biofilm formation. In wild-type KPC-2 and Δ1-48/N136D/M152I/L167P, introducing S70A led to a strong reduction in biofilm formation. In contrast, S70A/N136K only exhibited a slight reduction in biofilm forming capacity. This stands in contrast with findings from a previous study where mutating S70 either rescued (TEM-1) or had no effect (OXA-3) on biofilm formation [300]. Consequently, it seems that enzyme functionality affects biofilm formation differently among different β-lactamases. The differing effects of

S70A in different KPC-2 variants could indicate that these variants compensate biofilm formation through different molecular mechanisms.

The molecular mechanism of biofilm antagonization and compensation remains elusive. Prior studies have suggested that inhibition of biofilm formation is related to remodeling of peptidoglycans in the bacterial cell wall [300]. Although, one study has demonstrated that expression of β-lactamases can affect the peptidoglycan composition of *E. coli*, no direct evidence for this hypothesis exists [301]. KPC-2 primarily accumulated mutations within the A-site. For instance, position 136 and 167 resides within the A-site and in close proximity to the conserved residues S70 and E166, which are vital for the enzymatic activity of SBLs [60, 61, 65, 372, 373]. β-lactamases can exhibit promiscuous enzymatic activity [374–376]. Therefore, biofilm inhibition could potentially be mediated by promiscuous enzymatic activity towards other substrates than β-lactams. However, these are speculations and should be further investigated in future studies.

The generalizability of our findings still remains unclear. **Paper 3** combined with previous studies have demonstrated that multiple β-lactamases from different Ambler classes inhibit biofilm formation in *P. aeruginosa*, *E. coli* and *V. cholerae* [300, 301]. All of these studies employed artificial laboratory vectors with a medium to high copy number. Prior studies have demonstrated that certain multidrug resistance plasmids can negatively influence biofilm formation, although some plasmids also have a neutral or positive effect on biofilm formation [300–306]. Importantly, no studies have isolated the effect of plasmid-harbored β-lactamases, but rather investigated the effect of the entire plasmid. Natural conjugative and clinical MDR plasmids are often large (>40 kb) and can encode genes known to affect biofilm formation (e.g., c-di-GMP-metabolizing enzymes) [377–379]. Therefore, rigorous studies controlling for confounding effects from other plasmid-encoded genes are needed.

8 Conclusions

In **paper 1**, we established an improved version of the genome of *V. cholerae* C6706, which was linked to the current reference strain N16961. This should represent a valuable resource for the research community as *V. cholerae* C6706 is a commonly used model strain, but have lacked a reference genome with established linkages to N16961. The genome was leveraged to identify important genetic differences between *V. cholerae* C6706 and N16961 in genes related to c-di-GMP signaling and quorum sensing. These genetic changes alter the physiology of *V. cholerae* and induce changes in biofilm formation and motility between *V. cholerae* C6706 and N16961.

Biofilm formation is a hallmark of the life cycle of *V. cholerae*. Despite this, the evolution of *V. cholerae* in biofilms remains an understudied research topic. **Paper 2** demonstrates that evolution in biofilms strongly selects for increased biofilm formation. Increases in biofilm formation is mediated by single point mutations in the bi-functional c-di-GMP-metabolizing enzyme MbaA. These mutations seem to reduce PDE-activity, increase c-di-GMP synthesis and decouple MbaA from polyamine-mediated regulation by NspS. Taken together, our findings suggests that the increase in biofilm formation is mediated by a shift in the enzymatic output of MbaA from degradation to constitutive synthesis of c-di-GMP. Ultimately, **paper 2** sheds light on the evolution of *V. cholerae* in biofilms, and the function and evolutionary potential of bi-functional c-di-GMP-metabolizing enzymes. It also underlines how changes in the c-di-GMP turnover can facilitate biofilm adaptation. This is also supported by **paper 1**, which linked difference in motility and biofilm formation between *V. cholerae* C6706 and N16961, to mutations in c-di-GMP-metabolizing enzymes. So far, the molecular mechanism mediating the shift in the enzymatic output of MbaA remains unknown. Our findings so far suggest that regulatory crosstalk between the GGDEF- and EAL-domain could be involved.

In **paper 3**, we demonstrated how β-lactamases inhibit biofilm formation in *V. cholerae*. Using KPC-2 as model enzyme, we showcased how evolution in biofilm can reverse this inhibition through seemingly functional mutations in KPC-2. Thus, showcasing how living in biofilms can alter the evolutionary trajectories of AMR-enzymes of great clinical importance. Worryingly, reversal of biofilm inhibition, did not necessarily induce

functional trade-offs as some KPC-2 variants exhibited increased biofilm formation without any increase in susceptibility against β-lactams.

Collectively, this thesis expands our insight into the biology and evolution of *V. cholerae*. It demonstrates the feasibility of evolving *V. cholerae* in biofilms and demonstrates that living in biofilms can alter the evolution of *V. cholerae* and important AMR-enzymes. Furthermore, it showcases how the c-di-GMP signaling system is a potent evolutionary target for bacterial adaptation. Thus, this thesis also underlines the importance of studying the evolution of *V. cholerae* in more complex environments to better understand the biology of this pathogen.

9 Perspectives

This thesis lays the foundation for future studies on *V. cholerae*. **Paper 2** demonstrated how mutations in the bi-functional c-di-GMP-metabolizing enzyme MbaA can alter the enzymatic output of MbaA. So far, the molecular mechanism behind the change of activity in MbaA remains elusive. Future studies should strive to uncover the molecular mechanisms behind this and investigate if it's conserved across multiple bi-functional c-di-GMP-metabolizing enzymes. Doing so, would yield essential insights into the function and regulation of this enzyme class.

In addition, the work in this thesis enabled the characterization of novel traits acquired by *V. cholerae* or β-lactamases during biofilm evolution. However, the biofilm evolution model leveraged in this work is simplistic compared to the life cycle and aquatic environment of *V. cholerae*¸ which could limit the generalizability of these findings. The specific selective pressures imposed by the natural aquatic environment of *V. cholerae* still remain elusive. This is a major knowledge gap, which if closed, could improve our understanding of *V. cholerae* evolution and how it can persist in its aquatic niche and resurface to trigger new outbreaks. Future studies should build upon this thesis to develop more complex systems to study the evolution of *V. cholerae* under natural conditions. Furthermore, the current circulating strains of *V. cholerae* harbor multiple clinically relevant MGEs (e.g. SXT-element and MDR-plasmids). These represents suitable candidates to study the evolution of clinically relevant MGEs in complex structured environments. This thesis primarily employed biofilm evolution as a genetic screen to identify and characterize mutations that facilitate biofilm adaptation. It did not investigate the ecology and population biology of *V. cholerae* biofilms. Future studies should aim to investigate both evolutionary and ecological aspects, to attain a more comprehensive understanding of *V. cholerae* biofilms.

10 References

1. **Kanungo S, Azman AS, Ramamurthy T, Deen J, Dutta S**. Cholera. *The Lancet* 2022;399:1429–1440.

2. **Barua D**. History of Cholera. In: Barua D, Greenough WB (editors). *Cholera*. Boston, MA: Springer US. pp. 1–36.

3. **Balasubramanian D, López-Pérez M, Almagro-Moreno S**. Cholera Dynamics and the Emergence of Pandemic *Vibrio cholerae*. In: Almagro-Moreno S, Pukatzki S (editors). *Vibrio spp. Infections*. Cham: Springer International Publishing. pp. 127–147.

4. **Ali M, Nelson AR, Lopez AL, Sack DA**. Updated Global Burden of Cholera in Endemic Countries. *PLoS Negl Trop Dis* 2015;9:e0003832.

5. **Chin CS, Sorenson J, Harris JB, Robins WP, Charles RC, *et al.*** The origin of the Haitian cholera outbreak strain. *N Engl J Med* 2011;364:33–42.

6. **Eppinger M, Pearson T, Koenig SSK, Pearson O, Hicks N, *et al.*** Genomic Epidemiology of the Haitian Cholera Outbreak: a Single Introduction Followed by Rapid, Extensive, and Continued Spread Characterized the Onset of the Epidemic. *mBio* 2014;5:e01721-14.

7. **Weill F-X, Domman D, Njamkepo E, Almesbahi AA, Naji M, *et al.*** Genomic insights into the 2016–2017 cholera epidemic in Yemen. *Nature* 2019;565:230–233.

8. **Lassalle F, Al-Shalali S, Al-Hakimi M, Njamkepo E, Bashir IM, *et al.*** Genomic epidemiology of the cholera outbreak in Yemen reveals the spread of a multi-drug resistance plasmid between diverse lineages of *Vibrio cholerae*. *bioRxiv* 2022;2022.08.24.504966.

9. Ending Cholera, A global roadmap to 2030.

10. **Legros D**. Global Cholera Epidemiology: Opportunities to Reduce the Burden of Cholera by 2030. *J Infect Dis* 2018;218:S137–S140.

11. **Burki T**. ‘Things have gone seriously wrong’: global cholera surges. *The Lancet* 2023;401:633–634.

12. **Chatterjee SN, Chaudhuri K**. Lipopolysaccharides of *Vibrio cholerae*: I. Physical and chemical characterization. *Biochimica et Biophysica Acta (BBA) - Molecular Basis of Disease* 2003;1639:65–79.

13. **Ramamurthy T, Pragasam AK, Taylor-Brown A, Will RC, Vasudevan K, *et al.*** *Vibrio cholerae* O139 genomes provide a clue to why it may have failed to usher in the eighth cholera pandemic. *Nat Commun* 2022;13:3864.

14. **Ramamurthy T, Garg S, Sharma R, Bhattacharya SK, Balakrish Nair G, *et al.*** Emergence of novel strain of *Vibrio cholerae* with epidemic potential in southern and eastern India. *The Lancet* 1993;341:703–704.

15. **Hu D, Liu B, Feng L, Ding P, Guo X, *et al.*** Origins of the current seventh cholera pandemic. *Proc Natl Acad Sci U S A* 2016;113:E7730–E7739.

16. **Devault AM, Golding GB, Waglechner N, Enk JM, Kuch M, *et al.*** Second-Pandemic Strain of *Vibrio cholerae* from the Philadelphia Cholera Outbreak of 1849. *N Engl J Med* 2014;370:334–340.

17. **Chun J, Grim CJ, Hasan NA, Lee JH, Choi SY, *et al.*** Comparative genomics reveals mechanism for short-term and long-term clonal transitions in pandemic *Vibrio cholerae*. *Proc Natl Acad Sci U S A* 2009;106:15442–15447.

18. **Mutreja A, Kim DW, Thomson NR, Connor TR, Lee JH, *et al.*** Evidence for several waves of global transmission in the seventh cholera pandemic. *Nature* 2011;477:462–465.

19. **Woodward WE, Mosley WH**. The spectrum of cholera in rural Bangladesh. II. Comparison of El Tor Ogawa and classical Inaba infection. *Am J Epidemiol* 1972;96:342–351.

20. **Shahid NS, Samadi AR, Khan MU, Huq MI**. Classical vs El Tor cholera: a prospective family study of a concurrent outbreak. *J Diarrhoeal Dis Res* 1984;2:73–78.

21. **Cvjetanovic B, Barua D**. The Seventh Pandemic of Cholera. *Nature* 1972;239:137–138.

22. **Safa A, Nair GB, Kong RYC**. Evolution of new variants of *Vibrio cholerae* O1. *Trends Microbiol* 2010;18:46–54.

23. **Conner JG, Teschler JK, Jones CJ, Yildiz FH**. Staying Alive: *Vibrio cholerae*'s Cycle of Environmental Survival, Transmission, and Dissemination. *Microbiol Spectr* 4:10.1128/microbiolspec.vmbf-0015-2015

24. **Dziejman M, Balon E, Boyd D, Fraser CM, Heidelberg JF, *et al.*** Comparative genomic analysis of *Vibrio cholerae*: Genes that correlate with cholera endemic and pandemic disease. *Proc Natl Acad Sci U S A* 2002;99:1556–1561.

25. **Marsh JW, Sun D, Taylor RK**. Physical linkage of the *Vibrio cholerae* mannose-sensitive hemagglutinin secretory and structural subunit gene loci: identification of the mshG coding sequence. *Infect Immun* 1996;64:460–465.

26. **Yildiz FH, Schoolnik GK**. Role of rpoS in Stress Survival and Virulence of *Vibrio cholerae*. *J Bacteriol* 1998;180:773–784.

27. **Miller VL, DiRita VJ, Mekalanos JJ**. Identification of *toxS*, a regulatory gene whose product enhances *toxR*-mediated activation of the cholera toxin promoter. *J Bacteriol* 1989;171:1288–1293.

28. **Heidelberg JF, Eisen JA, Nelson WC, Clayton RA, Gwinn ML, *et al.*** DNA sequence of both chromosomes of the cholera pathogen *Vibrio cholerae*. *Nature* 2000;406:477–483.

29. **Thelin KH, Taylor RK**. Toxin-coregulated pilus, but not mannose-sensitive hemagglutinin, is required for colonization by *Vibrio cholerae* O1 El Tor biotype and O139 strains. *Infect Immun* 1996;64:2853–2856.

30. **Waldor MK, Tschäpe H, Mekalanos JJ**. A new type of conjugative transposon encodes resistance to sulfamethoxazole, trimethoprim, and streptomycin in *Vibrio cholerae* O139. *J Bacteriol* 1996;178:4157–4165.

31. **Satchell KJF, Jones CJ, Wong J, Queen J, Agarwal S, *et al.*** Phenotypic Analysis Reveals that the 2010 Haiti Cholera Epidemic Is Linked to a Hypervirulent Strain. *Infect Immun* 2016;84:2473–2481.

32. **Chin C-S, Sorenson J, Harris JB, Robins WP, Charles RC, *et al.*** The Origin of the Haitian Cholera Outbreak Strain. *N Engl J Med* 2010;364:33–42.

33. **Mashe T, Domman D, Tarupiwa A, Manangazira P, Phiri I, *et al.*** Highly Resistant Cholera Outbreak Strain in Zimbabwe. *N Engl J Med* 2020;383:687–689.

34. **Partridge SR, Kwong SM, Neville F, Jensen SO**. Mobile Genetic Elements Associated with Antimicrobial Resistance. *Clin Microbiol Rev* 2018;31:10.1128/cmr.00088-17.

35. **Castañeda-Barba S, Top EM, Stalder T**. Plasmids, a molecular cornerstone of antimicrobial resistance in the One Health era. *Nat Rev Microbiol* 2024:22:18–32

36. **Weisberg AJ, Chang JH**. Mobile Genetic Element Flexibility as an Underlying Principle to Bacterial Evolution. *Annu Rev Microbiol* 2023:15;77:603-624.

37. **Frost LS, Leplae R, Summers AO, Toussaint A**. Mobile genetic elements: the agents of open source evolution. *Nat Rev Microbiol* 2005;3:722–732.

38. **Chris S, Pilar G-BM, Victoria FM, C REP, Fernando de la C**. Mobility of Plasmids. *Microbiology and Molecular Biology Reviews* 2010;74:434–452.

39. **Hall RM, Collis CM**. Mobile gene cassettes and integrons: capture and spread of genes by site-specific recombination. *Mol Microbiol* 1995;15:593–600.

40. **Fluit AC, Schmitz F-J**. Resistance integrons and super-integrons. *Clinical Microbiology and Infection* 2004;10:272–288.

41. **Wozniak RA, Fouts DE, Spagnoletti M, Colombo MM, Ceccarelli D, *et al.*** Comparative ICE genomics: insights into the evolution of the SXT/R391 family of ICEs. *PLoS Genet* 2009;5:e1000786.

42. **Arnold BJ, Huang I-T, Hanage WP**. Horizontal gene transfer and adaptive evolution in bacteria. *Nat Rev Microbiol* 2022;20:206–218.

43. **Howard-Varona C, Hargreaves KR, Abedon ST, Sullivan MB**. Lysogeny in nature: mechanisms, impact and ecology of temperate phages. *ISME J* 2017;11:1511–1520.

44. **Fortier L-C, Sekulovic O**. Importance of prophages to evolution and virulence of bacterial pathogens. *Virulence* 2013;4:354–365.

45. **Johnston C, Martin B, Fichant G, Polard P, Claverys J-P**. Bacterial transformation: distribution, shared mechanisms and divergent control. *Nat Rev Microbiol* 2014;12:181–196.

46. **Brockhurst MA, Harrison E**. Ecological and evolutionary solutions to the plasmid paradox. *Trends Microbiol* 2022;30:534–543.

47. **Harrison E, Brockhurst MA**. Plasmid-mediated horizontal gene transfer is a coevolutionary process. *Trends Microbiol* 2012;20:262–267.

48. **Alvaro SM, Craig MR**. Fitness Costs of Plasmids: a Limit to Plasmid Transmission. *Microbiol Spectr* 2017;5:10.1128/microbiolspec.mtbp-0016–2017.

49. **Bouma JE, Lenski RE**. Evolution of a bacteria/plasmid association. *Nature* 1988;335:351–352.

50. **Kumar A, Das B, Kumar N**. Vibrio Pathogenicity Island-1: The Master Determinant of Cholera Pathogenesis. *Front Cell Infect Microbiol* 2020:6;10:56129610.

51. **Pant A, Bag S, Saha B, Verma J, Kumar P, *et al.*** Molecular insights into the genome dynamics and interactions between core and acquired genomes of *Vibrio cholerae*. *Proc Natl Acad Sci U S A* 2020;117:23762–23773.

52. **Vashist A, Verma J, Narendrakumar L, Das B**. Molecular Insights into Genomic Islands and Evolution of *Vibrio cholerae*. In: Mani I, Singh V, Alzahrani KJ, Chu D-T (editors). *Microbial Genomic Islands in Adaptation and Pathogenicity*. Singapore: Springer Nature Singapore. pp. 279–324.

53. **Beaber JW, Hochhut B, Waldor MK**. Genomic and functional analyses of SXT, an integrating antibiotic resistance gene transfer element derived from *Vibrio cholerae*. *J Bacteriol* 2002;184:4259–4269.

54. **Bordeleau E, Brouillette E, Robichaud N, Burrus V**. Beyond antibiotic resistance: integrating conjugative elements of the SXT/R391 family that

encode novel diguanylate cyclases participate to c-di-GMP signalling in *Vibrio cholerae*. *Environ Microbiol* 2010;12:510–523.

55. **Dalia AB, Seed KD, Calderwood SB, Camilli A**. A globally distributed mobile genetic element inhibits natural transformation of *Vibrio cholerae*. *Proc Natl Acad Sci U S A* 2015;112:10485–10490.

56. **Fayad AA, Rafei R, Njamkepo E, Ezzeddine J, Hussein H, *et al.*** An unusual two-strain cholera outbreak in Lebanon, 2022-2023: a genomic epidemiology study. *bioRxiv* 2023;2023.11.29.569232.

57. **Darby EM, Trampari E, Siasat P, Gaya MS, Alav I, *et al.*** Molecular mechanisms of antibiotic resistance revisited. *Nat Rev Microbiol* 2023;21:280–295.

58. **Murray CJL, Ikuta KS, Sharara F, Swetschinski L, Robles Aguilar G, *et al.*** Global burden of bacterial antimicrobial resistance in 2019: a systematic analysis. *The Lancet* 2022;399:629–655.

59. **Leibovici-Weissman Y, Neuberger A, Bitterman R, Sinclair D, Salam MA, *et al.*** Antimicrobial drugs for treating cholera. *Cochrane Database Syst Rev* 2014:19;2014(6):CD008625

60. **Bush K, Bradford PA**. β-Lactams and β-Lactamase Inhibitors: An Overview. *Cold Spring Harb Perspect Med* 2016:6(8): a025247.

61. **Bush K**. Past and Present Perspectives on β-Lactamases. *Antimicrob Agents Chemother* 2018;62:10.1128/aac.01076-18.

62. **Hutchings MI, Truman AW, Wilkinson B**. Antibiotics: past, present and future. *Curr Opin Microbiol* 2019;51:72–80.

63. **Cassini A, Högberg LD, Plachouras D, Quattrocchi A, Hoxha A, *et al.*** Attributable deaths and disability-adjusted life-years caused by infections with antibiotic-resistant bacteria in the EU and the European Economic Area in 2015: a population-level modelling analysis. *Lancet Infect Dis* 2019;19:56–66.

64. **Bush K, Bradford PA**. Epidemiology of β-Lactamase-Producing Pathogens. *Clin Microbiol Rev* 2020;33:10.1128/cmr.00047-19.

65. **Bonomo RA**. β-Lactamases: A Focus on Current Challenges. *Cold Spring Harb Perspect Med* 2017:3;7(1):a025239.

66. **Silva AJ, Benitez JA**. *Vibrio cholerae* Biofilms and Cholera Pathogenesis. *PLoS Negl Trop Dis* 2016;10:e0004330.

67. **Colwell RR, Kaper J, Joseph SW**. *Vibrio cholerae*, *Vibrio parahaemolyticus*, and Other *Vibrios*: Occurrence and Distribution in Chesapeake Bay. *Science (1979)* 1977;198:394–396.

68. **Akolkar JK, Matson JS**. Stress Responses in Pathogenic *Vibrios* and Their Role in Host and Environmental Survival. In: Almagro-Moreno S, Pukatzki S (editors). *Vibrio spp. Infections*. Cham: Springer International Publishing. pp. 213–232.

69. **Teschler JK, Nadell CD, Drescher K, Yildiz FH**. Mechanisms Underlying *Vibrio cholerae* Biofilm Formation and Dispersion. *Annu Rev Microbiol* 2022;76:503–532.

70. **Alam M, Sultana M, Nair GB, Siddique AK, Hasan NA, *et al.*** Viable but nonculturable *Vibrio cholerae* O1 in biofilms in the aquatic environment and their role in cholera transmission. *Proc Natl Acad Sci U S A* 2007;104:17801–17806.

71. **Flemming H-C, Wingender J, Szewzyk U, Steinberg P, Rice SA, *et al.*** Biofilms: an emergent form of bacterial life. *Nat Rev Microbiol* 2016;14:563–575.

72. **Tamplin ML, Gauzens AL, Huq A, Sack DA, Colwell RR**. Attachment of *Vibrio cholerae* serogroup O1 to zooplankton and phytoplankton of Bangladesh waters. *Appl Environ Microbiol* 1990;56:1977–1980.

73. **Lutz C, Erken M, Noorian P, Sun S, McDougald D**. Environmental reservoirs and mechanisms of persistence of *Vibrio cholerae*. *Front Microbiol* 2013:16;4:375

74. **White PB**. The rugose variant of *Vibrios*. *J Pathol Bacteriol* 1938;46:1–6.

75. **Ali A, Rashid MH, Karaolis DKR**. High-Frequency Rugose Exopolysaccharide Production by *Vibrio cholerae*. *Appl Environ Microbiol* 2002;68:5773–5778.

76. **Yildiz FH, Schoolnik GK**. *Vibrio cholerae* O1 El Tor: Identification of a gene cluster required for the rugose colony type, exopolysaccharide production, chlorine resistance, and biofilm formation. *Proc Natl Acad Sci U S A* 1999;96:4028.

77. **Beyhan S, Yildiz FH**. Smooth to rugose phase variation in *Vibrio cholerae* can be mediated by a single nucleotide change that targets c-di-GMP signalling pathway. *Mol Microbiol* 2007;63:995–1007.

78. **Meibom KL, Blokesch M, Dolganov NA, Wu C-Y, Schoolnik GK**. Chitin Induces Natural Competence in *Vibrio cholerae*. *Science (1979)* 2005;310:1824–1827.

79. **Faruque SM, Biswas K, Udden SMN, Ahmad QS, Sack DA, *et al.*** Transmissibility of cholera: In vivo-formed biofilms and their relationship to infectivity and persistence in the environment. *Proc Natl Acad Sci U S A* 2006;103:6350–6355.

80. **Gallego-Hernandez AL, DePas WH, Park JH, Teschler JK, Hartmann R, *et al.*** Upregulation of virulence genes promotes *Vibrio cholerae* biofilm hyperinfectivity. *Proc Natl Acad Sci USA* 2020;117:11010–11017.

81. **Rita T, Bharathi P, Andrew C**. Growth in a Biofilm Induces a Hyperinfectious Phenotype in *Vibrio cholerae*. *Infect Immun* 2010;78:3560–3569.

82. **Colwell RR, Huq A, Islam MS, Aziz KMA, Yunus M, *et al.*** Reduction of cholera in Bangladeshi villages by simple filtration. *Proc Natl Acad Sci U S A* 2003;100:1051–1055.

83. **Singh A, Barnard TG**. Surviving the acid barrier: responses of pathogenic *Vibrio cholerae* to simulated gastric fluid. *Appl Microbiol Biotechnol* 2015;100:815–824.

84. **Abel S, Abel zur Wiesch P, Chang H-H, Davis BM, Lipsitch M, *et al.*** Sequence tag-based analysis of microbial population dynamics. *Nat Meth* 2015;12:223–226.

85. **Nelson EJ, Harris JB, Glenn Morris J, Calderwood SB, Camilli A**. Cholera transmission: the host, pathogen and bacteriophage dynamic. *Nat Rev Microbiol* 2009;7:693–702.

86. **Nalin DR, Levine RJ, Levine MM, Hoover D, Bergquist E, *et al*.** Cholera, non-vibrio cholera, and stomach acid. Lancet 1978: 21;2(8095):856-9.

87. **Zhu J, Mekalanos JJ**. Quorum Sensing-Dependent Biofilms Enhance Colonization in *Vibrio cholerae*. *Dev Cell* 2003;5:647–656.

88. **Nalin DR, Daya V, Reid A, Levine MM, Cisneros L**. Adsorption and growth of *Vibrio cholerae* on chitin. *Infect Immun* 1979;25:768–770.

89. **Nhu NTQ, Lee JS, Wang HJ, Dufour YS**. Alkaline pH Increases Swimming Speed and Facilitates Mucus Penetration for *Vibrio cholerae*. *J Bacteriol* 2021;203:e00607-20.

90. **Merrell DS, Camilli A**. The cadA gene of *Vibrio cholerae* is induced during infection and plays a role in acid tolerance. *Mol Microbiol* 1999;34:836–849.

91. **Park Y-K, Bearson B, Bang SH, Bang IS, Foster JW**. Internal pH crisis, lysine decarboxylase and the acid tolerance response of *Salmonella typhimurium*. *Mol Microbiol* 1996;20:605–611.

92. **Meng SY, Bennett GN**. Nucleotide sequence of the *Escherichia coli* cad operon: a system for neutralization of low extracellular pH. *J Bacteriol* 1992;174:2659–2669.

93. **Angelichio MJ, Merrell SD, Camilli A**. Spatiotemporal Analysis of Acid Adaptation-Mediated *Vibrio cholerae* Hyperinfectivity. *Infect Immun* 2004;72:2405–2407.

94. **Koestler BJ, Waters CM**. Intestinal GPS: bile and bicarbonate control cyclic di-GMP to provide *Vibrio cholerae* spatial cues within the small intestine. *Gut Microbes* 2014;5:775–780.

95. **Koestler BJ, Waters CM**. Bile Acids and Bicarbonate Inversely Regulate Intracellular Cyclic di-GMP in *Vibrio cholerae*. *Infect Immun* 2014;82:3002–3014.

96. **Zhenyu L, Yuning W, Shengyan L, Ying S, Karl-Gustav R, *et al.*** *Vibrio cholerae* Represses Polysaccharide Synthesis To Promote Motility in Mucosa. *Infect Immun* 2015;83:1114–1121.

97. **Liu Z, Miyashiro T, Tsou A, Hsiao A, Goulian M, *et al.*** Mucosal penetration primes *Vibrio cholerae* for host colonization by repressing quorum sensing. *Proc Natl Acad Sci U S A* 2008;105:9769–9774.

98. **Silva AJ, Pham K, Benitez JA**. Haemagglutinin/protease expression and mucin gel penetration in El Tor biotype *Vibrio cholerae*. *Microbiology (N Y)* 2003;149:1883–1891.

99. **Millet YA, Alvarez D, Ringgaard S, von Andrian UH, Davis BM, *et al.*** Insights into *Vibrio cholerae* Intestinal Colonization from Monitoring Fluorescently Labeled Bacteria. *PLoS Pathog* 2014;10:e1004405-.

100. **Kirn TJ, Jude BA, Taylor RK**. A colonization factor links *Vibrio cholerae* environmental survival and human infection. *Nature* 2005;438:863–866.

101. **Krebs SJ, Taylor RK**. Protection and Attachment of *Vibrio cholerae* Mediated by the Toxin-Coregulated Pilus in the Infant Mouse Model. *J Bacteriol* 2011;193:5260–5270.

102. **Yamamoto T, Yokota T**. Electron microscopic study of *Vibrio cholerae* O1 adherence to the mucus coat and villus surface in the human small intestine. *Infect Immun* 1988;56:2753–2759.

103. **Joshi A, Kostiuk B, Rogers A, Teschler J, Pukatzki S, *et al.*** Rules of Engagement: The Type VI Secretion System in *Vibrio cholerae*. *Trends Microbiol* 2017;25:267–279.

104. **Zhao W, Caro F, Robins W, Mekalanos JJ**. Antagonism toward the intestinal microbiota and its effect on *Vibrio cholerae* virulence. *Science (1979)* 2018;359:210–213.

105. **Paul B, D WA, R TK, H WJ**. The *Vibrio cholerae* Type Six Secretion System Is Dispensable for Colonization but Affects Pathogenesis and the Structure of Zebrafish Intestinal Microbiome. *Infect Immun* 2021:16;89(9):e0015121.

106. **Logan SL, Thomas J, Yan J, Baker RP, Shields DS, *et al.*** The *Vibrio cholerae* type VI secretion system can modulate host intestinal mechanics to

displace gut bacterial symbionts. *Proc Natl Acad Sci U S A* 2018;115:E3779–E3787.

107. **Fu Y, Waldor MK, Mekalanos JJ**. Tn-Seq Analysis of *Vibrio cholerae* Intestinal Colonization Reveals a Role for T6SS-Mediated Antibacterial Activity in the Host. *Cell Host Microbe* 2013;14:652–663.

108. **Rivera-Chávez F, Mekalanos JJ**. Cholera toxin promotes pathogen acquisition of host-derived nutrients. *Nature* 2019;572:244–248.

109. **Chapman CML, Kapinos A, Rivera-Chávez F**. Modulation of Host-Microbe Metabolism by Cholera Toxin. *Infect Immun* 2023;91:e00435-22.

110. **Hartley DM, Morris Jr. JG, Smith DL**. Hyperinfectivity: A Critical Element in the Ability of *V. cholerae* to Cause Epidemics? *PLoS Med* 2005;3:e7.

111. **Alam A, LaRocque RC, Harris JB, Vanderspurt C, Ryan ET, *et al.*** Hyperinfectivity of Human-Passaged *Vibrio cholerae* Can Be Modeled by Growth in the Infant Mouse. *Infect Immun* 2005;73:6674–6679.

112. **Merrell DS, Butler SM, Qadri F, Dolganov NA, Alam A, *et al.*** Host-induced epidemic spread of the cholera bacterium. *Nature* 2002;417:642–645.

113. **Nielsen AT, Dolganov NA, Otto G, Miller MC, Wu CY, *et al.*** RpoS Controls the *Vibrio cholerae* Mucosal Escape Response. *PLoS Pathog* 2006;2:e109.

114. **Schild S, Tamayo R, Nelson EJ, Qadri F, Calderwood SB, *et al.*** Genes Induced Late in Infection Increase Fitness of *Vibrio cholerae* after Release into the Environment. *Cell Host Microbe* 2007;2:264–277.

115. **Kamp HD, Patimalla-Dipali B, Lazinski DW, Wallace-Gadsden F, Camilli A**. Gene Fitness Landscapes of *Vibrio cholerae* at Important Stages of Its Life Cycle. *PLoS Pathog* 2013;9:e1003800.

116. **Kamruzzaman M, Udden SMN, Cameron DE, Calderwood SB, Nair GB, *et al.*** Quorum-regulated biofilms enhance the development of conditionally viable, environmental *Vibrio cholerae*. *Proc Natl Acad Sci U S A* 2010;107:1588–1593.

117. **Romling U, Galperin M, Gomelsky M**. Cyclic di-GMP: the First 25 Years of a Universal Bacterial Second Messenger. *Microbiology and Molecular Biology Reviews* 2013;77:1–52.

118. **Hengge R**. Principles of c-di-GMP signalling in bacteria. *Nat Rev Microbiol* 2009;7:263–273.

119. **Jenal U, Reinders A, Lori C**. Cyclic di-GMP: second messenger extraordinaire. *Nat Rev Microbiol* 2017;15:271–284.

120. **Newton AC, Bootman MD, Scott JD**. Second Messengers. *Cold Spring Harb Perspect Biol* 2016:1;8(8):a005926.

121. **Yoon S hun, Waters CM**. The ever-expanding world of bacterial cyclic oligonucleotide second messengers. *Curr Opin Microbiol* 2021;60:96–103.

122. **Ross P, Weinhouse H, Aloni Y, Michaeli D, Weinberger-Ohana P, *et al.*** Regulation of cellulose synthesis in *Acetobacter xylinum* by cyclic diguanylic acid. *Nature* 1987;325:279–281.

123. **Hengge R**. High-specificity local and global c-di-GMP signaling. *Trends Microbiol* 2021;29:993–1003.

124. **Makitrynskyy R, Tsypik O, Nuzzo D, Paululat T, Zechel DL, *et al.*** Secondary nucleotide messenger c-di-GMP exerts a global control on natural product biosynthesis in streptomycetes. *Nucleic Acids Res* 2020;48:1583–1598.

125. **Fernandez NL, Hsueh BY, Nhu NTQ, Franklin JL, Dufour YS, *et al.*** *Vibrio cholerae* adapts to sessile and motile lifestyles by cyclic di-GMP regulation of cell shape. *Proc Natl Acad Sci U S A* 2020;117:29046–29054.

126. **Fernandez NL, Waters CM**. Cyclic di-GMP Increases Catalase Production and Hydrogen Peroxide Tolerance in *Vibrio cholerae*. *Appl Environ Microbiol* 2019;85:e01043-19.

127. **Tischler AD, Camilli A**. Cyclic diguanylate regulates *Vibrio cholerae* virulence gene expression. *Infect Immun* 2005;73:5873–5882.

128. **Ryan RP**. Cyclic di-GMP signalling and the regulation of bacterial virulence. *Microbiology (N Y)* 2013;159:1286–1297.

129. **Malone JG, Jaeger T, Spangler C, Ritz D, Spang A, *et al.*** YfiBNR mediates cyclic di-GMP dependent small colony variant formation and persistence in *Pseudomonas aeruginosa*. *PLoS Pathog* 2010;6:e1000804.

130. **Malone JG, Jaeger T, Manfredi P, Dötsch A, Blanka A, *et al.*** The YfiBNR signal transduction mechanism reveals novel targets for the evolution of persistent *Pseudomonas aeruginosa* in cystic fibrosis airways. *PLoS Pathog* 2012;8:e1002760.

131. **Obeng N, Czerwinski A, Schütz D, Michels J, Leipert J, *et al.*** Bacterial c-di-GMP has a key role in establishing host–microbe symbiosis. *Nat Microbiol* 2023;8:1809–1819.

132. **Seshasayee ASN, Fraser GM, Luscombe NM**. Comparative genomics of cyclic-di-GMP signalling in bacteria: post-translational regulation and catalytic activity. *Nucleic Acids Res* 2010;38:5970–5981.

134. **Barends TRM, Hartmann E, Griese JJ, Beitlich T, Kirienko N V, *et al.*** Structure and mechanism of a bacterial light-regulated cyclic nucleotide phosphodiesterase. *Nature* 2009;459:1015–1018.

135. **Savakis P, De Causmaecker S, Angerer V, Ruppert U, Anders K, *et al.*** Light-induced alteration of c-di-GMP level controls motility of *Synechocystis sp*. PCC 6803. *Mol Microbiol* 2012;85:239–251.

136. **Patterson DC, Ruiz MP, Yoon H, Walker JA, Armache J-P, *et al.*** Differential ligand-selective control of opposing enzymatic activities within a bifunctional c-di-GMP enzyme. *Proc Natl Acad Sci U S A* 2021;118:e2100657118.

137. **Conner JG, Zamorano-Sánchez D, Park JH, Sondermann H, Yildiz FH**. The ins and outs of cyclic di-GMP signaling in *Vibrio cholerae*. *Curr Opin Microbiol* 2017;36:20–29.

138. **Chou S-H, Galperin MY**. Diversity of Cyclic Di-GMP-Binding Proteins and Mechanisms. *J Bacteriol* 2016;198:32–46.

139. **Ryan RP, Tolker-Nielsen T, Dow JM**. When the PilZ don't work: effectors for cyclic di-GMP action in bacteria. *Trends Microbiol* 2012;20:235–242.

140. **Sudarsan N, Lee ER, Weinberg Z, Moy RH, Kim JN, *et al.*** Riboswitches in Eubacteria Sense the Second Messenger Cyclic Di-GMP. *Science* 2008;321:411–413.

141. **Yu S, Hu Z, Xu X, Liang X, Shen J, *et al.*** c-di-GMP modulates ribosome assembly by inhibiting rRNA methylation. *bioRxiv* 2024;2024.06.05.597503.

142. **Schirmer T**. C-di-GMP Synthesis: Structural Aspects of Evolution, Catalysis and Regulation. *J Mol Biol* 2016;428:3683–3701.

143. **Schirmer T, Jenal U**. Structural and mechanistic determinants of c-di-GMP signalling. *Nat Rev Microbiol* 2009;7:724–735.

144. **Hunter JL, Severin GB, Koestler BJ, Waters CM**. The *Vibrio cholerae* diguanylate cyclase VCA0965 has an AGDEF active site and synthesizes cyclic di-GMP. *BMC Microbiol* 2014;14:22.

145. **Dahlstrom KM, O'Toole GA**. A Symphony of Cyclases: Specificity in Diguanylate Cyclase Signaling. *Annu Rev Microbiol* 2017;71:179–195.

146. **Bridges AA, Bassler BL**. Inverse regulation of *Vibrio cholerae* biofilm dispersal by polyamine signals. *Elife* 2021;10:e65487.

147. **Bridges AA, Prentice JA, Fei C, Wingreen NS, Bassler BL**. Quantitative input–output dynamics of a c-di-GMP signal transduction cascade in *Vibrio cholerae*. *PLoS Biol* 2022;20:e3001585-.

148. **Pérez-Mendoza D, Coulthurst SJ, Humphris S, Campbell E, Welch M, *et al.*** A multi-repeat adhesin of the phytopathogen, *Pectobacterium atrosepticum*, is secreted by a Type I pathway and is subject to complex regulation involving a non-canonical diguanylate cyclase. *Mol Microbiol* 2011;82:719–733.

149. **Chan C, Paul R, Samoray D, Amiot NC, Giese B, *et al.*** Structural basis of activity and allosteric control of diguanylate cyclase. *Proc Natl Acad Sci U S A* 2004;101:17084–17089.

150. **Paul R, Abel S, Wassmann P, Beck A, Heerklotz H, *et al.*** Activation of the Diguanylate Cyclase PleD by Phosphorylation-mediated Dimerization. *J Biol Chem* 2007;282:29170–29177.

151. **Wassmann P, Chan C, Paul R, Beck A, Heerklotz H, *et al.*** Structure of BeF3−-Modified Response Regulator PleD: Implications for Diguanylate Cyclase Activation, Catalysis, and Feedback Inhibition. *Structure* 2007;15:915–927.

152. **De N, Pirruccello M, Krasteva PV, Bae N, Raghavan RV, *et al.*** Phosphorylation-Independent Regulation of the Diguanylate Cyclase WspR. *PLoS Biol* 2008;6:e67-.

153. **Christen B, Christen M, Paul R, Schmid F, Folcher M, *et al.*** Allosteric Control of Cyclic di-GMP Signaling. *Journal of Biological Chemistry* 2006;281:32015–32024.

154. **Schmidt AJ, Ryjenkov DA, Gomelsky M**. The Ubiquitous Protein Domain EAL Is a Cyclic Diguanylate-Specific Phosphodiesterase: Enzymatically Active and Inactive EAL Domains. *J Bacteriol* 2005;187:4774–4781.

155. **Bellini D, Hutchin A, Soren O, Webb JS, Tews I, *et al.*** Structure and Regulation of EAL Domain Proteins. In: Chou S-H, Guiliani N, Lee VT, Römling U (editors). *Microbial Cyclic Di-Nucleotide Signaling*. Cham: Springer International Publishing. pp. 27–48.

156. **Sundriyal A, Massa C, Samoray D, Zehender F, Sharpe T, *et al.*** Inherent Regulation of EAL Domain-catalyzed Hydrolysis of Second Messenger Cyclic di-GMP. *J Biol Chem* 2014;289:6978–6990.

157. **Tchigvintsev A, Xu X, Singer A, Chang C, Brown G, *et al.*** Structural insight into the mechanism of cyclic di-GMP hydrolysis by EAL domain phosphodiesterases. *J Mol Biol* 2010;402:524–538.

158. **Wierenga RK**. The TIM-barrel fold: a versatile framework for efficient enzymes. *FEBS Lett* 2001;492:193–198.

159. **Rao F, Yang Y, Qi Y, Liang Z-X**. Catalytic Mechanism of Cyclic Di-GMP-Specific Phosphodiesterase: a Study of the EAL Domain-Containing RocR from *Pseudomonas aeruginosa*. *J Bacteriol* 2008;190:3622–3631.

160. **Yang C, Cui C, Ye Q, Kan J, Fu S, *et al.*** Burkholderia cenocepacia integrates cis-2-dodecenoic acid and cyclic dimeric guanosine monophosphate signals to control virulence. *Proc Natl Acad Sci U S A* 2017;114:13006–13011.

161. **Feng Q, Ahator S Dela, Zhou T, Liu Z, Lin Q, *et al.*** Regulation of Exopolysaccharide Production by ProE, a Cyclic-Di-GMP Phosphodiesterase in *Pseudomonas aeruginosa* PAO1. *Front Microbiol* 2020:5;11:1226.

162. **Tamayo R, Tischler AD, Camilli A**. The EAL domain protein VieA is a cyclic diguanylate phosphodiesterase. *J Biol Chem* 2005;280:33324–33330.

163. **Galperin MY, Chou S-H**. Sequence Conservation, Domain Architectures, and Phylogenetic Distribution of the HD-GYP Type c-di-GMP Phosphodiesterases. *J Bacteriol* 2022;204:e00561-21.

164. **McKee RW, Kariisa A, Mudrak B, Whitaker C, Tamayo R**. A systematic analysis of the in vitro and in vivo functions of the HD-GYP domain proteins of *Vibrio cholerae*. *BMC Microbiol* 2014;14:272.

165. **Christen M, Christen B, Folcher M, Schauerte A, Jenal U**. Identification and Characterization of a Cyclic di-GMP-specific Phosphodiesterase and Its Allosteric Control by GTP. *J Biol Chem* 2005;280:30829–30837.

166. **Tamayo R, Schild S, Pratt JT, Camilli A**. Role of cyclic Di-GMP during el tor biotype *Vibrio cholerae* infection: characterization of the in vivo-induced cyclic Di-GMP phosphodiesterase CdpA. *Infect Immun* 2008;76:1617–1627.

167. **García B, Latasa C, Solano C, Portillo FG, Gamazo C, *et al.*** Role of the GGDEF protein family in Salmonella cellulose biosynthesis and biofilm formation. *Mol Microbiol* 2004;54:264–277.

168. **Ferreira RBR, Antunes LCM, Greenberg EP, McCarter LL**. *Vibrio parahaemolyticus* ScrC Modulates Cyclic Dimeric GMP Regulation of Gene Expression Relevant to Growth on Surfaces. *J Bacteriol* 2008;190:851–860.

169. **Tarutina M, Ryjenkov DA, Gomelsky M**. An Unorthodox Bacteriophytochrome from *Rhodobacter sphaeroides* Involved in Turnover of the Second Messenger c-di-GMP. *J Biol Chem* 2006;281:34751–34758.

170. **Bharati BK, Mukherjee R, Chatterji D**. Substrate-induced domain movement in a bifunctional protein, DcpA, regulates cyclic di-GMP turnover: Functional implications of a highly conserved motif. *J Biol Chem* 2018;293:14065–14079.

171. **Sharma IM, Prakash S, Dhanaraman T, Chatterji D**. Characterization of a dual-active enzyme, DcpA, involved in cyclic diguanosine monophosphate turnover in *Mycobacterium smegmatis*. *Microbiology (N Y)* 2014;160:2304–2318.

172. **Phippen CW, Mikolajek H, Schlaefli HG, Keevil CW, Webb JS, *et al.*** Formation and dimerization of the phosphodiesterase active site of the *Pseudomonas aeruginosa* MorA, a bi-functional c-di-GMP regulator. *FEBS Lett* 2014;588:4631–4636.

173. **Bomchil N, Watnick P, Kolter R**. Identification and Characterization of a *Vibrio cholerae* Gene, *mbaA*, Involved in Maintenance of Biofilm Architecture. *J Bacteriol* 2003;185:1384–1390.

174. **Hay ID, Remminghorst U, Rehm BHA**. MucR, a Novel Membrane-Associated Regulator of Alginate Biosynthesis in *Pseudomonas aeruginosa*. *Appl Environ Microbiol* 2009;75:1110–1120.

175. **Rick T, Kreiling V, Höing A, Fiedler S, Glatter T, *et al.*** GGDEF domain as spatial on-switch for a phosphodiesterase by interaction with landmark protein HubP. *NPJ Biofilms Microbiomes* 2022;8:35.

176. **Jonas K, Tomenius H, Römling U, Georgellis D, Melefors Ö**. Identification of YhdA as a regulator of the *Escherichia coli* carbon storage regulation system. *FEMS Microbiol Lett* 2006;264:232–237.

177. **Collins AJ, Smith TJ, Sondermann H, O'Toole GA**. From Input to Output: The Lap/c-di-GMP Biofilm Regulatory Circuit. *Annu Rev Microbiol* 2020;74:607–631.

178. **Hengge R**. Trigger phosphodiesterases as a novel class of c-di-GMP effector proteins. *Philosophical Transactions of the Royal Society B: Biological Sciences* 2016;371:20150498.

179. **Lindenberg S, Klauck G, Pesavento C, Klauck E, Hengge R**. The EAL domain protein YciR acts as a trigger enzyme in a c-di-GMP signalling cascade in *E. coli* biofilm control. *Embo j* 2013;32:2001–2014.

180. **Laventie B-J, Jenal U**. Surface Sensing and Adaptation in Bacteria. *Annu Rev Microbiol* 2020;74:735–760.

181. **Vrabioiu AM, Berg HC**. Signaling events that occur when cells of *Escherichia coli* encounter a glass surface. *Proc Natl Acad Sci U S A* 2022;119:e2116830119.

182. **Kaczmarczyk A, van Vliet S, Jakob RP, Teixeira RD, Scheidat I, *et al.*** A genetically encoded biosensor to monitor dynamic changes of c-di-GMP with high temporal resolution. *Nat Commun* 2024;15:3920.

183. **Hershey DM**. Integrated control of surface adaptation by the bacterial flagellum. *Curr Opin Microbiol* 2021;61:1–7.

184. **Sauer K, Stoodley P, Goeres DM, Hall-Stoodley L, Burmølle M, *et al.*** The biofilm life cycle: expanding the conceptual model of biofilm formation. *Nat Rev Microbiol* 2022;20:608–620.

185. **Wolfe AJ, Visick KL**. Get the Message Out: Cyclic-Di-GMP Regulates Multiple Levels of Flagellum-Based Motility. *J Bacteriol* 2008;190:463–475.

186. **Armitage JP, Berry RM**. Assembly and Dynamics of the Bacterial Flagellum. *Annu Rev Microbiol* 2020;74:181–200.

187. **Echazarreta MA, Klose KE**. Vibrio Flagellar Synthesis. *Front Cell Infect Microbiol* 2019:1;9:131.

188. **Dasgupta N, Wolfgang MC, Goodman AL, Arora SK, Jyot J, *et al.*** A four-tiered transcriptional regulatory circuit controls flagellar biogenesis in *Pseudomonas aeruginosa*. *Mol Microbiol* 2003;50:809–824.

189. **Arora SK, Ritchings BW, Almira EC, Lory S, Ramphal R**. A transcriptional activator, FleQ, regulates mucin adhesion and flagellar gene expression in *Pseudomonas aeruginosa* in a cascade manner. *J Bacteriol* 1997;179:5574–5581.

190. **Klose KE, Mekalanos JJ**. Differential Regulation of Multiple Flagellins in *Vibrio cholerae*. *J Bacteriol* 1998;180:303–316.

191. **Martin B, María-Trinidad G, J SD, Yuli G, D GJ**. The Bacterial Enhancer-Dependent ς54(ςN) Transcription Factor. *J Bacteriol* 2000;182:4129–4136.

192. **Prouty MG, Correa NE, Klose KE**. The novel σ54- and σ28-dependent flagellar gene transcription hierarchy of *Vibrio cholerae*. *Mol Microbiol* 2001;39:1595–1609.

193. **Srivastava D, Hsieh M-L, Khataokar A, Neiditch MB, Waters CM**. Cyclic di-GMP inhibits *Vibrio cholerae* motility by repressing induction of transcription and inducing extracellular polysaccharide production. *Mol Microbiol* 2013;90:1262–1276.

194. **Hickman JW, Harwood CS**. Identification of FleQ from *Pseudomonas aeruginosa* as a c-di-GMP-responsive transcription factor. *Mol Microbiol* 2008;69:376–389.

195. **Trampari E, Stevenson CE, Little RH, Wilhelm T, Lawson DM, *et al.*** Bacterial rotary export ATPases are allosterically regulated by the nucleotide second messenger cyclic-di-GMP. *J Biol Chem* 2015;290:24470–24483.

196. **Boehm A, Kaiser M, Li H, Spangler C, Kasper CA, *et al.*** Second Messenger-Mediated Adjustment of Bacterial Swimming Velocity. *Cell* 2010;141:107–116.

197. **Baker AE, Diepold A, Kuchma SL, Scott JE, Ha DG, *et al.*** PilZ Domain Protein FlgZ Mediates Cyclic Di-GMP-Dependent Swarming Motility Control in *Pseudomonas aeruginosa*. *J Bacteriol* 2016;198:1837–1846.

198. **Violeta Z, Begoña G, Cristina L, Maite E, Alejandro T-A, *et al.*** Coordinated Cyclic-Di-GMP Repression of *Salmonella* Motility through YcgR and Cellulose. *J Bacteriol* 2013;195:417–428.

199. **Paul K, Nieto V, Carlquist WC, Blair DF, Harshey RM**. The c-di-GMP Binding Protein YcgR Controls Flagellar Motor Direction and Speed to Affect Chemotaxis by a “Backstop Brake” Mechanism. *Mol Cell* 2010;38:128–139.

200. **Fang X, Gomelsky M**. A post-translational, c-di-GMP-dependent mechanism regulating flagellar motility. *Mol Microbiol* 2010;76:1295–1305.

201. **Floyd KA, Lee CK, Xian W, Nametalla M, Valentine A, *et al.*** c-di-GMP modulates type IV MSHA pilus retraction and surface attachment in *Vibrio cholerae*. *Nat Commun* 2020;11:1549.

202. **Jones CJ, Utada A, Davis KR, Thongsomboon W, Zamorano Sanchez D, *et al.*** C-di-GMP Regulates Motile to Sessile Transition by Modulating MshA Pili Biogenesis and Near-Surface Motility Behavior in *Vibrio cholerae*. *PLoS Pathog* 2015;11:e1005068.

203. **Teschler JK, Zamorano-Sanchez D, Utada AS, Warner CJA, Wong GCL, *et al.*** Living in the matrix: assembly and control of *Vibrio cholerae* biofilms. *Nat Rev Microbiol* 2015;13:255–268.

204. **Laventie B-J, Sangermani M, Estermann F, Manfredi P, Planes R, *et al.*** A Surface-Induced Asymmetric Program Promotes Tissue Colonization by *Pseudomonas aeruginosa*. *Cell Host Microbe* 2019;25:140-152.e6.

205. **Merritt JH, Ha DG, Cowles KN, Lu W, Morales DK, *et al.*** Specific control of *Pseudomonas aeruginosa* surface-associated behaviors by two c-di-GMP diguanylate cyclases. *mBio* 2010:19;1(4):e00183-10.

206. **Hug I, Deshpande S, Sprecher KS, Pfohl T, Jenal U**. Second messenger-mediated tactile response by a bacterial rotary motor. *Science* 2017;358:531–534.

207. **Ma LZ, Wang D, Liu Y, Zhang Z, Wozniak DJ**. Regulation of Biofilm Exopolysaccharide Biosynthesis and Degradation in *Pseudomonas aeruginosa*. *Annu Rev Microbiol* 2022;76:413–433.

208. **Beloin C, Roux A, Ghigo J-M**. *Escherichia coli* Biofilms. In: Romeo T (editor). *Bacterial Biofilms*. Berlin, Heidelberg: Springer Berlin Heidelberg. pp. 249–289.

209. **Hall-Stoodley L, Costerton JW, Stoodley P**. Bacterial biofilms: from the Natural environment to infectious diseases. *Nat Rev Micro* 2004;2:95–108.

210. **Beyhan S, Bilecen K, Salama SR, Casper-Lindley C, Yildiz FH**. Regulation of Rugosity and Biofilm Formation in *Vibrio cholerae*: Comparison of VpsT and VpsR Regulons and Epistasis Analysis of *vpsT*, *vpsR*, and *hapR*. *J Bacteriol* 2007;189:388–402.

211. **Zamorano-Sánchez D, Fong JCN, Kilic S, Erill I, Yildiz FH**. Identification and Characterization of VpsR and VpsT Binding Sites in *Vibrio cholerae*. *J Bacteriol* 2015;197:1221–1235.

212. **Krasteva P V, Fong JC, Shikuma NJ, Beyhan S, Navarro M V, *et al.*** *Vibrio cholerae* VpsT regulates matrix production and motility by directly sensing cyclic di-GMP. *Science* 2010;327:866–868.

213. **Shikuma NJ, Fong JCN, Yildiz FH**. Cellular Levels and Binding of c-di-GMP Control Subcellular Localization and Activity of the *Vibrio cholerae* Transcriptional Regulator VpsT. *PLoS Pathog* 2012;8:e1002719.

214. **Hsieh M-L, Hinton DM, Waters CM**. VpsR and cyclic di-GMP together drive transcription initiation to activate biofilm formation in *Vibrio cholerae*. *Nucleic Acids Res* 2018;46:8876–8887.

215. **Hsieh M-L, Waters CM, Hinton DM**. VpsR Directly Activates Transcription of Multiple Biofilm Genes in *Vibrio cholerae*. *J Bacteriol* 2020;202:10.1128/jb.00234-20.

216. **Hsieh M-L, Kiel N, Jenkins LMM, Ng W-L, Knipling L, *et al.*** The *Vibrio cholerae* master regulator for the activation of biofilm biogenesis genes, VpsR, senses both cyclic di-GMP and phosphate. *Nucleic Acids Res* 2022;50:4484–4499.

217. **Rumbaugh KP, Sauer K**. Biofilm dispersion. *Nat Rev Microbiol* 2020;18:571–586.

218. **Park S, Sauer K**. Controlling Biofilm Development Through Cyclic di-GMP Signaling. In: Filloux A, Ramos J-L (editors). *Pseudomonas aeruginosa: Biology, Pathogenesis and Control Strategies*. Cham: Springer International Publishing. pp. 69–94.

219. **Schleheck D, Barraud N, Klebensberger J, Webb JS, McDougald D, *et al.*** *Pseudomonas aeruginosa* PAO1 preferentially grows as aggregates in liquid batch cultures and disperses upon starvation. *PLoS One* 2009;4:e5513.

220. **Gjermansen M, Ragas P, Sternberg C, Molin S, Tolker-Nielsen T**. Characterization of starvation-induced dispersion in *Pseudomonas putida* biofilms. *Environ Microbiol* 2005;7:894–904.

221. **Díaz-Salazar C, Calero P, Espinosa-Portero R, Jiménez-Fernández A, Wirebrand L, *et al.*** The stringent response promotes biofilm dispersal in *Pseudomonas putida*. *Sci Rep* 2017;7:18055.

222. **Hay AJ, Zhu J**. Host Intestinal Signal-Promoted Biofilm Dispersal Induces *Vibrio cholerae* Colonization. *Infect Immun* 2015;83:317–323.

223. **Gjermansen M, Nilsson M, Yang L, Tolker-Nielsen T**. Characterization of starvation-induced dispersion in *Pseudomonas putida* biofilms: genetic elements and molecular mechanisms. *Mol Microbiol* 2010;75:815–826.

224. **Basu Roy A, Sauer K**. Diguanylate cyclase NicD-based signalling mechanism of nutrient-induced dispersion by *Pseudomonas aeruginosa*. *Mol Microbiol* 2014;94:771–793.

225. **E PO, Karin S**. PAS Domain Residues and Prosthetic Group Involved in BdlA-Dependent Dispersion Response by *Pseudomonas aeruginosa* Biofilms. *J Bacteriol* 2012;194:5817–5828.

226. **Bridges AA, Bassler BL**. The intragenus and interspecies quorum-sensing autoinducers exert distinct control over *Vibrio cholerae* biofilm formation and dispersal. *PLoS Biol* 2019;17:e3000429-.

227. **Barraud N, Schleheck D, Klebensberger J, Webb JS, Hassett DJ, *et al.*** Nitric Oxide Signaling in *Pseudomonas aeruginosa* Biofilms Mediates Phosphodiesterase Activity, Decreased Cyclic Di-GMP Levels, and Enhanced Dispersal. *J Bacteriol* 2009;191:7333–7342.

228. **Barraud N, Hassett DJ, Hwang S-H, Rice SA, Kjelleberg S, *et al.*** Involvement of Nitric Oxide in Biofilm Dispersal of *Pseudomonas aeruginosa*. *J Bacteriol* 2006;188:7344–7353.

229. **Li Y, Heine S, Entian M, Sauer K, Frankenberg-Dinkel N**. NO-Induced Biofilm Dispersion in *Pseudomonas aeruginosa* Is Mediated by an MHYT Domain-Coupled Phosphodiesterase. *J Bacteriol* 2013;195:3531–3542.

230. **Ha D-G, O'Toole GA**. c-di-GMP and its Effects on Biofilm Formation and Dispersion: a *Pseudomonas Aeruginosa* Review. *Microbiol Spectr* 2015;3:10.1128/microbiolspec.mb-0003–2014.

231. **Bridges AA, Prentice JA, Wingreen NS, Bassler BL**. Signal Transduction Network Principles Underlying Bacterial Collective Behaviors. *Annu Rev Microbiol* 2022;76:235–257.

232. **Christensen LD, van Gennip M, Rybtke MT, Wu H, Chiang W-C, *et al.*** Clearance of *Pseudomonas aeruginosa* Foreign-Body Biofilm Infections through Reduction of the Cyclic Di-GMP Level in the Bacteria. *Infect Immun* 2013;81:2705–2713.

233. **Bo AJ, Nørskov KK, Dahl HL, Morten R, Martin N, *et al.*** Induction of Native c-di-GMP Phosphodiesterases Leads to Dispersal of *Pseudomonas aeruginosa* Biofilms. *Antimicrob Agents Chemother* 2021;65:10.1128/aac.02431-20.

234. **Dahl HL, Bo AJ, Martin NC, Uldahl JC, Morten R, *et al.*** High efficacy treatment of murine *Pseudomonas aeruginosa* catheter-associated urinary tract infections using the c-di-GMP modulating anti-biofilm compound Disperazol in combination with ciprofloxacin. *Antimicrob Agents Chemother* 2024;68:e01481-23.

235. **Fernandez NL, Srivastava D, Ngouajio AL, Waters CM**. Cyclic di-GMP Positively Regulates DNA Repair in *Vibrio cholerae*. *J Bacteriol* 2018;200:e00005-18.

236. **Pratt JT, Tamayo R, Tischler AD, Camilli A**. PilZ Domain Proteins Bind Cyclic Diguanylate and Regulate Diverse Processes in *Vibrio cholerae*. *J Biol Chem* 2007;282:12860–12870.

237. **Crisan C V, Hammer BK**. The *Vibrio cholerae* type VI secretion system: toxins, regulators and consequences. *Environ Microbiol* 2020;22:4112–4122.

238. **Beyhan S, Tischler AD, Camilli A, Yildiz FH**. Transcriptome and Phenotypic Responses of *Vibrio cholerae* to Increased Cyclic di-GMP Level. *J Bacteriol* 2006;188:3600–3613.

239. **Tischler A, Lee SH, Camilli A**. The *Vibrio cholerae* vieSAB Locus Encodes a Pathway Contributing to Cholera Toxin Production. *J Bacteriol* 2002;184:4104–4113.

240. **Dey AK, Bhagat A, Chowdhury R**. Host Cell Contact Induces Expression of Virulence Factors and VieA, a Cyclic di-GMP Phosphodiesterase, in *Vibrio cholerae*. *J Bacteriol* 2013;195:2004–2010.

241. **Tamayo R, Schild S, Pratt JT, Camilli A**. Role of Cyclic Di-GMP during El Tor Biotype *Vibrio cholerae* Infection: Characterization of the *In Vivo*-Induced Cyclic Di-GMP Phosphodiesterase CdpA. *Infect Immun* 2008;76:1617–1627.

242. **Metzger LC, Stutzmann S, Scrignari T, Van der Henst C, Matthey N, *et al.*** Independent Regulation of Type VI Secretion in *Vibrio cholerae* by TfoX and TfoY. *Cell Rep* 2016;15:951–958.

243. **Lim B, Beyhan S, Yildiz FH**. Regulation of *Vibrio* Polysaccharide Synthesis and Virulence Factor Production by CdgC, a GGDEF-EAL Domain Protein, in *Vibrio cholerae*. *J Bacteriol* 2007;189:717–729.

244. **Beyhan S, Tischler AD, Camilli A, Yildiz FH**. Differences in Gene Expression between the Classical and El Tor Biotypes of *Vibrio cholerae* O1. *Infect Immun* 2006;74:3633–3642.

245. **Liu X, Beyhan S, Lim B, Linington RG, Yildiz FH**. Identification and Characterization of a Phosphodiesterase That Inversely Regulates Motility and Biofilm Formation in *Vibrio cholerae*. *J Bacteriol* 2010;192:4541–4552.

246. **Mukherjee S, Bassler BL**. Bacterial quorum sensing in complex and dynamically changing environments. *Nat Rev Microbiol* 2019;17:371–382.

247. **Hammer BK, Bassler BL**. Quorum sensing controls biofilm formation in *Vibrio cholerae*. *Mol Microbiol* 2003;50:101–104.

248. **Waters CM, Lu W, Rabinowitz JD, Bassler BL**. Quorum Sensing Controls Biofilm Formation in *Vibrio cholerae* through Modulation of Cyclic Di-GMP Levels and Repression of *vpsT*. *J Bacteriol* 2008;190:2527–2536.

249. **Tsou AM, Cai T, Liu Z, Zhu J, Kulkarni R V**. Regulatory targets of quorum sensing in *Vibrio cholerae*: evidence for two distinct HapR-binding motifs. *Nucleic Acids Res* 2009;37:2747–2756.

250. **Srivastava D, Harris RC, Waters CM**. Integration of Cyclic di-GMP and Quorum Sensing in the Control of *vpsT* and *aphA* in *Vibrio cholerae*. *J Bacteriol* 2011;193:6331–6341.

251. **Qin B, Bassler BL**. Quorum-sensing control of matrix protein production drives fractal wrinkling and interfacial localization of *Vibrio cholerae* pellicles. *Nat Commun* 2022;13:6063.

252. **Qin B, Fei C, Wang B, Stone HA, Wingreen NS, *et al.*** Hierarchical transitions and fractal wrinkling drive bacterial pellicle morphogenesis. *Proc Natl Acad Sci U S A* 2021;118:e2023504118.

253. **Jemielita M, Wingreen NS, Bassler BL**. Quorum sensing controls *Vibrio cholerae* multicellular aggregate formation. *Elife* 2018;7:e42057.

254. **Ciofu O, Moser C, Jensen PØ, Høiby N**. Tolerance and resistance of microbial biofilms. *Nat Rev Microbiol* 2022;20:621–635.

255. **Lebeaux D, Ghigo J-M, Beloin C**. Biofilm-Related Infections: Bridging the Gap between Clinical Management and Fundamental Aspects of Recalcitrance toward Antibiotics. *Microbiology and Molecular Biology Reviews* 2014;78:510–543.

256. **Coenye T, Bové M, Bjarnsholt T**. Biofilm antimicrobial susceptibility through an experimental evolutionary lens. *NPJ Biofilms Microbiomes* 2022;8:82.

257. **Brauner A, Fridman O, Gefen O, Balaban NQ**. Distinguishing between resistance, tolerance and persistence to antibiotic treatment. *Nat Rev Microbiol* 2016;14:320–330.

258. **Olsen I**. Biofilm-specific antibiotic tolerance and resistance. *European Journal of Clinical Microbiology & Infectious Diseases* 2015;34:877–886.

259. **Høiby N, Bjarnsholt T, Moser C, Bassi GL, Coenye T, *et al.*** ESCMID guideline for the diagnosis and treatment of biofilm infections 2014. *Clinical Microbiology and Infection* 2015;21:S1–S25.

260. **Yildiz F, Fong J, Sadovskaya I, Grard T, Vinogradov E**. Structural Characterization of the Extracellular Polysaccharide from *Vibrio cholerae* O1 El-Tor. *PLoS One* 2014;9:e86751-.

261. **Fong JCN, Syed KA, Klose KE, Yildiz FH**. Role of *Vibrio* polysaccharide (vps) genes in VPS production, biofilm formation and *Vibrio cholerae* pathogenesis. *Microbiology (N Y)* 2010;156:2757–2769.

262. **Hollenbeck EC, Fong JCN, Lim JY, Yildiz FH, Fuller GG, *et al.*** Molecular Determinants of Mechanical Properties of *V. cholerae* Biofilms at the Air-Liquid Interface. *Biophys J* 2014;107:2245–2252.

263. **Berk V, Fong JCN, Dempsey GT, Develioglu ON, Zhuang X, *et al.*** Molecular Architecture and Assembly Principles of *Vibrio cholerae* Biofilms. *Science* 2012;337:236–239.

264. **Absalon C, Van Dellen K, Watnick PI**. A Communal Bacterial Adhesin Anchors Biofilm and Bystander Cells to Surfaces. *PLoS Pathog* 2011;7:e1002210-.

265. **Singh PK, Rode DKH, Buffard P, Nosho K, Bayer M, *et al.*** *Vibrio cholerae* biofilm dispersal regulator causes cell release from matrix through type IV pilus retraction. *bioRxiv* 2021.05.02.442311

266. **Ali A, Johnson JA, Franco AA, Metzger DJ, Connell TD, *et al.*** Mutations in the extracellular protein secretion pathway genes (*eps*) interfere with rugose polysaccharide production in and motility of *Vibrio cholerae*. *Infect Immun* 2000;68:1967–1974.

267. **Steenackers HP, Parijs I, Foster KR, Vanderleyden J**. Experimental evolution in biofilm populations. *FEMS Microbiol Rev* 2016;40:373–397.

268. **Kawecki TJ, Lenski RE, Ebert D, Hollis B, Olivieri I, *et al.*** Experimental evolution. *Trends Ecol Evol* 2012;27:547–560.

269. **Bram V den B, Toon S, Maarten F, Jan M**. Experimental Design, Population Dynamics, and Diversity in Microbial Experimental Evolution. *Microbiology and Molecular Biology Reviews* 2018;82:10.1128/mmbr.00008-18.

270. **Lenski RE**. Convergence and Divergence in a Long-Term Experiment with Bacteria. *Am Nat* 2017;190:S57–S68.

271. **Lenski RE**. Revisiting the Design of the Long-Term Evolution Experiment with *Escherichia coli*. *J Mol Evol* 2023;91:241–253.

272. **Lenski RE**. Phenotypic and Genomic Evolution during a 20,000-Generation Experiment with the Bacterium *Escherichia coli*. In: *Plant Breeding Reviews*. pp. 225–265.

273. **Lenski RE**. Experimental evolution and the dynamics of adaptation and genome evolution in microbial populations. *ISME J* 2017;11:2181–2194.

274. **Cooper Vaughn S.** Experimental Evolution as a High-Throughput Screen for Genetic Adaptations. *mSphere* 2018;3:10.1128/msphere.00121-18.

275. **Cain AK, Barquist L, Goodman AL, Paulsen IT, Parkhill J, *et al.*** A decade of advances in transposon-insertion sequencing. *Nat Rev Genet* 2020;21:526–540.

276. **Rainey PB, Travisano M**. Adaptive radiation in a heterogeneous environment. *Nature* 1998;394:69–72.

277. **Korona R, Nakatsu CH, Forney LJ, Lenski RE**. Evidence for multiple adaptive peaks from populations of bacteria evolving in a structured habitat. *Proc Natl Acad Sci U S A* 1994;91:9037–9041.

278. **Kovács Á T, Dragoš A**. Evolved Biofilm: Review on the Experimental Evolution Studies of *Bacillus subtilis* Pellicles. *J Mol Biol* 2019;431:4749–4759.

279. **Poltak SR, Cooper VS**. Ecological succession in long-term experimentally evolved biofilms produces synergistic communities. *ISME J* 2011;5:369–378.

280. **Allegrucci M, Sauer K**. Characterization of Colony Morphology Variants Isolated from *Streptococcus pneumoniae* Biofilms. *J Bacteriol* 2007;189:2030–2038.

281. **Kraigsley AM, Finkel SE**. Adaptive evolution in single species bacterial biofilms. *FEMS Microbiol Lett* 2009;293:135–140.

282. **Zaborskytė G, Wistrand-Yuen E, Hjort K, Andersson DI, Sandegren L**. Modular 3D-Printed Peg Biofilm Device for Flexible Setup of Surface-Related Biofilm Studies. *Front Cell Infect Microbiol* 2022:3;11:802303.

283. **Boles BR, Thoendel M, Singh PK**. Self-generated diversity produces “insurance effects” in biofilm communities. *Proc Natl Acad Sci U S A* 2004;101:16630–16635.

284. **Traverse CC, Mayo-Smith LM, Poltak SR, Cooper VS**. Tangled bank of experimentally evolved *Burkholderia* biofilms reflects selection during chronic infections. *Proc Natl Acad Sci U S A* 2013;110:E250.

285. **McElroy KE, Hui JGK, Woo JKK, Luk AWS, Webb JS, *et al.*** Strain-specific parallel evolution drives short-term diversification during *Pseudomonas aeruginosa* biofilm formation. *Proc Natl Acad Sci U S A* 2014;111:E1419–E1427.

286. **Flynn Kenneth M, Dowell G, Johnson Thomas M, Koestler Benjamin J, Waters Christopher M, *et al.*** Evolution of Ecological Diversity in Biofilms of *Pseudomonas aeruginosa* by Altered Cyclic Diguanylate Signaling. *J Bacteriol* 2016;198:2608–2618.

287. **Collin K, Wook K**. Identification of Cyclic-di-GMP-Modulating Protein Residues by Bidirectionally Evolving a Social Behavior in *Pseudomonas fluorescens*. *mSystems* 2022;7:e00737-22.

288. **Zaborskytė G, Coelho P, Wrande M, Sandegren L**. Rapid evolution of *Klebsiella pneumoniae* biofilms in vitro delineates adaptive changes selected during infection. *bioRxiv* 2024;2024.03.16.585345.

289. **Zaborskytė G, Hjort K, Lytsy B, Sandegren L**. Convergent within-host evolution alters key virulence factors in a *Klebsiella pneumoniae* clone during a large hospital outbreak. *bioRxiv* 2024;2024.02.06.577356.

290. **Rossi E, La Rosa R, Bartell JA, Marvig RL, Haagensen JAJ, *et al.*** *Pseudomonas aeruginosa* adaptation and evolution in patients with cystic fibrosis. *Nat Rev Microbiol* 2021;19:331–342.

291. **Santos-Lopez A, Marshall CW, Scribner MR, Snyder DJ, Cooper VS**. Evolutionary pathways to antibiotic resistance are dependent upon environmental structure and bacterial lifestyle. *Elife* 2019;8:e47612.

292. **Ahmed MN, Abdelsamad A, Wassermann T, Porse A, Becker J, *et al.*** The evolutionary trajectories of *P. aeruginosa* in biofilm and planktonic growth modes exposed to ciprofloxacin: beyond selection of antibiotic resistance. *NPJ Biofilms Microbiomes* 2020;6:28.

293. **Scribner MR, Santos-Lopez A, Marshall CW, Deitrick C, Cooper VS**. Parallel Evolution of Tobramycin Resistance across Species and Environments. *mBio* 2020;11:10.1128/mbio.00932-20.

294. **Trubenová B, Roizman D, Moter A, Rolff J, Regoes RR**. Population genetics, biofilm recalcitrance, and antibiotic resistance evolution. *Trends Microbiol* 2022;30:841–852.

295. **Trampari E, Prischi F, Vargiu A V, Abi-Assaf J, Bavro VN, *et al.*** Functionally distinct mutations within AcrB underpin antibiotic resistance in different lifestyles. *npj Antimicrobials and Resistance* 2023;1:2.

296. **Rice EugeneW, Johnson CliffordJ, Clark RobertM, Fox KimR, Reasoner DonaldJ, *et al.*** Chlorine and survival of ‘rugose’ *Vibrio cholerae*. *The Lancet* 1992;340:740.

297. **Baltrus DA, Caitlin S, MacKenzie D, Courtney L, Zoe R, *et al.*** Genomic Background Governs Opposing Responses to Nalidixic Acid upon Megaplasmid Acquisition in *Pseudomonas*. *mSphere* 2021;6:10.1128/msphere.00008-21.

298. **Billane K, Harrison E, Cameron D, Brockhurst MA**. Why do plasmids manipulate the expression of bacterial phenotypes? *Philosophical Transactions of the Royal Society B: Biological Sciences* 2021;377:20200461.

299. **Roemhild R, Bollenbach T, Andersson DI**. The physiology and genetics of bacterial responses to antibiotic combinations. *Nat Rev Microbiol* 2022;20:478–490.

300. **Gallant C V, Daniels C, Leung JM, Ghosh AS, Young KD, *et al.*** Common β-lactamases inhibit bacterial biofilm formation. *Mol Microbiol* 2005;58:1012–1024.

301. **Fernández A, Pérez A, Ayala JA, Mallo S, Rumbo-Feal S, *et al.*** Expression of OXA-Type and SFO-1 β-Lactamases Induces Changes in Peptidoglycan Composition and Affects Bacterial Fitness. *Antimicrob Agents Chemother* 2012;56:1877–1884.

302. **Brülisauer L, Leon-Sampedro R, Hall AR**. Clinical Antibiotic-Resistance Plasmids Have Small Effects on Biofilm Formation and Population Growth in *Escherichia coli in vitro*. *bioRxiv* 2023;2023.03.01.530568.

303. **Schaufler K, Semmler T, Pickard DJ, de Toro M, de la Cruz F, *et al.*** Carriage of Extended-Spectrum Beta-Lactamase-Plasmids Does Not Reduce Fitness but Enhances Virulence in Some Strains of Pandemic *E. coli* Lineages. *Front Microbiol* 2016:17;7:336.

304. **Ghigo JM**. Natural conjugative plasmids induce bacterial biofilm development. *Nature* 2001;412:442–445.

305. **Teodósio JS, Simões M, Mergulhão FJ**. The influence of nonconjugative *Escherichia coli* plasmids on biofilm formation and resistance. *J Appl Microbiol* 2012;113:373–382.

306. **Nesse LL, Mo SS, Ramstad SN, Witsø IL, Sekse C, *et al.*** The Effect of Antimicrobial Resistance Plasmids Carrying blaCMY-2 on Biofilm Formation by *Escherichia coli* from the Broiler Production Chain. *Microorganisms* 2021:5;9(1):104.

307. **Metzger GA, Ridenhour BJ, France M, Gliniewicz K, Millstein J, *et al.*** Biofilms preserve the transmissibility of a multi-drug resistance plasmid. *NPJ Biofilms Microbiomes* 2022;8:95.

308. **Stalder T, Cornwell B, Lacroix J, Kohler B, Dixon S, *et al.*** Evolving Populations in Biofilms Contain More Persistent Plasmids. *Mol Biol Evol* 2020;37:1563–1576.

309. **Kizny Gordon AE, Mathers AJ, Cheong EYL, Gottlieb T, Kotay S, *et al.*** The Hospital Water Environment as a Reservoir for Carbapenem-Resistant Organisms Causing Hospital-Acquired Infections—A Systematic Review of the Literature. *Clinical Infectious Diseases* 2017;64:1435–1444.

310. **Johnson RC, Deming C, Conlan S, Zellmer CJ, Michelin A V, *et al.*** Investigation of a Cluster of *Sphingomonas koreensis* Infections. *New England Journal of Medicine* 2018;379:2529–2539.

311. **Constantinides B, Chau KK, Quan TP, Rodger G, Andersson MI, *et al.*** Genomic surveillance of *Escherichia coli* and *Klebsiella spp*. in hospital sink drains and patients. *Microb Genom 2020 Jul;6(7):mgen000391.*

312. **Aracil-Gisbert S, Fernández-De-Bobadilla MD, Guerra-Pinto N, Serrano-Calleja S, Pérez-Cobas AE, *et al.*** Long-term dynamics of the *Serratia*

marcescens complex" in the hospital-built environment. *bioRxiv* 2023;2023.10.15.562376.

313. **Weng Y, Bina XR, Bina JE**. Complete Genome Sequence of *Vibrio cholerae* O1 El Tor Strain C6706. *Microbiol Resour Announc* 2021;10:10.1128/mra.01301-20.

314. **Taviani E, Grim CJ, Choi J, Chun J, Haley B, *et al.*** Discovery of novel *Vibrio cholerae* VSP-II genomic islands using comparative genomic analysis. *FEMS Microbiol Lett* 2010;308:130–137.

315. **Morais LLC de S, Garza DR, Loureiro ECB, Vale ER, Santos DSA de S, *et al.*** Population and Genetic Study of *Vibrio cholerae* from the Amazon Environment Confirms that the WASA-1 Prophage Is the Main Marker of the Epidemic Strain that Circulated in the Region. *PLoS One* 2013;8:e81372-.

316. **Stutzmann S, Blokesch M**. Circulation of a Quorum-Sensing-Impaired Variant of *Vibrio cholerae* Strain C6706 Masks Important Phenotypes. *mSphere* 2016;1:e00098-16.

317. **Fröhlich C, Sørum V, Tokuriki N, Johnsen PJ, Samuelsen Ø**. Evolution of β-lactamase-mediated cefiderocol resistance. *Journal of Antimicrobial Chemotherapy* 2022;77:2429–2436.

318. **Hartmann R, Jeckel H, Jelli E, Singh PK, Vaidya S, *et al.*** Quantitative image analysis of microbial communities with BiofilmQ. *Nat Microbiol* 2021;6:151–156.

319. **Dubay MM, Acres J, Riekeles M, Nadeau JL**. Recent advances in experimental design and data analysis to characterize prokaryotic motility. *J Microbiol Methods* 2023;204:106658.

320. **Haney EF, Trimble MJ, Cheng JT, Vallé Q, Hancock REW**. Critical Assessment of Methods to Quantify Biofilm Growth and Evaluate Antibiofilm Activity of Host Defence Peptides. *Biomolecules* 2018:21;8(2):29.

321. **Wilson C, Lukowicz R, Merchant S, Valquier-Flynn H, Caballero J, *et al.*** Quantitative and Qualitative Assessment Methods for Biofilm Growth: A Mini-review. *Res Rev J Eng Technol* 2017;6(4)

322. **Heydorn A, Nielsen AT, Hentzer M, Sternberg C, Givskov M, *et al.*** Quantification of biofilm structures by the novel computer program comstat. *Microbiology (N Y)* 2000;146:2395–2407.

323. **O'Toole GA**. Microtiter Dish Biofilm Formation Assay. *JoVE* 2011;e2437.

324. **Prentice JA, van de Weerd R, Bridges AA**. Cell-lysis sensing drives biofilm formation in *Vibrio cholerae*. *Nat Commun* 2024;15:2018.

325. **Andersen JB, Rybtke M, Tolker-Nielsen T**. The dynamics of biofilm development and dispersal should be taken into account when quantifying biofilm via the crystal violet microtiter plate assay. *Biofilm* 2024;8:100207.

326. **Tittsler RP, Sandholzer LA**. The Use of Semi-solid Agar for the Detection of Bacterial Motility. *J Bacteriol* 1936;31:575–580.

327. **Partridge JD, Harshey RM, Partridge JD, Harshey RM**. Investigating Flagella-Driven Motility in *Escherichia coli* by Applying Three Established Techniques in a Series. *JoVE* 2020;e61364.

328. **Palma V, Gutiérrez MS, Vargas O, Parthasarathy R, Navarrete P**. Methods to Evaluate Bacterial Motility and Its Role in Bacterial–Host Interactions. *Microorganisms* 2022:4;10(3):563.

329. **Wick RR, Judd LM, Gorrie CL, Holt KE**. Unicycler: Resolving bacterial genome assemblies from short and long sequencing reads. *PLoS Comput Biol* 2017;13:e1005595–e1005595.

330. **Heather JM, Chain B**. The sequence of sequencers: The history of sequencing DNA. *Genomics* 2016;107:1–8.

331. **Amarasinghe SL, Su S, Dong X, Zappia L, Ritchie ME, *et al.*** Opportunities and challenges in long-read sequencing data analysis. *Genome Biol* 2020;21:30.

332. **De Maio N, Shaw LP, Hubbard A, George S, Sanderson ND, *et al.*** Comparison of long-read sequencing technologies in the hybrid assembly of complex bacterial genomes. *Microb Genom* 2019;5(9):e000294.

333. **Loman NJ, Quick J, Simpson JT**. A complete bacterial genome assembled de novo using only nanopore sequencing data. *Nat Methods* 2015;12:733–735.

334. **George S, Pankhurst L, Hubbard A, Votintseva A, Stoesser N, *et al.*** Resolving plasmid structures in *Enterobacteriaceae* using the MinION nanopore sequencer: assessment of MinION and MinION/Illumina hybrid data assembly approaches. *Microb Genom* 2017:9;3(8):e000118.

335. **Feng Y, Chen H-L, Chiu C-H**. Differential Genomic Variation between Short- and Long-Term Bacterial Evolution Revealed by Ultradeep Sequencing. *Genome Biol Evol* 2013;5:572–577.

336. **McElroy K, Thomas T, Luciani F**. Deep sequencing of evolving pathogen populations: applications, errors, and bioinformatic solutions. *Microb Inform Exp* 2014;4:1.

337. **Kloos J, Gama JA, Hegstad J, Samuelsen Ø, Johnsen PJ**. Piggybacking on Niche Adaptation Improves the Maintenance of Multidrug-Resistance Plasmids. *Mol Biol Evol* 2021;38:3188–3201.

338. **Sanger F, Nicklen S, Coulson AR**. DNA sequencing with chain-terminating inhibitors. *Proc Natl Acad Sci U S A* 1977;74:5463–5467.

339. **Cockerell SR, Rutkovsky AC, Zayner JP, Cooper RE, Porter LR, *et al.*** *Vibrio cholerae* NspS, a homologue of ABC-type periplasmic solute binding proteins, facilitates transduction of polyamine signals independent of their transport. *Microbiology (N Y)* 2014;160:832–843.

340. **Severin GB, Waters CM**. Spectrophotometric and Mass Spectroscopic Methods for the Quantification and Kinetic Evaluation of In Vitro c-di-GMP Synthesis. In: Sauer K (editor). *c-di-GMP Signaling: Methods and Protocols*. New York, NY: Springer New York. pp. 71–84.

341. **Webb MR**. A continuous spectrophotometric assay for inorganic phosphate and for measuring phosphate release kinetics in biological systems. *Proc Natl Acad Sci U S A* 1992;89:4884–4887.

342. **Eli D, Randall TE, Almblad H, Harrison JJ, Banin E**. Measuring Cyclic Diguanylate (c-di-GMP)-Specific Phosphodiesterase Activity Using the MANT-c-di-GMP Assay. In: Sauer K (editor). *c-di-GMP Signaling: Methods and Protocols*. New York, NY: Springer New York. pp. 263–278.

343. **Chao MC, Abel S, Davis BM, Waldor MK**. The design and analysis of transposon insertion sequencing experiments. *Nat Rev Microbiol* 2016;14:119–128.

344. **Abel S, Abel zur Wiesch P, Davis BM, Waldor MK, Hogan DA**. Analysis of Bottlenecks in Experimental Models of Infection. *PLoS Pathog* 2015;11:e1004823.

345. **Rolfs A, Montor WR, Yoon SS, Hu Y, Bhullar B, *et al.*** Production and sequence validation of a complete full length ORF collection for the pathogenic bacterium *Vibrio cholerae*. *Proc Natl Acad Sci U S A* 2008;105:4364–4369.

346. **van Opijnen T, Bodi KL, Camilli A**. Tn-seq: high-throughput parallel sequencing for fitness and genetic interaction studies in microorganisms. *Nat Methods* 2009;6:767–772.

347. **Lee SH, Butler SM, Camilli A**. Selection for in vivo regulators of bacterial virulence. *Proc Natl Acad Sci U S A* 2001;98:6889–6894.

348. **Osorio CG, Crawford JA, Michalski J, Martinez-Wilson H, Kaper JB, *et al.*** Second-Generation Recombination-Based In Vivo Expression Technology for Large-Scale Screening for *Vibrio cholerae* Genes Induced during Infection of the Mouse Small Intestine. *Infect Immun* 2005;73:972–980.

349. **Lombardo M-J, Michalski J, Martinez-Wilson H, Morin C, Hilton T, *et al.*** An in vivo expression technology screen for *Vibrio cholerae* genes expressed in human volunteers. *Proc Natl Acad Sci U S A* 2007;104:18229–18234.

350. **Cameron DE, Urbach JM, Mekalanos JJ**. A defined transposon mutant library and its use in identifying motility genes in *Vibrio cholerae*. *Proc Natl Acad Sci U S A* 2008;105:8736–8741.

351. **Chao MC, Pritchard JR, Zhang YJ, Rubin EJ, Livny J, *et al.*** High-resolution definition of the *Vibrio cholerae* essential gene set with hidden Markov model–based analyses of transposon-insertion sequencing data. *Nucleic Acids Res* 2013;41:9033–9048.

352. **Waters CM, Bassler BL**. Quorum sensing: Cell-to-Cell Communication in Bacteria. *Annu Rev Cell Dev Biol* 2005;21:319–346.

353. **Lung NS, Sophia K, Gabi S, Tobias H, J YP, *et al.*** Evolution of a cis-Acting SNP That Controls Type VI Secretion in *Vibrio cholerae*. *mBio* 2022;13:e00422-22.

354. **Drebes Dörr NC, Proutière A, Jaskólska M, Stutzmann S, Bader L, *et al.*** Single nucleotide polymorphism determines constitutive versus inducible type VI secretion in *Vibrio cholerae*. *ISME J* 2022;16:1868–1872.

355. **Proutière A, Drebes Dörr NC, Bader L, Stutzmann S, Metzger LC, *et al.*** Sporadic type VI secretion in seventh pandemic *Vibrio cholerae*. *Microbiology* 2023;169(5):001329.

356. **Mavian C, Tagliamonte M, Alam M, Sakib SN, Cash M, *et al.*** Ancestral Origin and Dissemination Dynamics of Reemerging Toxigenic *Vibrio cholerae*, Haiti. *Emerging Infectious Disease journal* 2023;29:2072.

357. **Walters C, Chen J, Stroika S, Katz LS, Turnsek M, *et al.*** Genome Sequences from a Reemergence of *Vibrio cholerae* in Haiti, 2022 Reveal Relatedness to Previously Circulating Strains. *J Clin Microbiol* 2023;61:e00142-23.

358. **Hoque MM, Noorian P, Espinoza-Vergara G, Manuneedhi Cholan P, Kim M, *et al.*** Adaptation to an amoeba host drives selection of virulence-associated traits in *Vibrio cholerae*. *ISME J* 2022;16:856–867.

359. **Wei Y, Ocampo P, Levin BR**. An experimental study of the population and evolutionary dynamics of *Vibrio cholerae* O1 and the bacteriophage JSF4. *Proceedings of the Royal Society B: Biological Sciences* 2010;277:3247–3254.

360. **Giacomucci S, Mathieu-Denoncourt A, Vincent AT, Jannadi H, Duperthuy M**. Experimental evolution of *Vibrio cholerae* identifies hypervesiculation as a way to increase motility in the presence of polymyxin B. *Front Microbiol* 2022;13:932165.

361. **Narendrakumar L, Chandrika SK, Thomas S**. Adaptive laboratory evolution of *Vibrio cholerae* to doxycycline associated with spontaneous mutation. *Int J Antimicrob Agents* 2020;56:106097.

362. **Larotonda L, Mornico D, Khanna V, Bernal-Bayard J, Ghigo JM, *et al.*** Chromosomal Position of Ribosomal Protein Genes Affects Long-Term Evolution of *Vibrio cholerae*. *mBio* 2023;14:e03432-22.

363. **Spiers AJ, Kahn SG, Bohannon J, Travisano M, Rainey PB**. Adaptive Divergence in Experimental Populations of *Pseudomonas fluorescens*. Genetic and Phenotypic Bases of Wrinkly Spreader Fitness. *Genetics* 2002;161:33.

364. **Mhatre E, Snyder DJ, Sileo E, Turner CB, Buskirk SW, *et al.*** One gene, multiple ecological strategies: A biofilm regulator is a capacitor for sustainable diversity. *Proc Natl Acad Sci U S A* 2020;117:21647–21657.

365. **Hall CL, Lee VT**. Cyclic-di-GMP regulation of virulence in bacterial pathogens. *WIREs RNA* 2018;9:e1454.

366. **Wang Y, Wang K-M, Zhang X, Wang W, Qian W, *et al.*** *Stenotrophomonas maltophilia* uses a c-di-GMP module to sense the mammalian body temperature during infection. *PLoS Pathog* 2024;20:1–26.

367. **Chong L, Wai LC, Hwa WY, Thing TS, Han PW, *et al.*** Insights into Biofilm Dispersal Regulation from the Crystal Structure of the PAS-GGDEF-EAL Region of RbdA from *Pseudomonas aeruginosa*. *J Bacteriol* 2018;200:e00515-17.

368. **Dahlstrom KM, Giglio KM, Collins AJ, Sondermann H, O'Toole GA**. Contribution of Physical Interactions to Signaling Specificity between a Diguanylate Cyclase and Its Effector. *mBio* 2015;6:e01978-15.

369. **David G, Jarrod ST, J CA, Holger S, J KL, *et al.*** Ligand-Mediated Biofilm Formation via Enhanced Physical Interaction between a Diguanylate Cyclase and Its Receptor. *mBio* 2018;9:10.1128/mbio.01254-18.

370. **Dahlstrom KM, Giglio KM, Sondermann H, O'Toole GA**. The Inhibitory Site of a Diguanylate Cyclase Is a Necessary Element for Interaction and Signaling with an Effector Protein. *J Bacteriol* 2016;198:1595–1603.

371. **Paunola E, Suntio T, Jämsä E, Makarow M**. Folding of Active β-Lactamase in the Yeast Cytoplasm before Translocation into the Endoplasmic Reticulum. *Mol Biol Cell* 1998;9:817–827.

372. **Philippon A, Jacquier H, Ruppé E, Labia R**. Structure-based classification of class A beta-lactamases, an update. *Curr Res Transl Med* 2019;67:115–122.

373. **Pemberton OA, Zhang X, Chen Y**. Molecular Basis of Substrate Recognition and Product Release by the *Klebsiella pneumoniae* Carbapenemase (KPC-2). *J Med Chem* 2017;60:3525–3530.

374. **Yang G, Miton CM, Tokuriki N**. A mechanistic view of enzyme evolution. *Protein Science* 2020;29:1724–1747.

375. **Fröhlich C, Chen JZ, Gholipour S, Erdogan AN, Tokuriki N**. Evolution of β-lactamases and enzyme promiscuity. *Protein Engineering, Design and Selection* 2021;34:gzab013.

376. **Baier F, Hong N, Yang G, Pabis A, Miton CM, *et al.*** Cryptic genetic variation shapes the adaptive evolutionary potential of enzymes. *Elife* 2019;8:e40789.

377. **Madsen JS, Riber L, Kot W, Basfeld A, Burmølle M, *et al.*** Type 3 Fimbriae Encoded on Plasmids Are Expressed from a Unique Promoter without Affecting Host Motility, Facilitating an Exceptional Phenotype That Enhances Conjugal Plasmid Transfer. *PLoS One* 2016;11:e0162390-.

378. **Madsen JS, Hylling O, Jacquiod S, Pécastaings S, Hansen LH, *et al.*** An intriguing relationship between the cyclic diguanylate signaling system and horizontal gene transfer. *ISME J* 2018;12:2330–2334.

379. **Madsen JS, Burmølle M, Hansen LH, Sørensen SJ**. The interconnection between biofilm formation and horizontal gene transfer. *FEMS Immunol Med Microbiol* 2012;65:183–195.

Appendix: Paper 1

A comparative genomic and phenotypic study of *Vibrio cholerae* model strains using hybrid sequencing

Øyvind M. Lorentzen (orcid.org/0009-0007-3386-0794)[1,#], Christina Bleis (orcid.org/0009-0003-7348-8123)[1], Sören Abel (orcid.org/0000-0002-4041-6989)[1,2,#]

[1] Department of Pharmacy, UiT The Arctic University of Norway, Tromsø, Norway

[2] Division of Infection Control, Norwegian Institute of Public Health, Oslo, Norway

[#] corresponding authors: oyvind.m.lorentzen@uit.no and soren.abel@fhi.no

Keywords

Vibrio cholerae, biofilm, motility, c-di-GMP signaling, quorum sensing, hybrid sequencing

Repositories

BioProject accession: PRJNA1109855. Accession number: CP157384, CP157385.

Abstract

Next-generation sequencing methods have become essential for studying bacterial biology and pathogenesis, often depending on high-quality, closed genomes. In this study, we utilized a hybrid sequencing approach to assemble the genome of C6706, a widely used *Vibrio cholerae* model strain. We present a manually curated annotation of the genome, enhancing user accessibility by linking each coding sequence to its counterpart in N16961, the first sequenced *V. cholerae* isolate and a commonly used reference genome. Comparative genomic analysis between *V. cholerae* C6706 and N16961 uncovered multiple genetic differences in genes associated with key biological functions. To determine whether these genetic variations result in phenotypic differences, we compared several phenotypes relevant to *V. cholerae* pathogenicity like genetic stability, acid sensitivity, biofilm formation, and motility. Notably, *V. cholerae* N16961 exhibited greater motility and reduced biofilm formation compared to *V. cholerae* C6706. These phenotypic differences appear to be mediated by variations in quorum sensing and cyclic di-GMP signaling pathways between the strains. This study provides valuable insights into the regulation of biofilm formation and motility in *V. cholerae*.

Impact Statement

This study utilizes hybrid sequencing and manually curated annotation to provide a high-quality genome of *V. cholerae* C6706 that serves as a user-friendly tool to study this commonly used model strain. We uncover genotypic and phenotypic variance compared to *V. cholerae* N16961, which is widely used as reference genome. Notably, distinct biofilm formation and motility patterns between the strains appear linked to differences in quorum sensing and c-di-GMP signaling pathways.

Introduction

Vibrio cholerae is the enteric pathogen that causes cholera, an acute diarrheal disease that can spread explosively and cause devastating outbreaks [1]. Annually, approximately 3 million people are infected, and 95 000 deaths are associated with the disease [2], making this pathogen a serious global health threat.

So far, the world has experienced seven cholera pandemics, spreading the pathogen globally [1, 3]. The most commonly studied strains today, all originate from the 7th pandemic and belong to the O1 serotype, biotype El Tor. The El Tor biotype is the currently dominating *V. cholerae* variant, responsible for the ongoing 7th pandemic [1, 4]. Among them are *V. cholerae* N16961, C6706, E7946, A1552 and 2010EL-1786 [5–9]. Even though they belong to the 7th pandemic, they differ in origin and belong to different transmission waves within the 7th pandemic [4]. *V. cholerae* C6706 and A1552 were isolated from an outbreak in the South America in the 1990s, while *V. cholerae* 2010EL-1786 stems from the 2010 Haiti cholera outbreak [5–9]. N16961 and E7946 were isolated in Asia in the 1970s. N16961 was the first sequenced *V. cholerae* isolate and has been used as reference genome for 7th pandemic *V. cholerae* El Tor strains [7]. While other *V. cholerae* variants have been sequenced more recently [9–12], including a *V. cholerae* C6706 strain [9–12], the original N16961 annotation is still widely used [13–19].

V. cholerae survives in the aquatic environment year-round in endemic regions and infects humans through contaminated water and food [1, 20]. Throughout its life cycle, the pathogen alternates between the aquatic environment and the human host. To successfully survive these transitions, *V. cholerae* depends on multiple cellular processes [1, 20, 21]. Biofilm formation plays an important role in the life cycle of *V. cholerae*. Growth in biofilms facilitates survival in the aquatic environment and increases the acid tolerance and infectivity of *V. cholerae* [21–25]. Two of the key regulators of biofilm formation in *V. cholerae* are quorum sensing (QS) and the cyclic diguanylate (c-di-GMP) signaling system. Quorum sensing is a key bacterial cell-cell communication system that governs collective behavior in bacteria in response to cell-population density and composition [19, 26].

Low cell-density (LCD) induces biofilm formation through phosphorylation of the response regulator LuxO, which in turn simultaneously represses HapR and activates AphA, which are high-cell- and low-cell-density master QS regulators [19, 27–29]. HapR and AphA repress and stimulate expression of biofilm genes, respectively. In contrast, high cell-density (HCD) leads to dephosphorylation of LuxO, which results in repression of AphA and expression of HapR, thereby, inhibiting biofilm formation [19, 27–29]. QS-states can differ between different 7th pandemic *V. cholerae* strains. For instance, the N16961 carries a frameshift mutation in HapR, which disrupts the QS signaling pathway and locks the strain into the state it assumes under low cell density conditions [7, 30, 31]. One of the mechanisms through which QS represses biofilm formation in *V. cholerae* involves regulation of c-di-GMP-metabolizing enzymes [28, 32–34]. C-di-GMP is a conserved nucleotide-based second messenger that regulates biofilm formation and motility in bacteria [35–37]. In short, c-di-GMP upregulates biofilm formation and inhibits motility. C-di-GMP regulates biofilm formation and motility through multiple regulatory mechanisms, which include flagellum synthesis and function, production of pilis and adhesins and secretion of extracellular polymeric substances (EPS)[35–37]. Strikingly, many Gram-negative pathogens with complex life cycles also boast complex c-di-GMP signaling systems [37]. In particular, *V. cholerae* possess more than 60 putative c-di-GMP-metabolizing proteins [35, 36].

One of the first barriers *V. cholerae* encounters in the human host is the acidic environment of the stomach [20, 38]. To overcome acidic conditions, *V. cholerae* employs a response called the “acid tolerance response” (ATR) [39]. This is a cascade of physiological responses that enable the bacterium to counteract the damaging effects of acid stress. One extensively studied component of ATR is the Cad system (*CadABC*), which maintains the intracellular pH balance by converting H^+ and lysine to cadaverine [20, 39–41]. After passage through the stomach, the pathogen enters and colonizes the small intestine to cause the characteristic symptoms of the disease [1, 20]. To summarize, the pathogenicity of *V. cholerae* depends on multiple physiological processes including acid tolerance, motility, chemotaxis, biofilm formation, and QS [1, 19–21].

In this study, we de novo assembled the genome of *V. cholerae* C6706 using short- and long-read next-generation sequencing technologies. As an effort to improve upon the prior version of the C6706 genome, we also manually curated the genome annotation and linked all open reading frames (ORF) with the corresponding ORF in the N16961 genome. We thereby created an accessible genome with a link to the N16961 reference genome. Finally, we conducted a genetic and phenotypic comparison of *V. cholerae* C6706 and N16961 to reveal differences between the two strains, thus contributing to the understanding of *V. cholerae* biology.

Material and methods

Strains, growth media and oligonucleotides

All bacterial strains used in this work are listed in table 1. Unless otherwise noted, cultures were grown from single colonies in Lysogeny-Broth-Miller (LB) media (10 g/L of tryptone, 10 g/L of sodium chloride and 5 g/L of yeast extract) at 37 °C with shaking at 700 rpm. Media were supplemented with carbenicillin (50 µg/mL) when *V. cholerae* strains carrying plasmids were grown to maintain the plasmid. For the acid killing assay the pH of the medium was adjusted to pH 4.6 with a 0.1 M solution of HCl. All oligonucleotides were synthetized by Sigma Aldrich and purified to remove salts.

Table 1: Strains and plasmids used in this study.

Strain no.	Strain background	Vector	Insert	References
3479	*V. cholerae* C6706 QS-deficient	None	None	[6]
1810	*V. cholerae* N16961	None	None	[7]
3802	*V. cholerae* C6706 QS-proficient	None	None	[30]
2832	*V. cholerae* C6706 QS-deficient	pANG01	None	This study
3002	*V. cholerae* C6706 QS-deficient	pOML27	VC1295-mRuby2	This study
3867	*V. cholerae* N16961	pOML27	VC1295-mRuby2	This study
3868	*V. cholerae* N16961	pANG01	None	This study
2844	*E. coli* DH5αpir	None	None	[42]
2988	*E. coli* DH5αpir	pOML27	VC1295-mRuby2	This study
2831	*E. coli* DH5αpir	pANG01	None	This study

Genomic DNA extraction

1 mL of liquid culture of *V. cholerae* in exponential phase was pelleted by centrifugation and resuspended in 50 µL of double-distilled sterile H_2O. Afterwards, 600 µL of lysis buffer (SDS 2% and 0.1 M EDTA) was added and the solution was incubated for 5 minutes at 80 °C to lyse the cells. After incubation, the solution was left to cool down to room temperature. 3 µL RNaseA was then added, and the solution was incubated for 60 minutes at 37 °C. Afterwards, the solution was cooled down to room temperature again, before 200 µL protein precipitation solution (7.5 M ammonium acetate) was added. The solution was incubated on ice for 5 minutes followed by centrifugation to precipitate proteins. The DNA-containing supernatant was recovered while the remaining pellet was discarded. Genomic DNA (gDNA) was then precipitated by adding 600 µL of isopropanol and gentle mixing. The precipitated gDNA was isolated from the tube with a glass pipette and washed in 600 µL of 70% EtOH. Lastly the DNA was centrifuged one more time and the supernatant discarded. The remaining DNA-pellet was carefully dried at room temperature for 30 min and dissolved overnight in Milli-Q filtered water.

Whole-genome data acquisition, assembly, and annotation

The sequencing service was provided by the Norwegian Sequencing Centre (www.sequencing.uio.no), a Norwegian national technology platform hosted by the University of Oslo and supported by the "Functional Genomics" and "Infrastructure" programs of the Research Council of Norway and the Southeastern Regional Health Authorities.

To create the paired-end fragment libraries for Illumina NGS genomic DNA was sheared on a Covaris E220 instrument aiming for a 350 bp fragment size. After fragmentation, the sample was transferred to a 96 plate for a half-volume Kapa Hyper library preparation kit (Roche). Unique dual indexing (Illumina UD adaptor plate, Illumina) was used in the ligation reaction, followed by a clean-up and one round of PCR (4- cycles) to boost library amount. The final library was cleaned twice to get rid of any leftover adapters/dimers. Quality was checked on a Fragment Analyzer instrument using a standard

NGS kit (AATI). Library was sequenced on an Hiseq4000 instrument (150bp PE), and quantified using qPCR (Kapa Library quantification kit, Kapa/Roche).

To conduct PacBio SMRT sequencing, genomic DNA was sheared to 12 kb fragments using g-tubes from Covaris. The library was prepared using Pacific Biosciences protocol for SMRTbell™ with PacBio® Barcoded Adapters for Multiplex SMRT® Sequencing. The sample was pooled together with ten other samples in roughly equimolar ratios. Final library was size selected using 0.45x Ampure PB beads. The library was sequenced on a Pacific Biosciences Sequel instrument using Sequel Polymerase v3.0, SMRT cells v3 LR and Sequencing chemistry v3.0. Loading was performed by diffusion. Sequencing was performed on one SMRT cell. Following sequencing, reads were demultiplexed using the barcoding pipeline on SMRT Link with 26 as minimum barcode score. Finally, HGAP4 assembly was performed using the Assembly (HGAP 4) pipeline on SMRT Link. Assembly was run using 4 Mb as expected genome size.

The final genome was assembled with the hybrid assembler Unicycler with both short and long reads as input sequence [43]. The genome was automatically annotated with the Rapid Annotation and Subsystem Technology (RAST) web tool hosted on PATRIC [44, 45]. Gene annotations in strain C6706 were linked to previously described *V. cholerae* strains by conducting a BLAST-search with every identified coding sequence (CDS) in C6706 against known genomic features in a selection of *V. cholerae* strains [46]. To improve upon the automated annotation of the C6706 genome, all CDS annotated as hypothetical proteins by RAST, were subjected to an additional proteinBLAST-search to identify gene function through comparison with homologs with an E-value <0.05 in other bacterial strains.

Attachment assay

Attachment was used as a proxy for biofilm formation and determined using a crystal violet attachment assay as described before, but in 24-well plates instead of 96-well plates [47]. Briefly, 2 mL LB-medium was inoculated 1:100 with an overnight-culture of *V. cholerae* and grown statically for 24 hours. After 24 hours, the bacterial culture was removed, and the plate was gently submerged in filtered water thrice to remove non-adherent cells. Afterwards, plates were dried for 1 h at 55 °C. To quantify biofilm

158 formation, wells were stained with 2 mL of 0.1% crystal violet (CV) for 10 minutes. After staining, the
159 crystal violet solution was removed, and the plates were again submerged in filtered water to remove
160 non-adherent dye and left to dry at room temperature. The CV was dissolved from the stained biomass
161 with 70% ethanol. Finally, the dissolved dye concentration was quantified by measuring absorbance at
162 595 nm in a Spark® multimode plate reader (Tecan).

163 **Motility on semi-solid agar plates**

164 Colony size on semi-solid agar plates was used as a proxy for motility and was assessed as previously
165 described [48]. Briefly, semi-solid agar plates were made with 60 mL of LB-media containing 0.3%
166 agarose in 140 mm diameter petri dishes. 1 µL of cells grown to exponential phase in LB medium was
167 stabbed into the surface of the swarmer plates with a sterile inoculation loop. The plates were
168 incubated at 37 °C for 12 hours. Afterwards plates were imaged. To quantify the motility, images was
169 imported into FIJI and the diameter of each individual swarm was measured in FIJI with the line and
170 measure function [49].

171 **Variation analysis and genome comparison**

172 Variation analysis was performed with the variation analysis tool hosted by PATRIC [45]. Mutations
173 were called using standard settings with BWA-mem-strict and FreeBayes as aligner and snpcaller,
174 respectively. Mutations called in homopolymeric regions and when comparing the hybrid sequencing
175 assembled genome from this study (BioProject accession PRJNA1109855) to the paired read library of
176 Illumina short read sequences also from this study (Table S1) were omitted. Genome comparison was
177 conducted with progressivMauve [50].

178 **Fluctuation assays**

179 Wild-type *V. cholerae* C6706 and N16961 were grown overnight. A dilution series of the overnight
180 cultures were created and plated onto LB-plate with or without 50 µg/mL rifampicin. After overnight
181 growth at 37 °C, the rifampicin resistant and the total number (resistant and susceptible) of colonies
182 were counted. Mutation rate was calculated with the FALCOR web application using the Ma-Sandri-
183 Sarkar Maximum Likelihood Estimator (MSS-MLE) method [51]. The Student

's t-test was used to determine the significance between observed number of mutational events in C6706 and N16961 based on 9 biological replicates [52].

Acid killing assay

Survival in acidic media was determined as previously described [39]. Briefly, two 100 mL LB cultures were inoculated 1:100 with a starter culture of *V. cholerae* C6706 and N16961, respectively. The two cultures were grown to exponential phase and subsequently diluted to OD_{600} 0.0125. These were used as inoculum into acidic media (LB adjusted to pH 4.6 with 0.1 M HCl). Samples were taken out at time points 0 min, 25 min, 40 min, and 60 min and CFUs was enumerated by plating on LB agar. Experiment was performed in biological triplicates.

Bacterial Fitness Measurements

To start the growth curve experiments, overnight cultures were diluted 1:100 into 300 µL LB-medium and pipetted into a 100-well honeycomb plates (Oy Growth Curves Ab Ltd, Finland). Growth curves were recorded by measuring optical density at 600 nm (OD_{600}) every four minutes for 24 h at 37 °C with continuous shaking in a Bioscreen C instrument (Oy Growth Curves Ab Ltd, Finland). Bacterial fitness was quantified as the area under the curve (AUC) in the growth curves with the flux package in R [53]. Each biological replicate is always based on three technical replicates.

Cloning of VC1295 for expression and fluorescent microscopy

All primers used in this study are listed in table 2. *VC1295* was amplified by PCR with its native promotor from genomic DNA extracted from *V. cholerae* N16961 using primer #153 and #154. The PCR was conducted with Phusion polymerase (New England Biolabs). Afterwards, *VC1295* with its native promotor was cloned onto the pENTRY vector pMaRo1 through a Gibson assembly reaction, which was conducted at 50 °C for 60 min [54]. The correct sequence was confirmed by Sanger sequencing by Macrogen Europe using primer #3 and #4 .

Table 2: Primers used in this study.

No.	Name	Sequence (5' to 3')	Ref.
3	P0003_pEntry_F	gatctcgggccccaaataat	[55]
4	P0004_pEntry_R	gcagctggatggcaaataat	[55]
153	P0153_VC1295_F	TTTTATAATGCCAACTTTGTACAAAAAAGCAGGCT*gtatcttaacagtattccttgataca*	This study
154	P0154_VC1295_R	TCTTATAATGCCAACTTTGTACAAGAAAGCTGGGTtgcggcatctttaaagtgtgct	This study
159	P0159_pANG_Ins_F	cagtgccaacatagtaagccag	This study
160	P0160_pANG_Ins_R	gaagcatttatcagggttattgtctc	This study

The final vector construct carrying *VC1295-mRuby2* under the control of its native promotor was assembled by a Gateway cloning reaction between the pENTRY vector containing *VC1295* and a pDESTINATION vector carrying *mRuby2* [55, 56]. The correct assembly was confirmed by PCR using primer #159 and #160. This vector was then conjugated into *V. cholerae via* the intermediate strain *Escherichia coli* SM10(λpir) [57].

V. cholerae strain carrying a plasmid expressing *VC1295*-mRuby2 was grown to exponential phase. Upon reaching exponential phase, 2 µL of the suspension was spotted on a 1% agarose patched and imaged with an Deltavision Elite (GE Healthcare) inverted microscope with a Deltavision CMOS camera and a UPlanFLN 100× PH NA 1.30 phase contrast objective (Olympus). Images were processed with softWoRx (GE Healthcare), FIJI, and Photoshop CS6 (Adobe) to find focused slide, crop the area of interest and adjust levels [49].

Results

Building a circularized *V. cholerae* C6706 genome

We created a closed circularized genome for *V. cholerae* C6706 with a hybrid sequencing approach that combines both long- and short-read sequencing technology [43]. Long-read sequencing with PacBio sequencing yielded 504,131 subreads with a mean length of 6,801 base pairs generating a total of 1.89x10^9 bases. The assembly yielded two contigs totaling 4,090,295 bp, with an average read depth of 444x. Short-read sequencing using Illumina technology generated a total of 15,841,698 reads, with an average length of 151 base pairs, resulting in an average read depth of 585x. The resulting genome consists of two closed, circular chromosomes of 3,019,923 and 1,070,364 base pairs, respectively. Genome quality evaluation hosted by PATRIC [45] confirmed the assembled genome's completeness at 100%, with a minimal contamination of 0.6 %. Additionally, the genome sequence is of high quality, with coarse and fine consistency values reaching 99.9% and 99.5 %, respectively (Table 3) [58]. Automatic annotation with the Rapid Annotation and Subsystem Technology (RAST), hosted by PATRIC, yielded 3,788 coding sequences (CDS) [44, 45]. To increase usability, every CDS in the C6706 genome has also been linked to the corresponding CDS in *V. cholerae* N16961 by searching for homologues by BLAST (Table S2).

237 **Table 3: Sequencing and genome assembly metrics and genome quality control.**

Table 3. Sequencing and genome assembly metrics and genome quality control	
PacBio sequencing	
Subreads	504,131
Subreads mean length (bp)	6,801
Total reads (bp)	1.89×10^9
Assembly	
2 contigs total (bp)	4,090,295
Average read depth	444x
Illumina sequencing	
Reads total	15,841,698
Mean length (bp)	151
Average read depth	585x
RAST	
Completeness (%)	100
Coarse consistency (%)	99.9
Fine consistency (%)	99.5
Contamination (%)	0.6

238

239

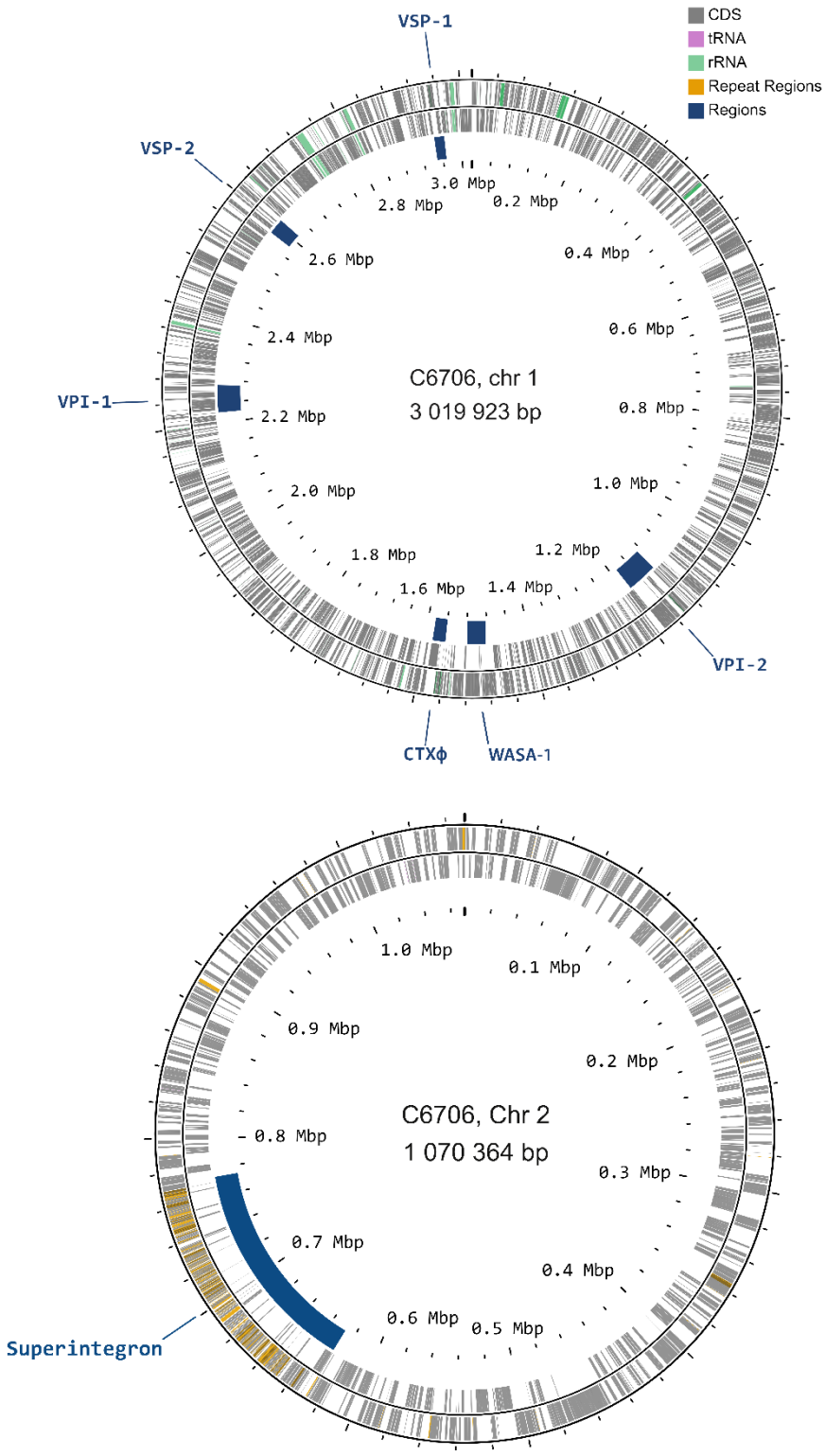

240

241 **Figure 1: Genetic maps of chromosome 1 and 2 of *V. cholerae* C6706.**

242 Maps of chromosome 1 and 2 of *V. cholerae* C6706. Each grey bar represents a coding sequence (CDS),
243 pink bar represents tRNAs, green bars represent rRNAs and orange bars represent repeat regions.
244 Important mobile genetic elements ("regions") are underlined in blue. Maps were created with
245 CGView [59, 60].

V. cholerae C6706 carries multiple genetic changes compared to N16961

The *V. cholerae* El Tor variant C6706 is a commonly used strain by researchers and represents the wild-type in many studies [13, 17, 18, 61, 62]. For a long time, only the genome of *V. cholerae* N16961, another El Tor isolate, was available [7] and researchers have used and are still using it as the de facto reference genome [13–18] despite potential differences between the El Tor variants [4, 9, 10]. To identify the genetic differences between *V. cholerae* C6706 and N16961, we conducted a genome comparison and a variant analysis. The paired read library of Illumina short read sequences from our hybrid sequencing of *V. cholerae* C6706 was used as input. The updated closed genome of *V. cholerae* N16961 (GenBank accession numbers: LT906614, LT906615; PATRIC Genome ID: 243277.254) was used as reference genome. This identified 76 differences, which included 6 deletions, 3 insertions and 67 point mutations. Of the 67 point mutations, there were 44 nonsynonymous mutations and 23 synonymous mutations (Table S3). A genome comparison of *V. cholerae* C6706 and N16961, showcased that C6706 also contained the WASA-1 prophage specific to the West African–South American (WASA) clade of *V. cholerae* isolates, which is not present in N16961 [4, 63]. Similar to what has been observed in other *V. cholerae* strains, chromosome 1 contained a large inversion (Fig. S1) [64, 65]. Comparison to previously sequenced *V. cholerae* C6706 showcased that the inversion varied between assemblies (Fig. S2). Finally, C6706 contained a different variant of the *Vibrio* seventh pandemic island II (VSP-2), which differs from N16961 in the region encompassing VC0511-VC0515 [4, 66, 67]. Overall, the genomes of C6706 and N16961 are very similar except for the two abovementioned mobile genetic elements and inversion in chromosome 1.

Several of the identified mutations in C6706 were located in genes previously linked to important biological functions, such as biofilm formation, motility, quorum sensing, genome stability and repair, and acid tolerance (Table 4). Among the mutated genes was the previously published point mutation (Gly333Ser) in LuxO, which induces a deficiency in quorum sensing (QS) that locks *V. cholerae* into the same state it assumes under low cell density conditions [30]. We also found multiple mutations in c-di-GMP-metabolizing genes, potentially affecting the c-di-GMP turnover of *V. cholerae* C6706

relative to N16961. This included a frameshift mutation in VC1295, a HD-GYP-domain protein predicted to degrade c-di-GMP [68]. In addition, we identified mutations in genes coding for proteins important for flagellar function and chemotaxis. Lastly, we identified mutations in CadB, an enzyme crucial for acid adaptation in several enteric pathogens and RecA, which is essential for the SOS response, DNA repair, and mutagenicity in bacteria [39, 41, 69–71].

Our genetic comparison of *V. cholerae* C6706 and N16961 identified a selection of mutations likely affecting the physiology and adaptability of these strains. To understand the role of these mutations, we employed phenotypic assays to accurately quantify differences in key bacterial phenotypes between *V. cholerae* C6706 and N16961.

Table 4: Selected genes with changes from N16961 to C6706.

Gene accession number N16961	Gene accession number C6706	Nucleotide change	Amino acid change	Gene name	Function	Cellular process
VC0280	VCC2568	C686T	Thr229Ile	*cadB*	Lysine/cadaverine antiporter membrane protein CadB	Acid adaptation
VC0543	VCC2308	A914G	Tyr305Cys	*recA*	RecA protein	Stress response
VC0543	VCC2271	217_218insT*	Val74fs#	*hapR*	Quorum-sensing regulator of virulence	Quorum sensing
VC0653	VCC2204	T1664C	Val555Ala	*rocS*	Diguanylate cyclase / phosphodiesterase	c-di-GMP signaling
VC1021	VCC1859	G997A	Gly333Ser	*luxO*	LuxO global quorum sensing regulator	Quorum sensing
VC1295	VCC1597 /1598	1153delT$	Phe385fs	n/a	c-di-GMP phosphodiesterase (HD-GYP domain)	c-di-GMP signaling
VC1399	VCC1499	837_838insA	Gly279_ Lys280fs	*cheR*	Chemotaxis protein methyltransferase CheR	Motility/ chemotaxis
VC1653	VCC1185	C1675T	His559Tyr	*vieS*	Response regulator VieS	c-di-GMP signaling
VC1967	VCC0880	A277G	Thr93Ala	n/a	Methyl-accepting chemotaxis sensor/transducer protein	Motility/ chemotaxis
VC2191	VCC0672	C863T	Pro288Leu	*flgK*	Flagellar hook-associated protein FlgK	Motility/ chemotaxis
VC2208	VCC0655	G283A	Ala95Thr	*flgT*	Flagellar protein FlgT	Motility/ chemotaxis
VC2338	VCC0536	C1237T	Leu413Phe	*lacZ*	Beta-galactosidase	Metabolism
VCA0557	VCCA0844	A926G	Asp309Gly	n/a	Diguanylate cyclase	c-di-GMP signaling
VCA0931	VCCA0133	G1207A	Ala403Thr	n/a	c-di-GMP phosphodiesterase (HD-GYP domain)	c-di-GMP signaling
VCA1084	VCCA0275	G339A	Met113Ile	*lapB*	Type I secretion system ATPase, LssB family LapB	Type II secretion systems

* "ins" indicates an insertion between the two given positions within a gene.

"fs" indicates a frame shift after the first amino acid that is affected by the change.

$ "del" indicates a deletion of the indicated base at the indicated position.

Mutation rate is increased in *V. cholerae* C6706

The *recA* gene codes for a protein essential for DNA repair and has been shown to affect the mutagenicity of bacteria [69, 70, 72]. The A914G substitution identified in C6706 is a missense mutation that results in a tyrosine-to-cysteine change at position 305 in the C-terminal domain of RecA [73]. To assess whether this mutation affects the mutation rate in *V. cholerae* C6706, we quantified the mutation rate and number of mutations per culture (*m*) with a rifampicin fluctuation assay [74]. The mutation rate and *m* were calculated using the FALCOR web application, employing the Ma-Sandri-Sarkar Maximum Likelihood Estimator (MSS-MLE) method [50]. The mutation rate was higher in *V. cholerae* C6706 (7.85×10^{-9}) compared to N16961 (5.65×10^{-9}) (Fig. 2A) and we observed a significant increase in mutations per culture (*m*) in *V. cholerae* C6706 (39.3) compared to N16961 (18.2) (p = 0.0236 in two-tailed t-test comparing the natural logarithm of *m* of C6706 and N1691) (Fig. 2B). We did not identify any additional mutations in genes predicted to be involved in genome stability and repair. This suggests that the observed difference in mutation rates could stem from functional differences in the RecA variants.

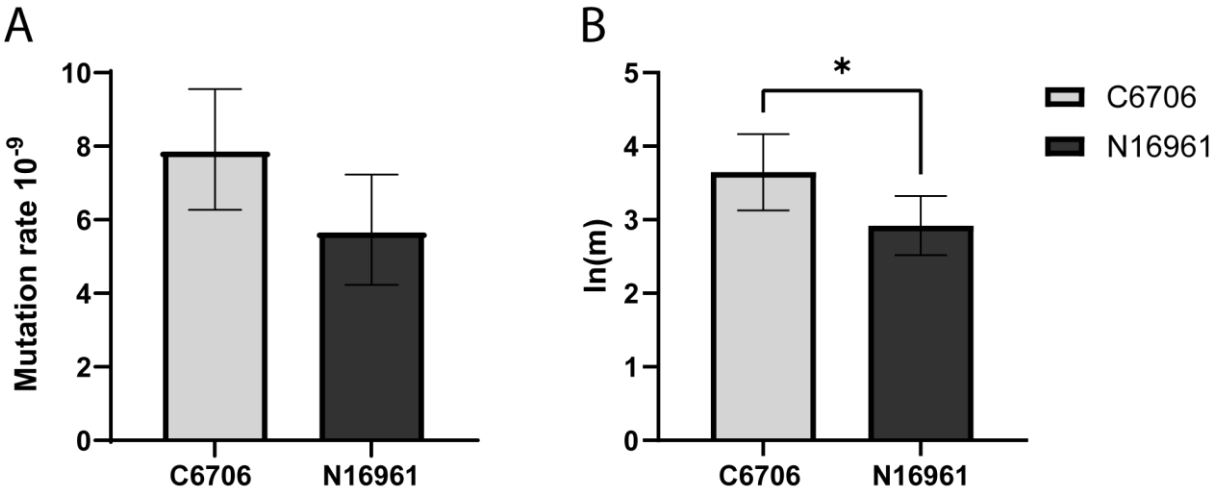

Figure 2: *V. cholerae* C6706 has a higher mutation rate than N16961.

Comparison of mutation rate and the natural logarithm of number of mutations per culture [ln(*m*)] of *V. cholerae* C6706 and N16961 measured with a rifampicin fluctuation assay [51][51]**(A)** Mutation rate of *V. cholerae* C6706 and N16961. **(B)** Ln(*m)* of *V. cholerae* C6706 and N16961. Bars depict the means based on nine biological replicates. Error bars represent the 95% confidence intervals. Statistical significance was tested using an unpaired two-tailed T-test, *, $p<0.05$.

***V. cholerae* C6706 and N16961 have similar tolerance to acidic conditions**

To understand the impact of the point mutation in *cadB* (Thr229Ile), we compared the acid tolerance of *V. cholerae* C6706 and N16961. Both strains were exposed to a pH of 4.6 in LB medium and CFUs were enumerated over time (Fig. 3). The two strains did not grow in pH 4.6. Instead, CFUs declined over time, indicating cell death. There was no significant survival difference between *V. cholerae* C6706 and N16961 in acid at any time point (p = 0.4-0.9, two-tailed T-test), indicating that the observed mutation in *cadB* does not significantly affect the acid tolerance of *V. cholerae* C6706.

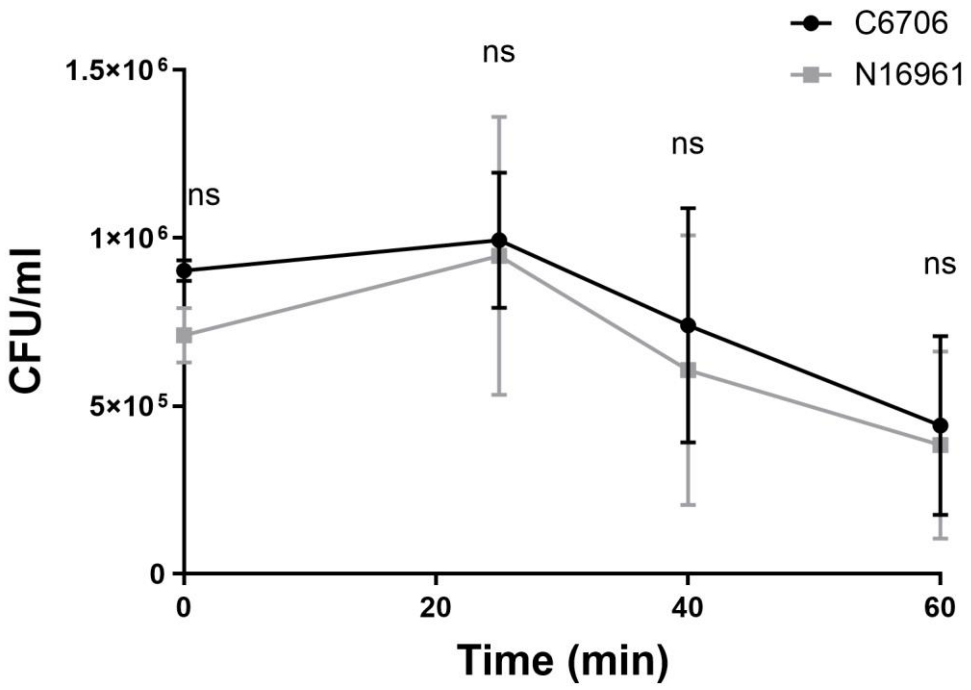

Figure 3. Both *V. cholerae* strains, C6706 and N16961, are equally sensitive to acid.

CFU per mL measurements over time of *V. cholerae* C6706 and N16961 exposed to pH 4.6 in LB medium. The dots represent the mean of three biologically independent replicates and error bars indicate the standard deviation. Statistical significance was tested using a two-tailed T-test for each individual time point; non-significant (ns), p>0.05.

Biofilm formation and motility differ between *V. cholerae* C6706 and N16961

V. cholerae C6706 harbored multiple genetic changes in genes predicted to regulate biofilm formation and motility, including several c-di-GMP-associated genes, *luxO*, and multiple proteins involved in flagellar function and chemotaxis (Table 4). In bacteria, biofilm formation and motility are often inversely regulated, where increasing biofilm formation leads to decreased motility and *vice versa* [35, 36, 75, 76]. To investigate if the sum of these genetic changes affected biofilm formation and motility in *V. cholerae* C6706 and N16961, we quantified these phenotypes. As already stated, N16961 contains a non-functional *hapR* due to a frameshift mutation that locks it in a low cell density QS-state, independent of the actual cell density [7, 30, 31]. This defective QS is known to affect biofilm formation and motility [22, 28]. The strain of *V. cholerae* C6706 sequenced in this study is locked in the same QS-state, but due to a different mutation in *luxO* [30]. To compare N16961 to the naïve, QS-proficient C6706 we also included a variant with harboring wild-type *luxO* [22]. We conducted a variant analysis to identify genetic differences between QS-proficient C6706 (GenBank accession numbers: CP064350, CP064351; PATRIC Genome ID: 948564.8) sequenced by Weng et al. [11] and QS-deficient C6706 (BioProject accession PRJNA1109855) strains, which did not reveal any additional mutations other than the expected G997A in *luxO* (Table S4).

The QS-deficient variant of *V. cholerae* C6706 formed 85% and 53% more biofilm compared to QS-proficient variant of *V. cholerae* C6706 and QS-deficient N16961, respectively (Fig. 4A, one-way ANOVA, $p<0.0001$). In addition, N16961 formed 20% more biofilm compared to the QS-proficient variant of C6706 (Fig. 4A, one-way ANOVA, $p<0.01$). The QS-deficient *V. cholerae* C6706 exhibited 14% lower motility compared to *V. cholerae* N16961 (Fig. 4B, one-way ANOVA, $p<0.0001$). In contrast, QS-deficient C6706 exhibited a 12% increase in motility compared to QS-proficient C6706 (Fig. 4B, one-way ANOVA, $p<0.0001$). To ensure that the differences in biofilm formation and motility were not due to large variations in bacterial fitness, we recorded growth curves. Comparisons of these curves revealed small differences in the area under the curve. Although these differences were statistically significant, the resulting minor changes in relative fitness (QS-deficient C6706: 1.00, N16961: 0.96, QS-

proficient C6706: 1.03) are unlikely to account for the substantial differences observed in biofilm formation and motility (Fig. 4C, Table S5).

QS-deficient C6706 and N16961 had inverse behavior when comparing biofilm formation and motility, where the strain with the highest level of biofilm formation had the lowest motility. In contrast, QS-proficient *V. cholerae* C6706 did not exhibit this pattern and had both the lowest biofilm formation and the lowest motility out of the three strains. The observed differences in biofilm formation and motility between the QS-proficient and QS-deficient variants of *V. cholerae* C6706 are likely due to differences in QS-state, as QS is known to impact biofilm formation and motility [22, 28]. The same explanation could explain the differences between QS-proficient and N16961. However, the QS-deficient variant of *V. cholerae* C6706 and N16961 are locked in the same low cell density state. Therefore, the difference in biofilm formation and motility between these two strains is likely not mediated by differences in QS-state, but caused by additional mutations (e.g., mutations in the c-di-GMP signaling system or flagellar protein).

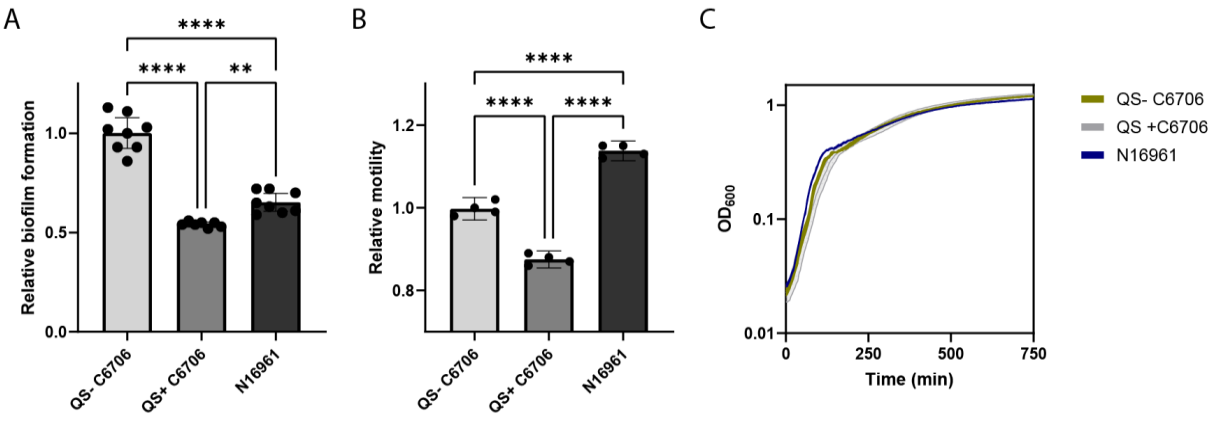

Figure 4: *V. cholerae* biofilm formation and motility.

Comparison of the capacity to form biofilms, motility on semi-solid agar plates, and growth of the naturally QS-deficient N16961, a laboratory acquired QS deficient C6706 (QS- C6706), and a naturally QS proficient C6706 (QS+ C6706). **(A)** Relative biofilm formation normalized to QS- C6706 after static growth at 37 °C for 24 hours in 24-well plates. The bars represent the mean of eight (QS- C6706 and N16961) or seven (QS+ C6706) biological replicates and the error bars indicate the 95% confidence interval. Statistical significance was tested using a one-way ANOVA followed by Tukey's multiple comparisons tests. **, p<0.01; ****, p<0.0001. **(B)** Relative motility normalized to QS- C6706 after growth on semi-solid agar for 12 hours. The bars represent the mean of four biological replicates and the error bars indicate the 95% confidence interval. Statistical significance was tested using a one-way ANOVA followed by Tukey's multiple comparisons tests. ****, p<0.0001. **(C)** Growth curves of N16961, QS-deficient *V. cholerae* C6706, and QS-proficient C6706 measured as OD_{600} over time.

Altered c-di-GMP signaling and QS shape biofilm and motility in *V. cholerae* strains C6706 vs. N16961

Comparison of N16961, QS-deficient *V. cholerae* C6706, and QS-proficient C6706 indicated that QS was not the sole cause of the observed differences in biofilm formation and motility. We therefore wanted to investigate whether variations in the c-di-GMP signaling system, particularly the frameshift mutation in the putative c-di-GMP-degrading protein VC1295, contributed to the observed phenotypic differences. First, we investigated the expression of VC1295 under the control of its native promotor. In agreement with Koestler et al. [77] and McKee et al. [68] fluorescence microscopy demonstrated that VC1295 was expressed and translated in *V. cholerae* C6706 (Fig. 5A). Furthermore, the protein was correctly translocated to its expected subcellular compartment in the cell membrane.

V. cholerae N16961 contains a functional copy of VC1295 and is naturally QS deficient. Therefore, we next investigated biofilm formation and motility in N16961 harboring an empty control vector (N16961 pCTRL) and QS-deficient *V. cholerae* C6706 expressing either a plasmid-born VC1295 (QS- C6706 p*VC1295*) or an empty control vector (QS- C6706 pCTRL). Comparing QS-deficient *V. cholerae* C6706 harboring pVC1295 with N16961 harboring pCTRL, the two strains displayed identical biofilm formation (Fig. 5B), while QS- C6706 p*VC1295* demonstrated a 12% increase in motility compared to N16961 pCTRL (Fig. 5C). This indicates that the plasmid-borne VC1295 can complement the frameshifted genomic VC1295. Therefore, VC1295 seemed to be expressed and enzymatically active under the tested biofilm and motility assay conditions, and the frameshift mutation in *VC1295* in *V. cholerae* C6706 seems to contribute to the differences in biofilm formation and motility between C6706 and N16961.

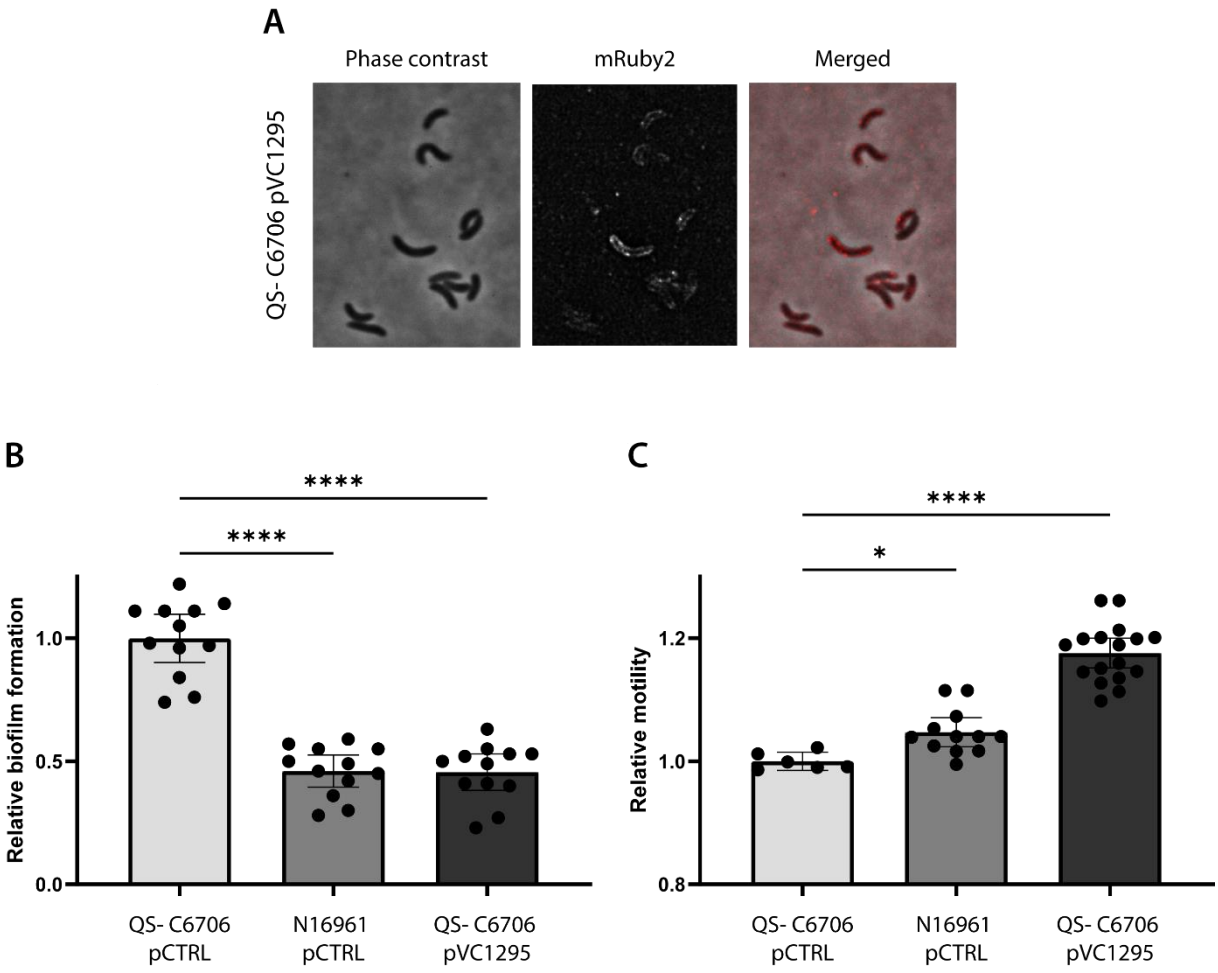

397

398 **Figure 5: VC1295 is expressed in *V. cholerae* C6706, inhibits biofilm formation, and increases motility.**
399 **(A)** Fluorescent images of *V. cholerae* C6706 expressing VC1295 fused to a C-terminal mRuby2 on a
400 medium-copy number plasmid under control of its native promoters in exponential growth phase (QS-
401 C6706 pVC1295). A phase contrast (PC), a corresponding fluorescence (mRuby2) image, and an overlay
402 of both images (merged) are shown. **(B)** Biofilm formation of QS- C6706 pCTRL, N16961 pCTRL and QS-
403 C6706 pVC1295 normalized to QS- C6706 pCTRL after static growth at 37 °C for 24 hours in 24-well
404 plates (n = 12). **(C)** Motility of the same strains test in (B) after growth on semi-solid agar at 37 °C for
405 12 hours ($n \geq 6$). The bars represent the mean and the error bars represent the 95% confidence interval.
406 Statistical significance was tested using a one-way ANOVA- followed by Dunnet multiple comparison
407 correction . *, p<0.05, ****, p<0.0001.

Discussion

In this study, we have assembled a high-quality, carefully annotated genome of *V. cholerae* C6706 and employed it to conduct a genetic and phenotypic comparison of *V. cholerae* C6706 and N16961. Assessment of genome quality in our assembled genome, aligned well with the criteria suggested by Parello et al. [58] for defining a high-quality genome with low contamination score (0.6%), fine consistency score of 99.5% and a completeness score of 100%. A genetic comparison demonstrates how these strains, isolated from different outbreaks in the 7th pandemic, carry mutations that alter their physiology. Indeed, when comparing our assembled C6706 genome with the genome of N16961, we identified multiple mutations in genes with potential to affect *V. cholerae* biology (Table 4). One set of striking differences were the multiple mutations in enzymes metabolizing c-di-GMP, a well-known regulator of biofilm and motility in bacteria [35–37]. In addition, we observed mutations in genes involved in acid stress, stress response and genome stability, flagellum biosynthesis, and chemotaxis. Comparison of our genome to previously assembled genomes of *V. cholerae* C6706 only identified the known laboratory-acquired mutation in *luxO* [11, 30]. However, a large inversion in chromosome 1 had occurred (Fig. S1-2), which seems to occur intermittently in *V. cholerae* 7th pandemic strains, as this has occurred in multiple *V. cholerae* model strains [10, 64, 65]. Importantly, a previous study did not find any fitness costs associated with large inversions in chromosome 1 [64].

To better understand if these mutations really affect the biology of *V. cholerae* C6706, we quantified selected phenotypes. Firstly, this revealed a difference in mutation rate between the two strains (Fig 1), which could potentially be attributed to a point mutation (C305Y) in RecA. This is a ubiquitous recombinase conserved throughout the bacterial kingdom, which evolves with a slow speed [73, 78, 79]. The protein is involved in multiple important cellular processes including the SOS-response, genome stability and repair, and homologous recombination [69–72]. An increased mutation rate can be beneficial in some circumstances as it has been shown to accelerate evolution and increases the rate of adaptation [80–82].

The most striking phenotypic differences between the strains were differences in biofilm formation and motility (Fig 4A-B). QS-deficient *V. cholerae* C6706 formed increased biofilms and larger colonies on semi-solid agar plates compared to the QS-proficient C6706. These findings are in line with the current literature that QS inhibits both motility and biofilm formation [22, 28]. Prior studies have demonstrated that QS regulates biofilm formation through control of multiple c-di-GMP-metabolizing genes [27, 28, 32–34, 83]. Typically, c-di-GMP regulates motility and biofilm formation inversely, i.e., high c-di-GMP concentrations increase biofilms and decrease motility, while low c-di-GMP concentrations do the opposite [35–37]. How QS inhibits both biofilm formation and motility at the same time in *V. cholerae* remains unclear. In certain cases, specific c-di-GMP-metabolizing enzymes asymmetrically regulate both biofilm formation and motility [35, 84]. Consequently, quorum sensing might influence c-di-GMP-degrading enzymes that primarily inhibit biofilm formation without necessarily promoting increased motility. Alternatively, additional signaling pathways could also be involved, thereby modulating biofilm formation or motility independently of c-di-GMP.

V. cholerae N16961 exhibited higher motility than both variants of C6706 (Fig. 4B). This is in agreement with a previous study that showed that *V. cholerae* N16961 had increased motility compared to South-American *V. cholerae* isolates closely related to C6706 [85]. In addition to increased motility due to QS-deficiency, this could come from an altered c-di-GMP metabolism with decreased levels of c-di-GMP in *V. cholerae* N16961, e.g., due to the presence of a functional copy of the putative c-di-GMP-degrading enzyme VC1295. Alternatively, the genetic differences in multiple flagellar and chemotaxis-related proteins could also contribute to the observed difference in motility.

Interestingly, QS-deficient *V. cholerae* C6706 formed more biofilm and had lower motility compared to N16961 even though they should both be locked in the same QS-state (Fig. 4)[30]. This indicates that additional signaling pathways other than QS are mediating the observed phenotypic differences. The inverse effect on biofilm formation and motility resembles the effect of increased levels of c-di-GMP [35–37]. While some c-di-GMP-metabolizing enzymes in *V. cholerae* are known to be regulated by QS, many of them are seemingly regulated independently of QS [32, 83, 86]. Therefore,

459 we hypothesized that the differences between QS-deficient C6706 and N16961 could be due to
460 differences in the strains' QS-independent c-di-GMP signaling systems. Indeed, *V. cholerae* C6706
461 contains multiple mutations in putative c-di-GMP-metabolizing enzymes (Table 4). This includes a
462 frameshift mutation in VC1295, a functional c-di-GMP-degrading enzyme [68]. Indeed, expression of a
463 functional copy of VC1295 in QS-deficient C6706 reversed the observed differences in biofilm
464 formation and motility (Fig. 5B-C), indicating that the observed differences were at least partly due to
465 differences in c-di-GMP-metabolism between the strains. Although, the difference could also be due
466 to additional QS-related signaling pathways as *V. cholerae* C6706 and N16961 contain different
467 mutations, LuxO and HapR, respectively, in the quorum sensing signaling pathway. Even though the
468 mutations lead to the same QS-state, we cannot exclude that they have additional confounding
469 downstream effects. Altogether, the results of this work are consistent with a model where the
470 observed differences in biofilm formation and motility are due to a combination of effects from QS and
471 c-di-GMP signaling.

472 *V. cholerae* N16961 and QS-proficient *V. cholerae* C6706 exhibited differences in biofilm
473 formation and motility, and the difference in motility exceeded biofilm formation (Fig. 4A-B). In QS-
474 proficient *V. cholerae* C6706, this might be attributed to QS-mediated repression of biofilm formation
475 [28, 32, 34, 83]. In addition, it harbors a frameshift mutation in the active c-di-GMP-degrading enzyme
476 VC1295 (Table 4) [68]. This leads to putatively increased c-di-GMP levels and increased biofilm
477 formation, which could partially balance out the QS-mediated biofilm repression (Fig. 4A). N16961
478 lacks QS-mediated biofilm repression, but also lacks the frameshift mutation in VC1295. For motility,
479 the QS-state and c-di-GMP levels of QS-proficient *V. cholerae* C6706 would both act to repress motility
480 (Fig. 4B) [22, 36, 87]. In contrast, the QS-state and putatively lower c-di-GMP levels of *V. cholerae*
481 N16961 would both promote motility (Fig. 4B) [22, 36, 87]. Therefore, the observed differences in
482 biofilm formation and motility are consistent with the identified genetic changes between *V. cholerae*
483 C6706 and N16961 (Table 4).

In conclusion, our study offers a genomic analysis of *V. cholerae* C6706, utilizing a hybrid sequencing approach. This yielded a high-quality genome of *V. cholerae* C6706, which we carefully annotated and cross referenced to N16961. We believe that this will be a valuable resource for the scientific community and represents an improvement of the previous version of the *V. cholerae* C6706 genome [11]. By characterizing genotypic and phenotypic differences between *V. cholerae* C6706 and N16961, we have uncovered potential targets of adaptive evolution in the 7th cholera pandemic. Furthermore, the comparison of biofilm formation and motility between *V. cholerae* C6706 and N16961, sheds further light on the complex interplay of factors regulating biofilm formation and motility in *V. cholerae* 7th pandemic strains.

Author statements

Author contributions

The project was conceptualized by O.M.L. and S.A. Funding was acquired by S.A. The experiments were carried out and the data analyzed by O.M.L. and C.B. under the supervision of S.A. The manuscript was drafted by O.M.L. and C.B. and edited and revised by all authors.

Conflicts of interest

The authors declare that there are no conflicts of interest.

Funding information

This work was funded by Research Council of Norway (NFR) 249979 (to S.A.). The funders had no role in study design, data collection and interpretation, or the decision to submit the work for publication.

Acknowledgements

We thank the Norwegian Sequencing Centre hosted at the University of Oslo for sequencing our laboratory's strain of *Vibrio cholerae*. In addition, we thank Erik Hjerde for assistance with the de novo assembly of the closed genome of *Vibrio cholerae* C6706. We thank Prof. Melanie Blokesch for providing us with the QS-proficient variant of *V. cholerae* C6706. We thank João Alves Gama for assisting in the analysis of bacterial fitness.

References

1. **Kanungo S, Azman AS, Ramamurthy T, Deen J, Dutta S**. Cholera. *The Lancet* 2022;399:1429–1440.

2. **Ali M, Nelson AR, Lopez AL, Sack DA**. Updated Global Burden of Cholera in Endemic Countries. *PLoS Negl Trop Dis* 2015;9:e0003832.

3. **Barua D**. History of Cholera. In: Barua D, Greenough WB (editors). *Cholera*. Boston, MA: Springer US. pp. 1–36.

4. **Mutreja A, Kim DW, Thomson NR, Connor TR, Lee JH, *et al.*** Evidence for several waves of global transmission in the seventh cholera pandemic. *Nature* 2011;477:462–465.

5. **Yildiz FH, Schoolnik GK**. Role of rpoS in Stress Survival and Virulence of *Vibrio cholerae*. *J Bacteriol* 1998;180:773–784.

6. **Thelin KH, Taylor RK**. Toxin-coregulated pilus, but not mannose-sensitive hemagglutinin, is required for colonization by *Vibrio cholerae* O1 El Tor biotype and O139 strains. *Infect Immun* 1996;64:2853–2856.

7. **Heidelberg JF, Eisen JA, Nelson WC, Clayton RA, Gwinn ML, *et al.*** DNA sequence of both chromosomes of the cholera pathogen *Vibrio cholerae*. *Nature* 2000;406:477–483.

8. **Miller VL, DiRita VJ, Mekalanos JJ**. Identification of *toxS*, a regulatory gene whose product enhances toxR-mediated activation of the cholera toxin promoter. *J Bacteriol* 1989;171:1288–1293.

9. **Reimer AR, Domselaar G Van, Stroika S, Walker M, Kent H, *et al.*** Comparative Genomics of *Vibrio cholerae* from Haiti, Asia, and Africa. *Emerging Infectious Disease journal* 2011;17:2113.

10. **Matthey N, Drebes Dörr NC, Blokesch M**. Long-Read-Based Genome Sequences of Pandemic and Environmental *Vibrio cholerae* Strains. *Microbiol Resour Announc* 2018;7:e01574-18.

11. **Weng Y, Bina XR, Bina JE**. Complete Genome Sequence of *Vibrio cholerae* O1 El Tor Strain C6706. *Microbiol Resour Announc* 2021;10:10.1128/mra.01301-20.

12. **Creasy-Marrazzo A, Saber MM, Kamat M, Bailey LS, Brinkley L, *et al.*** Genome-wide association studies reveal distinct genetic correlates and increased heritability of antimicrobial resistance in *Vibrio cholerae* under anaerobic conditions. *Microb Genom* 2022 Dec;8(12):mgen000905.

13. **Rivera-Chávez F, Mekalanos JJ**. Cholera toxin promotes pathogen acquisition of host-derived nutrients. *Nature* 2019;572:244–248.

14. **Sit B, Srisuknimit V, Bueno E, Zingl FG, Hullahalli K, *et al.*** Undecaprenyl phosphate translocases confer conditional microbial fitness. *Nature* 2023;613:721–728.

15. **Dalia AB, McDonough E, Camilli A**. Multiplex genome editing by natural transformation. *Proceedings of the National Academy of Sciences* 2014;111:8937–8942.

16. **Jaskólska M, Adams DW, Blokesch M**. Two defence systems eliminate plasmids from seventh pandemic *Vibrio cholerae*. *Nature* 2022;604:323–329.

17. **Vidakovic L, Mikhaleva S, Jeckel H, Nisnevich V, Strenger K, *et al.*** Biofilm formation on human immune cells is a multicellular predation strategy of *Vibrio cholerae*. *Cell* 2023;186:2690-2704.e20.

18. **Prentice JA, van de Weerd R, Bridges AA**. Cell-lysis sensing drives biofilm formation in *Vibrio cholerae*. *Nat Commun* 2024;15:2018.

19. **Bridges AA, Prentice JA, Wingreen NS, Bassler BL**. Signal Transduction Network Principles Underlying Bacterial Collective Behaviors. *Annu Rev Microbiol* 2022;76:235–257.

20. **Conner JG, Teschler JK, Jones CJ, Yildiz FH**. Staying Alive: *Vibrio cholerae*'s Cycle of Environmental Survival, Transmission, and Dissemination. *Microbiol Spectr*. 2016 Apr;4(2)

21. **Silva AJ, Benitez JA**. *Vibrio cholerae* Biofilms and Cholera Pathogenesis. *PLoS Negl Trop Dis* 2016;10:e0004330.

22. **Zhu J, Mekalanos JJ**. Quorum Sensing-Dependent Biofilms Enhance Colonization in *Vibrio cholerae*. *Dev Cell* 2003;5:647–656.

23. **Gallego-Hernandez AL, DePas WH, Park JH, Teschler JK, Hartmann R, *et al.*** Upregulation of virulence genes promotes *Vibrio cholerae* biofilm hyperinfectivity. *Proc Natl Acad Sci U S A* 2020;117:11010–11017.

24. **Rita T, Bharathi P, Andrew C**. Growth in a Biofilm Induces a Hyperinfectious Phenotype in *Vibrio cholerae*. *Infect Immun* 2010;78:3560–3569.

25. **Faruque SM, Biswas K, Udden SMN, Ahmad QS, Sack DA, *et al.*** Transmissibility of cholera: In vivo-formed biofilms and their relationship to infectivity and persistence in the environment. *Proceedings of the National Academy of Sciences* 2006;103:6350–6355.

26. **Waters CM, Bassler BL**. QUORUM SENSING: Cell-to-Cell Communication in Bacteria. *Annu Rev Cell Dev Biol* 2005;21:319–346.

27. **Bridges AA, Bassler BL**. The intragenus and interspecies quorum-sensing autoinducers exert distinct control over *Vibrio cholerae* biofilm formation and dispersal. *PLoS Biol* 2019;17:e3000429-.

28. **Hammer BK, Bassler BL**. Quorum sensing controls biofilm formation in *Vibrio cholerae*. *Mol Microbiol* 2003;50:101–104.

29. **Rutherford ST, van Kessel JC, Shao Y, Bassler BL**. AphA and LuxR/HapR reciprocally control quorum sensing in *vibrios*. *Genes Dev* 2011;25:397–408.

30. **Stutzmann S, Blokesch M**. Circulation of a Quorum-Sensing-Impaired Variant of *Vibrio cholerae* Strain C6706 Masks Important Phenotypes. *mSphere* 2016;1:e00098-16.

31. **Meibom KL, Blokesch M, Dolganov NA, Wu C-Y, Schoolnik GK**. Chitin Induces Natural Competence in *Vibrio cholerae*. *Science (1979)* 2005;310:1824–1827.

32. **Waters CM, Lu W, Rabinowitz JD, Bassler BL**. Quorum Sensing Controls Biofilm Formation in *Vibrio cholerae* through Modulation of Cyclic Di-GMP Levels and Repression of vpsT. *J Bacteriol* 2008;190:2527–2536.

33. **Hammer BK, Bassler BL**. Distinct Sensory Pathways in *Vibrio cholerae* El Tor and Classical Biotypes Modulate Cyclic Dimeric GMP Levels To Control Biofilm Formation. *J Bacteriol* 2009;191:169–177.

34. **Zhao X, Koestler BJ, Waters CM, Hammer BK**. Post-transcriptional activation of a diguanylate cyclase by quorum sensing small RNAs promotes biofilm formation in *Vibrio cholerae*. *Mol Microbiol* 2013;89:989–1002.

35. **Hengge R**. Principles of c-di-GMP signalling in bacteria. *Nat Rev Microbiol* 2009;7:263–273.

36. **Conner JG, Zamorano-Sánchez D, Park JH, Sondermann H, Yildiz FH**. The ins and outs of cyclic di-GMP signaling in *Vibrio cholerae*. *Curr Opin Microbiol* 2017;36:20–29.

37. **Romling U, Galperin M, Gomelsky M**. Cyclic di-GMP: the First 25 Years of a Universal Bacterial Second Messenger. *Microbiology and Molecular Biology Reviews* 2013;77:1–52.

38. **Hornick RB, Music SI, Wenzel R, Cash R, Libonati JP, *et al.*** The Broad Street pump revisited: response of volunteers to ingested cholera *vibrios*. *Bull NY Acad Med* 1971;47:1181–1191.

39. **Merrell DS, Camilli A**. The *cadA* gene of *Vibrio cholerae* is induced during infection and plays a role in acid tolerance. *Mol Microbiol* 1999;34:836–849.

40. **Singh A, Barnard TG**. Surviving the acid barrier: responses of pathogenic *Vibrio cholerae* to simulated gastric fluid. *Appl Microbiol Biotechnol* 2015;100:815–824.

41. **Meng SY, Bennett GN**. Nucleotide sequence of the *Escherichia coli* cad operon: a system for neutralization of low extracellular pH. *J Bacteriol* 1992;174:2659–2669.

42. **Platt R, Drescher C, Park SK, Phillips GJ**. Genetic system for reversible integration of DNA constructs and lacZ gene fusions into the *Escherichia coli* chromosome. *Plasmid* 2000;43:12–23.

43. **Wick RR, Judd LM, Gorrie CL, Holt KE**. Unicycler: Resolving bacterial genome assemblies from short and long sequencing reads. *PLoS Comput Biol* 2017;13:e1005595–e1005595.

44. **Aziz RK, Bartels D, Best AA, DeJongh M, Disz T, *et al.*** The RAST Server: rapid annotations using subsystems technology. *BMC Genomics* 2008;9:75.

45. **Wattam AR, Abraham D, Dalay O, Disz TL, Driscoll T, *et al.*** PATRIC, the bacterial bioinformatics database and analysis resource. *Nucleic Acids Res* 2014;42:D581–D591.

46. **Madden T**. The BLAST Sequence Analysis Tool. 2002 Oct 9. The NCBI Handbook. Bethesda (MD): National Center for Biotechnology Information (US); 2002-. Chapter 16.

47. **O'Toole GA**. Microtiter Dish Biofilm Formation Assay. *JoVE* 2011;e2437.

48. **Zhu J, Miller MB, Vance RE, Dziejman M, Bassler BL, *et al.*** Quorum-sensing regulators control virulence gene expression in *Vibrio cholerae*. *Proceedings of the National Academy of Sciences* 2002;99:3129–3134.

49. **Schindelin J, Arganda-Carreras I, Frise E, Kaynig V, Longair M, *et al.*** Fiji: an open-source platform for biological-image analysis. *Nat Methods* 2012;9:676–682.

50. **Darling Aaron E. AND Mau BANDPNT**. progressiveMauve: Multiple Genome Alignment with Gene Gain, Loss and Rearrangement. *PLoS One* 2010;5:1–17.

51. **Hall BM, Ma C-X, Liang P, Singh KK**. Fluctuation analysis CalculatOR: a web tool for the determination of mutation rate using Luria-Delbruck fluctuation analysis. *Bioinformatics* 2009;25:1564–1565.

52. **Rosche WA, Foster PL**. Determining Mutation Rates in Bacterial Populations. *Methods* 2000;20:4–17.

53. **Jurasinski G, Koebsch F, Guenther A, Beetz S**. Flux Rate Calculation from Dynamic Closed Chamber. *R package version 03-01*. https://CRAN.R-project.org/package=flu (2022).

54. **Gibson DG, Young L, Chuang R-Y, Venter JC, Hutchison CA, *et al.*** Enzymatic assembly of DNA molecules up to several hundred kilobases. *Nat Meth* 2009;6:343–345.

55. **House BL, Mortimer MW, Kahn ML**. New recombination methods for *Sinorhizobium meliloti* genetics. *Appl Environ Microbiol* 2004;70:2806–2815.

56. **Hartley JL, Temple GF, Brasch MA**. DNA cloning using in vitro site-specific recombination. *Genome Res* 2000;10:1788–1795.

57. **Simon R, Priefer U, Pühler A**. A Broad Host Range Mobilization System for In Vivo Genetic Engineering: Transposon Mutagenesis in Gram Negative Bacteria. *Bio/Technology* 1983;1:784–791.

58. **Parrello B, Butler R, Chlenski P, Olson R, Overbeek J, *et al.*** A machine learning-based service for estimating quality of genomes using PATRIC. *BMC Bioinformatics* 2019;20:486.

59. **Stothard P, Wishart DS**. Circular genome visualization and exploration using CGView. *Bioinformatics* 2005;21:537–539.

60. **Grant JR, Stothard P**. The CGView Server: a comparative genomics tool for circular genomes. *Nucleic Acids Res* 2008;36:W181–W184.

61. **Abel S, Abel zur Wiesch P, Chang H-H, Davis BM, Lipsitch M, *et al.*** Sequence tag-based analysis of microbial population dynamics. *Nat Meth* 2015;12:223–226.

62. **Cameron DE, Urbach JM, Mekalanos JJ**. A defined transposon mutant library and its use in identifying motility genes in Vibrio cholerae. *Proceedings of the National Academy of Sciences* 2008;105:8736–8741.

63. **Morais LLC de S, Garza DR, Loureiro ECB, Vale ER, Santos DSA de S, *et al.*** Population and Genetic Study of *Vibrio cholerae* from the Amazon Environment Confirms that the WASA-1 Prophage Is the Main Marker of the Epidemic Strain that Circulated in the Region. *PLoS One* 2013;8:e81372-.

64. **Val M-E, Marbouty M, de Lemos Martins F, Kennedy SP, Kemble H, *et al.*** A checkpoint control orchestrates the replication of the two chromosomes of *Vibrio cholerae*. *Sci Adv* 2016;2:e1501914.

65. **Matthey N, Stutzmann S, Stoudmann C, Guex N, Iseli C, *et al.*** Neighbor predation linked to natural competence fosters the transfer of large genomic regions in *Vibrio cholerae*. *Elife* 2019;8:e48212.

66. **Nusrin S, Gil AI, Bhuiyan NA, Safa A, Asakura M, *et al.*** Peruvian *Vibrio cholerae* O1 El Tor strains possess a distinct region in the *Vibrio* seventh pandemic island-II that differentiates them from the prototype seventh pandemic El Tor strains. *J Med Microbiol* 2009;58:342–354.

67. **Taviani E, Grim CJ, Choi J, Chun J, Haley B, *et al.*** Discovery of novel *Vibrio cholerae* VSP-II genomic islands using comparative genomic analysis. *FEMS Microbiol Lett* 2010;308:130–137.

68. **McKee RW, Kariisa A, Mudrak B, Whitaker C, Tamayo R**. A systematic analysis of the in vitro and in vivo functions of the HD-GYP domain proteins of *Vibrio cholerae*. *BMC Microbiol* 2014;14:272.

69. **Thi T Do, López E, Rodríguez-Rojas A, Rodríguez-Beltrán J, Couce A, *et al.*** Effect of recA inactivation on mutagenesis of *Escherichia coli* exposed to sublethal concentrations of antimicrobials. *Journal of Antimicrobial Chemotherapy* 2011;66:531–538.

70. **Cirz RT, Chin JK, Andes DR, de Crécy-Lagard V, Craig WA, *et al.*** Inhibition of Mutation and Combating the Evolution of Antibiotic Resistance. *PLoS Biol* 2005;3:e176-.

71. **Friedberg EC, Walker GC, Siede W**. DNA Repair and Mutagenesis. ASM Press; 2005.

72. **Kanie S, Horibata K, Kawano M, Isogawa A, Sakai A, *et al.*** Roles of RecA protein in spontaneous mutagenesis in *Escherichia coli*. *Genes Genet Syst* 2007;82:99–108.

73. **Bell JC, Kowalczykowski SC**. RecA: Regulation and Mechanism of a Molecular Search Engine. *Trends Biochem Sci* 2016;41:491–507.

74. **Krašovec R, Richards H, Gomez G, Gifford DR, Mazoyer A, *et al.*** Measuring Microbial Mutation Rates with the Fluctuation Assay. *JoVE* 2019;e60406.

75. **Teschler JK, Nadell CD, Drescher K, Yildiz FH**. Mechanisms Underlying *Vibrio cholerae* Biofilm Formation and Dispersion. *Annu Rev Microbiol* 2022;76:503–532.

76. **Flemming H-C, Wingender J, Szewzyk U, Steinberg P, Rice SA, *et al.*** Biofilms: an emergent form of bacterial life. *Nat Rev Microbiol* 2016;14:563–575.

77. **Koestler BJ, Waters CM**. Bile Acids and Bicarbonate Inversely Regulate Intracellular Cyclic di-GMP in *Vibrio cholerae*. *Infect Immun* 2014;82:3002–3014.

78. **Rocha EPC, Cornet E, Michel B**. Comparative and Evolutionary Analysis of the Bacterial Homologous Recombination Systems. *PLoS Genet* 2005;1:e15-.

79. **Karlin S, Brocchieri L**. Evolutionary conservation of RecA genes in relation to protein structure and function. *J Bacteriol* 1996;178:1881–1894.

80. **Ram Y, Hadany L**. The evolution of stress-induced hypermutation in asexual populations. *Evolution (NY)* 2012;66:2315–2328.

81. **Swings T, Van den Bergh B, Wuyts S, Oeyen E, Voordeckers K, *et al.*** Adaptive tuning of mutation rates allows fast response to lethal stress in *Escherichia coli*. *Elife* 2017;6:e22939.

82. **Taddei F, Radman M, Maynard-Smith J, Toupance B, Gouyon PH, *et al.*** Role of mutator alleles in adaptive evolution. *Nature* 1997;387:700–702.

83. **Srivastava D, Harris RC, Waters CM**. Integration of Cyclic di-GMP and Quorum Sensing in the Control of vpsT and aphA in Vibrio cholerae. *J Bacteriol* 2011;193:6331–6341.

84. **Hengge R**. High-specificity local and global c-di-GMP signaling. *Trends Microbiol* 2021;29:993–1003.

699 85. **Satchell KJF, Jones CJ, Wong J, Queen J, Agarwal S, *et al.*** Phenotypic Analysis Reveals that the
700 2010 Haiti Cholera Epidemic Is Linked to a Hypervirulent Strain. *Infect Immun* 2016;84:2473–
701 2481.

702 86. **Walker LM, Haycocks JRJ, Van Kessel JC, Dalia TN, Dalia AB, *et al.*** A simple mechanism for
703 integration of quorum sensing and cAMP signalling in *Vibrio cholerae*. *Elife* 2023;12:RP86699.

704 87. **Srivastava D, Hsieh M-L, Khataokar A, Neiditch MB, Waters CM**. Cyclic di-GMP inhibits *Vibrio*
705 *cholerae* motility by repressing induction of transcription and inducing extracellular
706 polysaccharide production. *Mol Microbiol* 2013;90:1262–1276.

707

Appendix: Paper 2

Appendix: Paper 3

The Biofilm Lifestyle Shapes the Evolution of β-Lactamases

Øyvind M. Lorentzen [1,*,†], Anne Sofie B. Haukefer[1], Pål J. Johnsen[1], and Christopher Frøhlich[1,*,†]

[1]Department of Pharmacy, UiT The Arctic University of Norway, Tromsø, Norway

[†]Equal contribution.

*Corresponding authors: E-mails: oyvind.m.lorentzen@uit.no; christopher.frohlich@uit.no.

Accepted: February 08, 2024

Abstract

The evolutionary relationship between the biofilm lifestyle and antibiotic resistance enzymes remains a subject of limited understanding. Here, we investigate how β-lactamases affect biofilm formation in *Vibrio cholerae* and how selection for a biofilm lifestyle impacts the evolution of these enzymes. Genetically diverse β-lactamases expressed in *V. cholerae* displayed a strong inhibitory effect on biofilm production. To understand how natural evolution affects this antagonistic pleiotropy, we randomly mutagenized a β-lactamase and selected for elevated biofilm formation. Our results revealed that biofilm evolution selects for β-lactamase variants able to hydrolyze β-lactams without inhibiting biofilms. Mutational analysis of evolved variants demonstrated that restoration of biofilm development was achieved either independently of enzymatic function or by actively leveraging enzymatic activity. Taken together, the biofilm lifestyle can impose a profound selective pressure on antimicrobial resistance enzymes. Shedding light on such evolutionary interplays is of importance to understand the factors driving antimicrobial resistance.

Graphical Abstract

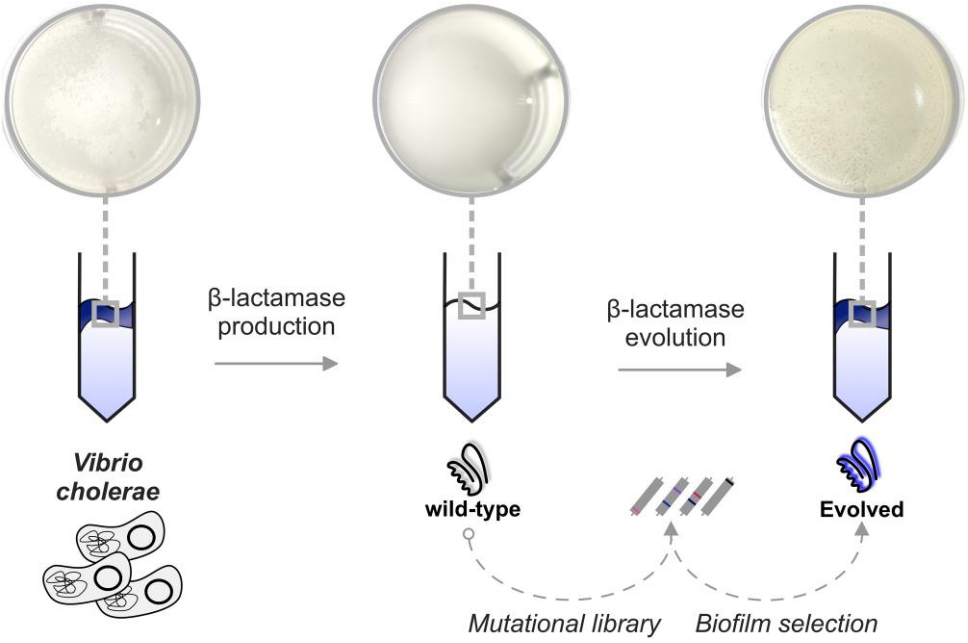

Significance

β-Lactamases inhibit biofilm formation, and the selection for increased biofilm production can mitigate this antagonistic pleiotropic effect. The emergence of β-lactamase variants avoiding biofilm inhibition suggests that the biofilm lifestyle affects the evolutionary fate of these enzymes.

Key words: *Vibrio cholerae*, β-lactamases, evolution, AMR, biofilm.

Introduction

Biofilms, which are structured bacterial communities covered in a protective extracellular matrix, represent one of the most prevalent bacterial lifestyles (Flemming et al. 2016; Ciofu et al. 2022). Biofilm-embedded bacteria demonstrate a remarkable ability to endure harsh conditions and exhibit increased tolerance toward external stressors, including antimicrobials (Flemming et al. 2016; Ciofu et al. 2022). These structured communities further serve as hotspots that facilitate the dissemination of mobile genetic elements harboring antimicrobial resistance genes (Madsen et al. 2012; Abe et al. 2020; Castañeda-Barba et al. 2023). It has been shown that a biofilm lifestyle can select for distinct evolutionary trajectories and profoundly influences the evolution of both bacteria and mobile genetic elements, when compared to bacteria evolving in unstructured environments (Steenackers et al. 2016; Kovács and Dragoš 2019; Coenye et al. 2022; Castañeda-Barba et al. 2023). However, our current understanding of how biofilms influence the evolution of antimicrobial resistance enzymes is limited.

Upon acquisition, plasmid-harbored genes can induce pleiotropy, resulting in unpredictable effects on multiple cellular traits such as reduced basal bacterial growth or collateral responses to antimicrobials (Baltrus et al. 2021; Billane et al. 2021; Roemhild et al. 2022). Consequently, pleiotropy plays a pivotal role in shaping natural selection in a given environment, potentially requiring compensatory mutations to counteract these adverse effects.

Among Gram-negative pathogens, the most prominent cause of β-lactam resistance is the production of β-lactamases (Cassini et al. 2019). These enzymes display significant sequence- and functional-variability and are often encoded on mobile genetic elements, which facilitates horizontal transmission to closely and more distantly related bacteria (Castañeda-Barba et al. 2023). They can be classified into Ambler classes A to D based on sequence diversity or grouped into 2 major functional categories: serine-type (classes A, C, and D) and metallo-β-lactamases (class B) (Bush 2018). Enzymes grouped into classes A and D have been shown to antagonize biofilm formation in *Escherichia coli* and *Pseudomonas aeruginosa* (Gallant et al. 2005; Fernández et al. 2012). We hypothesize that the occurrence of such pleiotropic effects can significantly alter the evolutionary trajectory of the pleiotropy-inducing resistance enzymes.

In this study, we utilize *Vibrio cholerae* as a model organism, due to the importance of biofilm in its life cycle, to study the impact of β-lactamases on biofilm formation (Teschler et al. 2015; Conner et al. 2016; Silva and Benitez 2016; Teschler et al. 2022). We employed a combination of directed and experimental evolution techniques (Fig. 1a) to evaluate how selection for pellicle production, a specific type of biofilm formed at the air-liquid interface, influences the evolutionary trajectories of β-lactamases (Kovács and Dragoš 2019; Qin et al. 2021; Qin and Bassler 2022). Gaining insights into these intricate evolutionary relationships is essential for comprehending the dissemination and evolution of antimicrobial resistance enzymes.

Results and Discussion

β-Lactamases From All Ambler Classes Inhibit Biofilm Formation

To determine the inhibitory effect of β-lactamases on biofilm formation, we quantified biomass produced by *V. cholerae* strains harboring a medium copy number vector with or without β-lactamase genes (Fig. 1a and b). Crystal violet staining of adherent biomass after 24 h of static growth was used as a proxy for biofilm development. Compared to the control vector, 7 out of 8 tested β-lactamase-producing strains exhibited a significant reduction in biomass ranging from 43% to 61% (Table 1 and Fig. 1b, one-way analysis of variance [ANOVA], $P < 0.0001$). Notably, NDM-1 was the only exception, showing a statistically nonsignificant reduction of 17% (Table 1 and Fig. 1b, one-way ANOVA, $P > 0.05$). While it has been previously suggested that biofilm inhibition is mainly attributed to class A and D β-lactamases, due to their evolutionary relationship to low-molecular-weight penicillin-binding proteins (Gallant et al. 2005; Fernández et al. 2012), our data demonstrate that this antagonistic pleiotropy can be more general across the different classes of β-lactamases.

To ensure that the expressed β-lactamases were functional, we determined the ampicillin resistance and bacterial fitness of the β-lactamase-producing strains. Our data show that the β-lactamases conferred a 6- to 64-fold

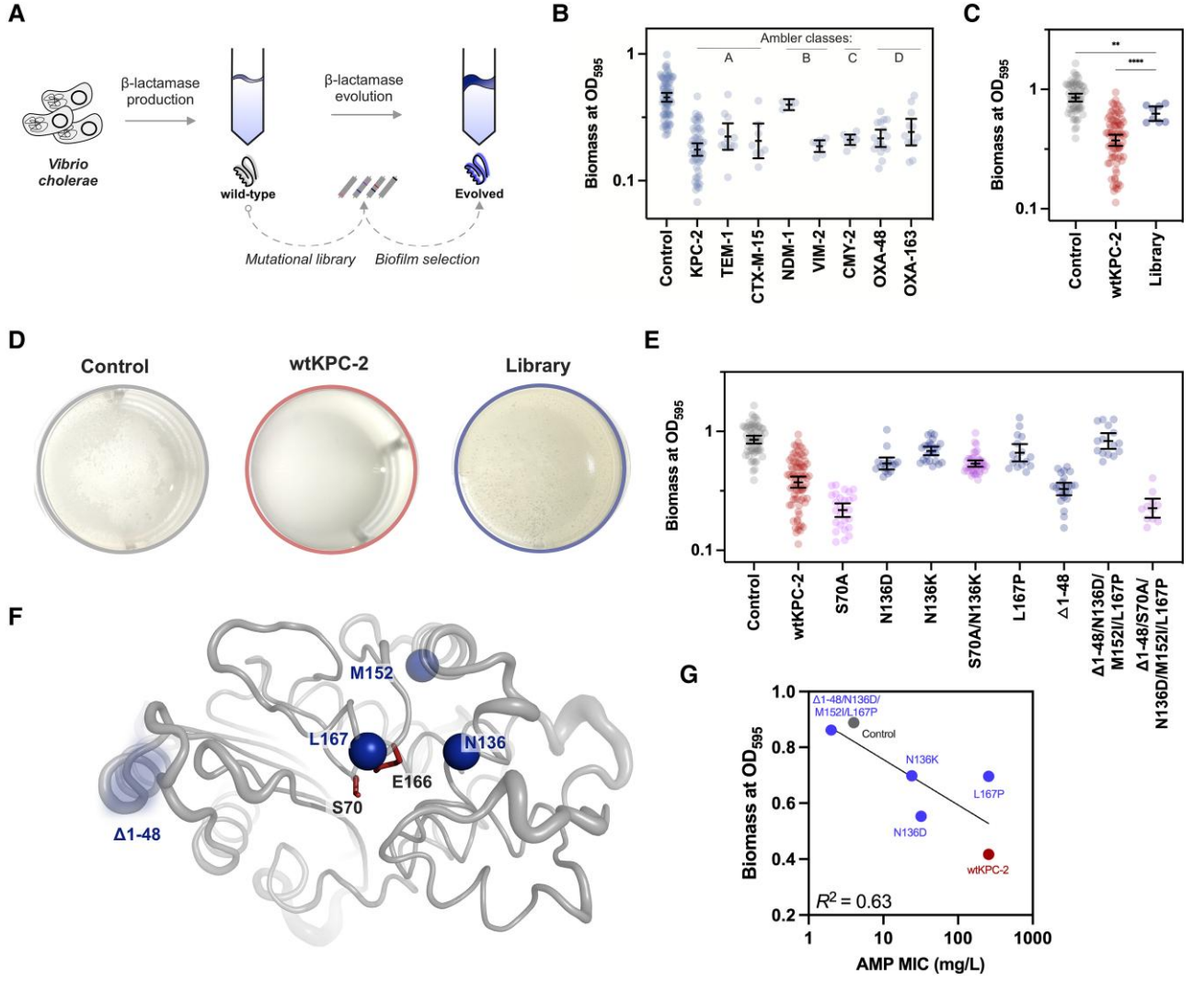

Fig. 1.—Biofilm lifestyle shapes the evolution of β-lactamases in *V. cholerae*. a. We first explored the influence of β-lactamase gene expression on the *V. cholerae* biofilm phenotype (left). Second, by subjecting a mutant library of KPC-2 to experimental evolution, we revealed how the biofilm lifestyle affects β-lactamase evolution (right). b. The expression of β-lactamase genes from Ambler classes A to D (top) significantly hindered biofilm formation in *V. cholerae* compared to the control vector. c. Our mutational library of KPC-2 (>5,000 mutants) exhibited significantly enhanced biofilm formation compared to wild-type KPC-2 (wtKPC-2) (****; one-way ANOVA, $P < 0.0001$), although it remained less than the vector control (**; one-way ANOVA, $P = 0.001$). d. Differences in biomass production related to *V. cholerae*'s ability to form pellicles. While our control displayed signs of pellicle formation after 24 h incubation, the presence of KPC-2 completely suppressed biofilm pellicle development. In contrast, the presence of our KPC-2 mutational library resulted in a well-structured biofilm pellicle. e. While wtKPC-2 led to reduced biofilm capacity, N136K and Δ1-48/N136D/M152I/L167P, which were selected from and were enriched in the pellicle, demonstrated significant improvement in biofilm formation (*P* values reported in Table 2). β-Lactam binding-deficient (serine-to-alanine at position 70) variants of wtKPC-2 and Δ1-48/N136D/M152I/L167P strongly reduced the biofilm phenotype. On the contrary, S70A/N136K maintained high levels of biofilm formation compared to the evolved variant N136K. Deconvolution of mutations within Δ1-48/N136D/M152I/L167P displayed that, in contrast to N136D and L167P, the deletion Δ1-48 did not significantly increase biofilm formation compared to wtKPC-2 (*P* values reported in Table 2). f. Location of mutational sites compared to the key active site residues S70 and E166. g. Pearson correlation ($R^2 = 0.63$, $P = 0.059$) between ampicillin resistance and biofilm formation for wtKPC-2 (black), control (gray), and evolved mutants Δ1-48/N136D/M152I/L167P, N136K, N136D, and L167P (blue). Each datapoint in b, c, and e represents a biological replicate, and error bars display 95% confidence intervals.

decrease in ampicillin susceptibility compared to our vector control, confirming the functional activity of the enzymes (Table 1). Evaluation of the area under the growth curve, used as a proxy for bacterial fitness, uncovered that 7 out of 8 β-lactamase-producing strains did not suffer a detrimental effect on fitness (Table 1, supplementary fig. S1, Supplementary Material online, and supplementary table S1, Supplementary Material online). Unexpectedly, the TEM-1-producing strain demonstrated reduced fitness (20%) compared to the empty vector control strain. The

Table 1
Biofilm inhibitory effect of β-lactamases from all Ambler classes

Strain no.	β-Lactamases	Ambler class	Biomass at OD_{595} [a]	*P* values[b]	*N*[c]	Relative fitness[d]	Ampicillin MICs (mg/L)
30-73	wtVC[e]	—	0.800 ± 0.021	<0.0001	10	1.48 ± 0.01	4
30-71	Control[f]	—	0.483 ± 0.019	—	77	1	4
30-70	KPC-2	A	0.191 ± 0.011	<0.0001	56	1.34 ± 0.01	>256
32-56	TEM-1	A	0.238 ± 0.028	0.0002	12	0.80 ± 0.01	24
32-57	CTX-M-15	A	0.220 ± 0.034	0.0036	8	1.22 ± 0.01	>256
32-58	NDM-1	B	0.399 ± 0.012	0.1397	4	1.07 ± 0.1	>256
32-59	VIM-2	B	0.189 ± 0.008	<0.0001	8	1.26 ± 0.01	>256
32-53	CMY-2	C	0.211 ± 0.008	<0.0001	8	0.94 ± 0.03	32
32-54	OXA-48	D	0.225 ± 0.016	<0.0001	16	1.32 ± 0.01	>256
32-55	OXA-163	D	0.259 ± 0.030	0.0008	12	0.97 ± 0.03	>256

Errors are reported as the standard error of the mean.
MIC, minimal inhibitory concentration; OD, opitcal density.
[a]OD measurements were performed in a 96-well plate.
[b]Brown–Forsythe one-way ANOVA to test for differences in biomass formation compared to the vector control ($\alpha = 0.05$) and followed by Dunnett test to correct for multiple testing; F (DFn, DFd) = 48.50 (8, 77); overall $P < 0.0001$.
[c]Sample size (biological replicates) tested to determine the biomass at OD_{595}.
[d]Determined as area under the growth curve compared to control (see supplementary fig. S1, Supplementary Material online for bacterial growth curves and supplementary table S1, Supplementary Material online for areas under curve).
[e]Wild-type *V. cholerae* C6706. Parental strain for all downstream strain constructs.
[f]*V. cholerae* harboring the pA15 vector without β-lactamase gene.

same strain conferred only a 6-fold increase in ampicillin minimal inhibitory concentration (MIC), despite the overall high catalytic activity of TEM-1 (k_{cat}/K_M ~10^7 M^{-1} s^{-1}) (Brown et al. 2009). Therefore, in the case of TEM-1, it cannot be excluded that the observed mediated biofilm inhibition was unrelated to the intracellular enzyme production. However, correlation analysis of the relationship bacterial fitness of all β-lactamase-producing strains and their ability to produce biofilms did not reveal any significant correlation (Pearson correlation, $R^2 = 0.15$, $P = 0.31$; supplementary fig. S1, Supplementary Material online). Thus, the overall antagonization of biofilms mediated by β-lactamases was likely not attributable to nonfunctional proteins or detrimental effects on bacterial fitness but appeared to be connected to their enzymatic activity.

The Biofilm Lifestyle Shapes the Evolution of β-Lactamases

To understand whether genetic changes within β-lactamases could modulate biofilm formation, we focused on the contemporary β-lactamase KPC-2 (wtKPC-2), as it conferred a strong biofilm inhibitory effect, and employed random mutagenesis as a mean to generate genetic diversity (Fig. 1a). Expression of the gene library in *V. cholerae* significantly improved biofilm formation, resulting in higher biomass (OD_{595}) compared to the wtKPC-2 (Fig. 1c, one-way ANOVA, $P < 0.0001$). Improvements were also evident in the strains' ability to form biofilm pellicles (Fig. 1d). The presence of wtKPC-2 completely suppressed pellicle formation, while both the control and mutant library formed visible biofilm pellicles at the air-liquid interface. Thus, our results indicate that the library harbors bla_{KPC-2} mutants able to compensate for the initial biofilm antagonization.

To identify potential variants displaying compensatory behavior, we harvested the biofilm pellicles formed by the library population-mix ($n = 2$) and isolated 12 random clones. Sanger sequencing revealed that 33% of the selected clones contained mutations within KPC-2 at position 136 (N136K and N136D), indicating strong selection for pellicle production and parallel evolution. The clone displaying N136D also exhibited additional amino acid substitutions (M152I/L167P) and a deletion which led to a frameshift mutation (supplementary fig. S2, Supplementary Material online). This frameshift resulted in the loss of the first 48 amino acids, including the signal peptide, and the recruitment of an alternative methionine start codon at position 49 (Δ1-48/N136D/M152I/L167P) (supplementary fig. S2, Supplementary Material online).

To remove the effect of potential confounding mutations on the vector backbone and chromosome, we subcloned N136K and Δ1-48/N136D/M152I/L167P into an isogenic vector backbone and assayed biofilm formation. N136K and Δ1-48/N136D/M152I/L167P displayed 68% and 107% higher biomass relative to wtKPC-2, respectively (one-way ANOVA, $P < 0.0001$ and $P = 0.0008$; Table 2 and Fig. 1e). To deconvolute the contributions from the different mutations in the Δ1-48/N136D/M152I/L167P variant, we selected and constructed variants displaying either loss of the signal peptide (Δ1-48) or mutations around the active site (N136D and L167P; Table 2 and Fig. 1e). While Δ1-48 alone did not significantly (one-way ANOVA, $P = 0.79$) improve biofilm formation relative to wtKPC-2, N136D and L167P increased biofilm formation by 33% (one-way ANOVA, $P = 0.0003$) and 67% (one-way

Table 2
KPC-2 variants resulting in improved biofilm development

Strain no.	Inserts	Biomass at OD_{595}[a]	*P* values[b]	*N*[c]	Relative fitness[d]	Ampicillin MICs (mg/L)
30-70	wtKPC-2	0.417 ± 0.020	—	81	1	>256
30-71	Control[e]	0.889 ± 0.032	<0.0001	61	0.75 ± 0.01	4
30-65	S70A	0.229 ± 0.014	<0.0001	27	ND	4
30-77	Δ1-48/N136D/M152I/L167P[e]	0.862 ± 0.063	<0.0001	15	0.78 ± 0.04	2
30-67	Δ1-/S70A/N136D/M152I/L167P[e]	0.235 ± 0.021	0.0008	11	ND	4
32-13	Δ1-48	0.341 ± 0.019	0.7914	24	0.79 ± 0.03	2
32-07	N136D	0.553 ± 0.037	0.0003	16	0.97 ± 0.02	32
30-75	N136K	0.698 ± 0.028	<0.0001	24	1.00 ± 0.01	24
30-69	S70A/N136K	0.547 ± 0.019	<0.0001	39	ND	2
32-06	L167P	0.696 ± 0.061	<0.0001	16	0.99 ± 0.01	>256

MIC, minimal inhibitory concentration; ND, not determined; OD, opitcal density.
[a]OD measurement was performed in 24-well plates.
[b]Brown–Forsythe one-way ANOVA to test for differences in biomass formation compared to wtKPC-2 ($\alpha = 0.05$) and followed by Dunnett test to correct for multiple testing; F (DFn, DFd) = 62 (15, 293); overall *P* value < 0.0001.
[c]Sample size (biological replicates) tested to determine the biomass at OD_{595}.
[d]Determined as area under the growth curve compared to wtKPC-2 (see supplementary fig. S3, Supplementary Material online for bacterial growth curves and supplementary table S1, Supplementary Material online for area under curves).
[e]*V. cholerae* harboring the pA15 vector without β-lactamase gene.
Errors are reported as the standard error of the mean.

ANOVA, $P < 0.0001$), respectively (Table 2 and Fig. 1e). Translocation of β-lactamases into the periplasmic space depends on the presence of a signal peptide, and the loss of a signal peptide (e.g. Δ1-48/N136D/M152I/L167P) prevents this. Thus, KPC-2 variants without this signal peptide are likely retained in the cytoplasm. Our data demonstrate that these mutants still exert a detrimental effect on biofilm formation. In addition, β-lactamases bearing a signal peptide (e.g. N136D/K and L167P) can be enzymatically active within the cytosol before the translocation (Paunola et al. 1998). This observation suggests that the mechanistic interaction by which they interfere with biofilm formation likely occurs in the cytoplasm. Taken together, our result shows that a biofilm lifestyle can select for mutations in β-lactamases that reverse their initial antagonistic pleiotropic effect on biofilm formation. Thus, evolution in biofilms shapes the evolution of antimicrobial resistance enzymes.

Functional Mutations in KPC-2 Reverse Biofilm Inhibition

Next, we investigated the functional and structural role of mutations acquired during evolution. To study the functionality of selected and constructed mutants, we investigated their ability to confer ampicillin resistance (Table 2). As expected, all mutants lacking the signal peptide exhibited ampicillin susceptibility similar to the vector control (Table 2). Other mutations, such as N136D/K and L167P, clustered around the active site of KPC-2 (Fig. 1f) maintained ampicillin MICs 6- to >64-fold higher than the control strain. Generally, increased biofilm formation coincided with lower ampicillin resistance (Pearson correlation, $R^2 = 0.63$, $P = 0.059$). However, our L167P mutant maintained ampicillin susceptibility similar to KPC-2 while compensating for biofilm formation. L167P exemplifies that biofilm compensation can occur without compromising the enzyme's ability to confer ampicillin resistance (Fig. 1g). Furthermore, the fitness effect of these mutants did not significantly correlate with biofilm formation (Pearson correlation, $R^2 = 0.004$ and $P = 0.89$, supplementary fig. S3, Supplementary Material online). Altogether, our combined findings on bacterial growth and biofilm formation indicate that the reversal of biofilm inhibition was not related to changes in bacterial fitness.

Our mutant analysis (Fig. 1e) suggests that the compensatory effects of the evolved mutants may be linked to cytosolic processes, where they could be either permanently active due to loss of the signal peptide (Δ1-48/N136D/M152I/L167P) or temporarily (N136D/K and L167P) prior to translocation (Paunola et al. 1998). To investigate whether the enzymatic activity of wtKPC-2 and evolved variants was linked to biofilm formation, we constructed serine-to-alanine mutants at position 70 which are unable to covalently bind and efficiently hydrolyze β-lactam substrates (Table 2 and Fig. 1e) (Stojanoski et al. 2016). As expected, introducing S70A in the wtKPC-2, N136K, and Δ1-48/N136D/M152I/L167P backgrounds resulted in MICs similar to the vector control (Table 2). Introducing S70A in wtKPC-2 led to a 45% reduction in biofilm formation compared to the wtKPC-2. Similarly, the introduction of S70A in the evolved Δ1-48/N136D/M152I/L167P variant caused a 73% decrease in biofilm formation compared to the evolved variant, resulting in biofilm levels similar to KPC-2:S70A (Fig. 1e). On the contrary, S70A/N136K displayed only a 21% reduction in biofilm formation compared to the evolved N136K variant and maintained a strong biofilm phenotype relative to the other serine-to-alanine mutants. Our findings stand in contrast to a previous study where the removal of the active site

serine either rescued (TEM-1) or had no effect (OXA-3) on biofilm formation (Gallant et al. 2005). Therefore, how enzyme functionality affects biofilm inhibition seems to vary greatly between different β-lactamases. While the exact molecular mechanisms of biofilm antagonization and compensation remain elusive, informed by our data, we hypothesize that the evolved variants compensate for biofilm inhibition either independently of enzymatic activity (N136K) or by employing its enzymatic activity (Δ1-48/N136D/M152I/L167P). For Δ1-48/N136D/M152I/L167P, the reversal of biofilm inhibition seemingly relies on the indispensable active site serine (S70), since introducing S70A into Δ1-48/N136D/M152I/L167P nullifies the reversal. This indicates that Δ1-48/N136D/M152I/L167P relies on the enzymatic activity of KPC-2 (Fig. 1e) to increase biofilm formation. Alternatively, observed differences in biofilm formation between mutants may be related to differences in structural integrity and/or stability of the evolved variants. However, this seems unlikely since S70A usually does not compromise the stability of β-lactamases (Brown et al. 2009).

Taken together, our findings demonstrate that a broad range of highly diverse β-lactamases inhibits biofilm formation in *V. cholerae,* and that selection for a biofilm lifestyle significantly affects the evolution of these enzymes. Such pleiotropy, where genes can affect a multitude of bacterial phenotypes, has been observed in multiple model systems (Andersson and Hughes 2010; Noda-García et al. 2019; Burmeister et al. 2020). We argue that the selection pressure generated through pleiotropic effects represents a substantial selective force, which influences the genetic adaption and evolution of antimicrobial resistance enzymes.

Methods and Material

Growth Media and Chemicals

All strains and primers used and constructed within this study are shown in supplementary tables S2 and S3, Supplementary Material online. Strains were grown in Lysogeny-Broth (LB) media supplemented with chloramphenicol (5 or 25 mg/L for *V. cholerae* and *E. coli* strains, respectively). LB media and chloramphenicol were purchased from Sigma-Aldrich (USA). Restriction enzymes and T4 ligase were supplied by ThermoFisher (USA).

Strain Construction

The gene sequences of bla_{TEM-1}, bla_{CMY-2}, $bla_{CTX-M-15}$, and bla_{NDM-1} were previously synthesized by Genewiz (Germany) and subcloned in a medium copy number vector (p15A origin) according to the gene sequences NG_050145.1, NG_048935.1, NG_048814.1, and NG_049326.1, respectively (Fröhlich et al. 2022). In addition, bla_{VIM-2} (NG_050347.1), bla_{OXA-48} (CP033880), and bla_{KPC-2} (KU665642) were subcloned from *E. coli* 50579417 and *Klebsiella pneumoniae* K47-25, respectively, into the same vector backbone (Samuelsen et al. 2013; Di Luca et al. 2017; Taiaroa et al. 2018; Fröhlich et al. 2022). All β-lactamases carried an additional glycine after their start codon, allowing us to use a *Xho*I restriction site at the N-terminus. Amplification was performed with Phusion polymerase (NEB). PCR products were digested using *Dpn*I, *Xho*I, and *Nco*I and ligated with the backbone using T4 ligase. Ligated vectors were transformed into the *E. coli* E. cloni (MP21-5) and then subsequently transformed into *V. cholerae* C6706.

OXA-163 was constructed by site-directed mutagenesis and whole vector amplification using Phusion polymerase (NEB, USA), primers P54F/R, and bla_{OXA-48} (CP033880) as a template (Fröhlich et al. 2019). The PCR product was digested for 1 h at 37 °C using *Dpn*I and *Lgu*I. The digested product was ligated for 1 h at room temperature using T4 ligase and transformed into *E. coli* E. cloni (MP21-5). Cells were selected on chloramphenicol 25 mg/L, and mutations were confirmed with Sanger sequencing.

To subclone mutant bla_{KPC-2} alleles, the target genes and vector backbone were amplified using primers P7/P8 and P3/P4, respectively (supplementary table S3, Supplementary Material online), and Phusion polymerase (NEB). PCR products were digested using *Dpn*I, *Xho*I, and *Nco*I and ligated with the backbone using T4 ligase. Ligated vectors were transformed into the MP21-5 and then subsequently transformed into *V. cholerae* C6706.

Active site serine of KPC-2 was mutated to alanine (S70A) using whole vector site-directed mutagenesis with primers P108/P115 containing *Lgu*I cutting sites. The bla_{KPC-2} genes were amplified using primers P108/P115 and Phusion polymerase (NEB). The PCR products were digested with *Lgu*I and *Dpn*I for 1 h at 37 °C following self-ligation using T4 ligase. Ligated vectors were transformed into MP21-5 and then subsequently transformed into *V. cholerae* C6706.

Bacterial Fitness Measurements

Single colonies were grown overnight at 37 °C with shaking at 700 rpm and subsequently diluted 1:100 into LB medium supplemented with 5 μg/L chloramphenicol to a final volume of 300 μL. Growth curve experiments were conducted in 100-well honeycomb plates in a Bioscreen C instrument (Oy Growth Curves Ab Ltd, Finland). Briefly, growth curves were recorded by measuring optical density at 600 nm (OD_{600}) in 4 min intervals for 18 h at 37 °C with continuous shaking. The relative bacterial fitness was calculated as the area under the curve of the individual growth curves using the flux package in R (Jurasinski et al. 2014) and normalized to either *V. cholerae* harboring an empty control vector (Table 1) or wtKPC-2 (Table 2). Fitness was

calculated based on a minimum of 3 biological replicates each based on 3 technical replicates per biological replicate.

Biomass Determining Using Crystal Violet

Overnight cultures were grown in 2 mL LB medium supplemented with 5 μg/L chloramphenicol and incubated overnight at 37 °C with shaking (700 rpm). The following day, the cultures were diluted 1:100 in 2 mL LB medium in a 24-well plate (Corning, USA) and incubated statically at 37 °C for 24 h. Pellicle formation was imaged with a NexiusZoom stereo microscope (Euromex, Netherlands) at 6.7× magnification. Next, the bacterial cultures were removed from the 24-well plate, and the plate was gently washed in distilled water to remove non-adherent bacterial cells. Biofilms were fixed by incubation for 1 h at 55 °C. To quantify the attached biomass, cells were stained with 2 mL of 0.1% crystal violet (Sigma-Aldrich) for 10 min. The crystal violet solution was then removed, and the plates were washed in filtered water and dried at room temperature. Crystal violet-stained biofilms were dissolved in 2.25 mL 70% ethanol (Sigma-Aldrich). Afterwards, biofilm formation was quantified by directly measuring optical density at 595 nm (OD_{595}) in a Spark multimode plate reader (Tecan, Switzerland) in the 24-well plates or by transferring 200 μL of the dissolved crystal violet into a 96-well plate and then measure OD_{595} in an Epoch 2 plate reader (Biotek). Datasets were tested for normality using a Shapiro–Wilk test ($\alpha = 0.05$). The log transformed datasets were analyzed using a Brown–Forsythe one-way analysis of variance (ANOVA, $\alpha = 0.05$) followed by a Dunnett test to correct for multiple comparisons tests. All statistical analyses were performed using Prism v. 9 (GraphPad, USA).

MIC Determination

To assess the functionality of the constructed β-lactamases in *V. cholerae* (Tables 1 and 2), antimicrobial susceptibility against ampicillin was determined using MIC Test Strips (Liofilchem, Italy). Briefly, a bacterial suspension with an optical density of 0.5 McFarland (1.5×10^8 CFU/mL) units was prepared in 0.9% saline (Sigma-Aldrich). This suspension was then plated on LB agar supplemented with 5 mg/L chloramphenicol before the ampicillin MIC test strip was added. The ampicillin MIC was visually determined after incubation for 20 h at 37 °C.

Mutagenesis of KPC-2

The KPC-2 mutant library used in this study was constructed using error-prone PCR to introduce mutations in the bla_{KPC-2} gene as previously described (Fröhlich et al. 2022). Briefly, the mutational library was constructed by error-prone PCR using 10 ng vector DNA, GoTag DNA polymerase (Promega, USA), 25 mM $MgCl_2$ (Promega), 10 μM of primers P7/P8, and either 50 μM oxo-dGTP or 1 μM dPTP. PCR products were *Dpn*I digested for 1 h at 37 °C. Five nanograms of each product was used for a second PCR, which was performed as described above, but without mutagenic nucleotides. The PCR product from the 2nd PCR was digested using *Nco*I and *Xho*I and ligated into the digested and purified vector backbone. The resulting ligation reaction was transformed into MP21-5 (*E. coli* E. cloni). To ensure that the entire sequence space was sampled, >5,000 mutants were harvested. The mutational library was isolated from *E. coli* E. cloni and transformed into *V. cholerae* C6706 (resulting in MP30-72), and selected on LB plates containing 5 mg/L chloramphenicol. Once again, >5,000 colonies were harvested to ensure that the entire sequence space of KPC-2 was sampled.

Biofilm Selection and Isolation of Novel KPC-2 Variants

Overnight cultures of MP30-72 were prepared in 3 mL LB medium ($n = 2$) supplemented with 5 mg/L chloramphenicol and incubated overnight at 37 °C with shaking (700 rpm). Cultures were diluted 1:100 in 2 mL LB supplemented with 5 mg/L chloramphenicol in a 24-well plate and incubated statically at 37 °C for 48 h. After 48 h, biofilm pellicles were harvested and transferred into 1 mL phosphate saline buffer (Fisher Bioreagents, USA, 0.137 M NaCl, 0.0027 M KCl, and 0.01 M phosphate, pH 7.4) using a sterile inoculation loop. Afterwards, the suspension was vortexed for 120 s to disintegrate the biofilm and dislodge biofilm-embedded bacterial cells. To isolate single biofilm-evolved clones, 1 μL of the bacterial suspension was spread onto LB agar supplemented with 5 mg/L chloramphenicol and incubated overnight at 37 °C. Single clones were randomly harvested and subsequently Sanger sequenced (Genewiz) to identify genetic changes in KPC-2. Finally, isolated mutants harboring mutations in KPC-2 were subcloned into the original isogenic backgrounds.

Supplementary Material

Supplementary material is available at *Genome Biology and Evolution* online.

Acknowledgments

We thank Rebekka Rolfsnes Hovd for assisting in strain construction. We thank João Alves Gama for assisting in the analysis of bacterial fitness.

Author Contributions

Ø.M.L. and C.F. conceived the study. Ø.M.L., A.S.B.H., and C.F. performed the experimental work. Ø.M.L., A.S.B.H., P.J.J., and C.F. wrote the manuscript.

Funding

Funding was obtained from the Centre for new antibacterial strategies (CANS) at UiT—The Arctic University of Norway (https://uit.no/research/cans) (C.F., A.S.B.H.). Ø.M.L. was funded by UiT—The Arctic University of Norway. P.J.J. thanks Olav Thon Stiftelsen for funding.

Conflict of Interest

The authors declare no conflict of interest.

Data Availability

The data underlying the figures in this article are published alongside the article as source file.

Literature Cited

Abe K, Nomura N, Suzuki S. Biofilms: hot spots of horizontal gene transfer (HGT) in aquatic environments, with a focus on a new HGT mechanism. FEMS Microbiol Ecol. 2020:96(5):fiaa031. https://doi.org/10.1093/femsec/fiaa031.

Andersson DI, Hughes D. Antibiotic resistance and its cost: is it possible to reverse resistance? Nat Rev Microbiol. 2010:8(4):260–271. https://doi.org/10.1038/nrmicro2319.

Baltrus DA, Smith C, Derrick M, Leligdon C, Rosenthal Z, Mollico M, Moore A, Clark M. Genomic background governs opposing responses to nalidixic acid upon megaplasmid acquisition in *Pseudomonas*. mSphere. 2021:6(1):e00008-21. https://doi.org/10.1128/mSphere.00008-21.

Billane K, Harrison E, Cameron D, Brockhurst MA. Why do plasmids manipulate the expression of bacterial phenotypes? Philos Trans R Soc B Biol Sci. 2021:377(1842):20200461. https://doi.org/10.1098/rstb.2020.0461.

Brown NG, Shanker S, Prasad BVV, Palzkill T. Structural and biochemical evidence that a TEM-1 β-lactamase N170G active site mutant acts via substrate-assisted catalysis. J Biol Chem. 2009:284(48):33703–33712. https://doi.org/10.1074/jbc.M109.053819.

Burmeister AR, Fortier A, Roush C, Lessing AJ, Bender RG, Barahman R, Grant R, Chan BK, Turner PE. Pleiotropy complicates a trade-off between phage resistance and antibiotic resistance. Proc Natl Acad Sci USA. 2020:117(21):11207–11216. https://doi.org/10.1073/pnas.1919888117.

Bush K. Past and present perspectives on β-lactamases. Antimicrob Agents Chemother. 2018:62(10):e01076-18. https://doi.org/10.1128/AAC.01076-18.

Cassini A, Högberg LD, Plachouras D, Quattrocchi A, Hoxha A, Simonsen GS, Colomb-Cotinat M, Kretzschmar ME, Devleesschauwer B, Cecchini M, et al. Attributable deaths and disability-adjusted life-years caused by infections with antibiotic-resistant bacteria in the EU and the European Economic Area in 2015: a population-level modelling analysis. Lancet Infect Dis. 2019:19(1):56–66. https://doi.org/10.1016/S1473-3099(18)30605-4.

Castañeda-Barba S, Top EM, Stalder T. Plasmids, a molecular cornerstone of antimicrobial resistance in the One Health era. Nat Rev Microbiol. 2023:22(1):18–32. https://doi.org/10.1038/s41579-023-00926-x.

Ciofu O, Moser C, Jensen PØ, Høiby N. Tolerance and resistance of microbial biofilms. Nat Rev Microbiol. 2022:20(10):621–635. https://doi.org/10.1038/s41579-022-00682-4.

Coenye T, Bové M, Bjarnsholt T. Biofilm antimicrobial susceptibility through an experimental evolutionary lens. NPJ Biofilms Microbiomes. 2022:8(1):82. https://doi.org/10.1038/s41522-022-00346-4.

Conner JG, Teschler JK, Jones CJ, Yildiz FH. Staying alive: *Vibrio cholerae*'s cycle of environmental survival, transmission, and dissemination. Microbiol Spectr. 2016:4(2):10.1128/microbiolspec.VMBF-0015-2015. https://doi.org/10.1128/microbiolspec.VMBF-0015-2015.

Di Luca MC, Sørum V, Starikova I, Kloos J, Hülter N, Naseer U, Johnsen PJ, Samuelsen Ø. Low biological cost of carbapenemase-encoding plasmids following transfer from *Klebsiella pneumoniae* to *Escherichia coli*. J Antimicrob Chemother. 2017:72(1):85–89. https://doi.org/10.1093/jac/dkw350.

Fernández A, Pérez A, Ayala JA, Mallo S, Rumbo-Feal S, Tomás M, Poza M, Bou G. Expression of OXA-type and SFO-1 β-lactamases induces changes in peptidoglycan composition and affects bacterial fitness. Antimicrob Agents Chemother. 2012:56(4):1877–1884. https://doi.org/10.1128/AAC.05402-11.

Flemming H-C, Wingender J, Szewzyk U, Steinberg P, Rice SA, Kjelleberg S. Biofilms: an emergent form of bacterial life. Nat Rev Microbiol. 2016:14(9):563–575. https://doi.org/10.1038/nrmicro.2016.94.

Fröhlich C, Sørum V, Molden AT, Johnsen PJ, Leiros H-KS, Samuelsen Ø. OXA-48-mediated ceftazidime–avibactam resistance is associated with evolutionary trade-offs. mSphere. 2019:4(2):e00024-19. https://doi.org/10.1128/mSphere.00024-19.

Fröhlich C, Sørum V, Tokuriki N, Johnsen PJ, Samuelsen Ø. Evolution of β-lactamase-mediated cefiderocol resistance. J Antimicrob Chemother. 2022:77(9):2429–2436. https://doi.org/10.1093/jac/dkac221.

Gallant CV, Daniels C, Leung JM, Ghosh AS, Young KD, Kotra LP, Burrows LL. Common β-lactamases inhibit bacterial biofilm formation. Mol Microbiol. 2005:58(4):1012–1024. https://doi.org/10.1111/j.1365-2958.2005.04892.x.

Jurasinski G, Koebsch F, Guenther A, Beetz S. 2014. Flux rate calculation from dynamic closed chamber measurements. R package version 0.3-0.1. https://cran.r-project.org/web/packages/flux/flux.pdf

Kovács ÁT, Dragoš A. Evolved biofilm: review on the experimental evolution studies of *Bacillus subtilis* pellicles. J Mol Biol. 2019:431(23):4749–4759. https://doi.org/10.1016/j.jmb.2019.02.005.

Madsen JS, Burmølle M, Hansen LH, Sørensen SJ. The interconnection between biofilm formation and horizontal gene transfer. FEMS Immunol Med Microbiol. 2012:65(2):183–195. https://doi.org/10.1111/j.1574-695X.2012.00960.x.

Noda-García L, Davidi D, Korenblum E, Elazar A, Putintseva E, Aharoni A, Tawfik DS. Chance and pleiotropy dominate genetic diversity in complex bacterial environments. Nat Microbiol. 2019:4(7):1221–1230. https://doi.org/10.1038/s41564-019-0412-y.

Paunola E, Suntio T, Jämsä E, Makarow M. Folding of active β-lactamase in the yeast cytoplasm before translocation into the endoplasmic reticulum. Mol Biol Cell. 1998:9(4):817–827. https://doi.org/10.1091/mbc.9.4.817.

Qin B, Bassler BL. Quorum-sensing control of matrix protein production drives fractal wrinkling and interfacial localization of *Vibrio cholerae* pellicles. Nat Commun. 2022:13(1):6063. https://doi.org/10.1038/s41467-022-33816-6.

Qin B, Fei C, Wang B, Stone HA, Wingreen NS, Bassler BL. Hierarchical transitions and fractal wrinkling drive bacterial pellicle morphogenesis. Proc Natl Acad Sci USA. 2021:118(20):e2023504118. https://doi.org/10.1073/pnas.2023504118.

Roemhild R, Bollenbach T, Andersson DI. The physiology and genetics of bacterial responses to antibiotic combinations. Nat Rev Microbiol. 2022:20(8):478–490. https://doi.org/10.1038/s41579-022-00700-5.

Samuelsen Ø, Naseer U, Karah N, Lindemann PC, Kanestrøm A, Leegaard TM, Sundsfjord A. Identification of Enterobacteriaceae

isolates with OXA-48 and coproduction of OXA-181 and NDM-1 in Norway. J Antimicrob Chemother. 2013:68(7):1682–1685. https://doi.org/10.1093/jac/dkt058.

Silva AJ, Benitez JA. *Vibrio cholerae* biofilms and cholera pathogenesis. PLoS Negl Trop Dis. 2016:10(2):e0004330. https://doi.org/10.1371/journal.pntd.0004330.

Steenackers HP, Parijs I, Foster KR, Vanderleyden J. Experimental evolution in biofilm populations. FEMS Microbiol Rev. 2016:40(3):373–397. https://doi.org/10.1093/femsre/fuw002.

Stojanoski V, Adamski CJ, Hu L, Mehta SC, Sankaran B, Zwart P, Prasad BVV, Palzkill T. Removal of the side chain at the active-site serine by a glycine substitution increases the stability of a wide range of serine β-lactamases by relieving steric strain. Biochemistry. 2016:55(17):2479–2490. https://doi.org/10.1021/acs.biochem.6b00056.

Taiaroa G, Samuelsen Ø, Kristensen T, Løchen Økstad OA, Heikal A. Complete genome sequence of pseudomonas aeruginosa K34-7, a carbapenem-resistant isolate of the high-risk sequence type 233. Microbiol Resour Announc. 2018:7(4):e00886–18. https://doi.org/10.1128/mra.00886-18.

Teschler JK, Nadell CD, Drescher K, Yildiz FH. Mechanisms underlying *Vibrio cholerae* biofilm formation and dispersion. Annu Rev Microbiol. 2022:76(1):503–532. https://doi.org/10.1146/annurev-micro-111021-053553.

Teschler JK, Zamorano-Sanchez D, Utada AS, Warner CJA, Wong GCL, Linington RG, Yildiz FH. Living in the matrix: assembly and control of *Vibrio cholerae* biofilms. Nat Rev Microbiol. 2015:13(5):255–268. https://doi.org/10.1038/nrmicro3433.

Associate editor: Lucy van Dorp